

1,3-Dipolar Cycloadditions with Porphyrins

by

Jeffery Flemming

B. Sc. (Hons), Wilfrid Laurier University, 1997

A THESIS SUBMITTED IN PARTIAL FULFILMENT OF
THE REQUIREMENTS FOR THE DEGREE OF

MASTER OF SCIENCE

In

THE FACULTY OF GRADUATE STUDIES

DEPARTMENT OF CHEMISTRY

We accept this thesis as conforming
to the required standard

THE UNIVERSITY OF BRITISH COLUMBIA

August 2001

© Jeffery Flemming, 2001

In presenting this thesis in partial fulfilment of the requirements for an advanced degree at the University of British Columbia, I agree that the Library shall make it freely available for reference and study. I further agree that permission for extensive copying of this thesis for scholarly purposes may be granted by the head of my department or by his or her representatives. It is understood that copying or publication of this thesis for financial gain shall not be allowed without my written permission.

Department of Chemistry

The University of British Columbia
Vancouver, Canada

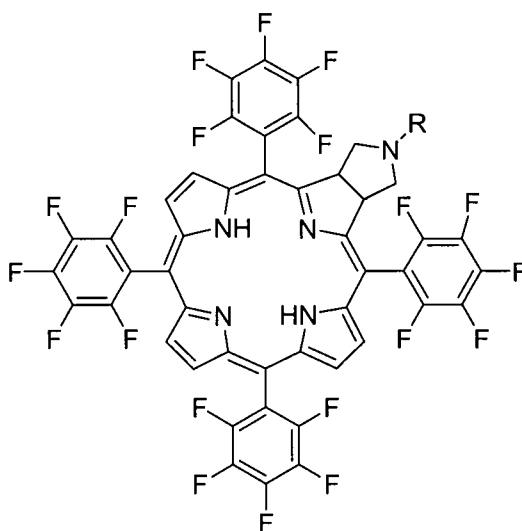
Date Aug. 15 / 2001

Abstract

The objective of this work is to use 1,3-dipolar cycloadditions to synthesize novel aromatic compounds based on meso-phenyl substituted porphyrins. These compounds are potential photosensitizers for use in photodynamic therapy.

Tetraphenylporphyrins with a variety of substituents were reacted with selected 1,3-dipoles. Tetraphenylporphyrin (TPP), 5,10-diphenylporphyrin (DPP), and tetrakis(pentafluorophenyl)porphyrin (pFTPP) were used in reactions with azomethine ylides, carbonyl ylides, diazoalkanes, nitrile oxides, thiocarbonyl ylides, nitrile ylides, and ozone, with varying results. Centrally metallated porphyrins were also used.

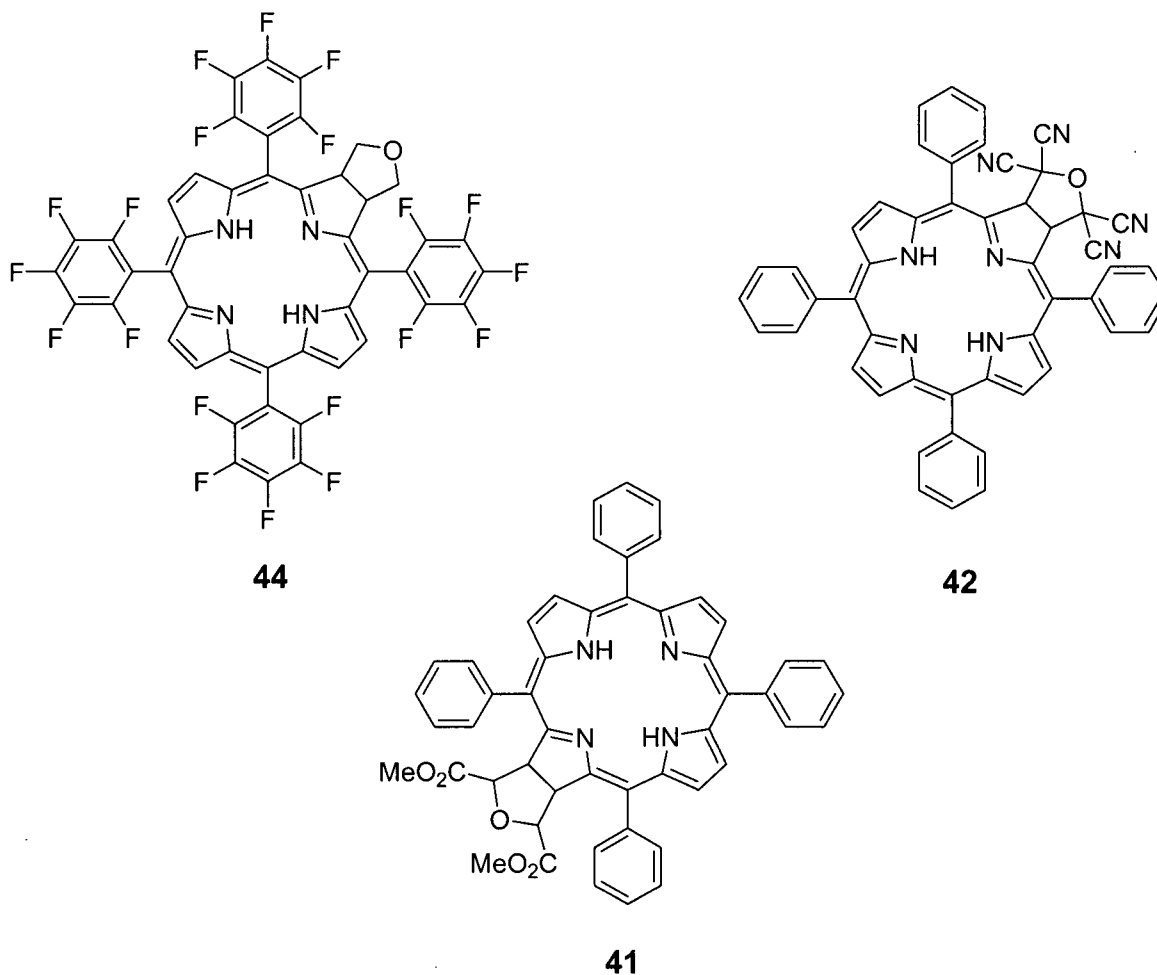
Azomethine ylides reacted with pFTPP efficiently giving cycloadducts of



36a-38a

pFTPP. Three n-substituted azomethine ylides (R = benzyl, 3,5-dimethoxybenzyl, and propyl) were used. The different substituents on the pyrrolidine ring did not affect the ultra-violet / visible (UV-Vis) spectra of the chlorin.

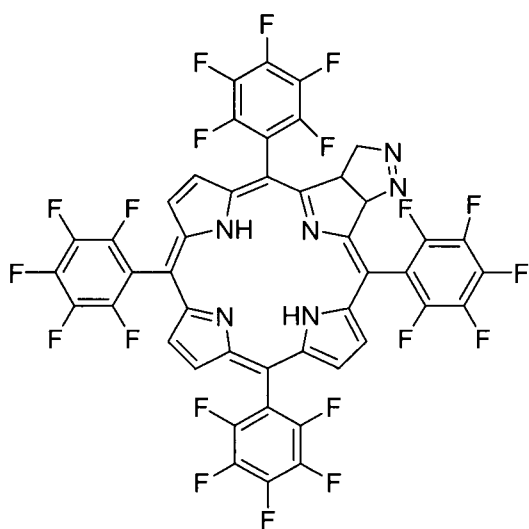
Carbonyl ylides form cycloadducts with both TPP and pFTPP. The



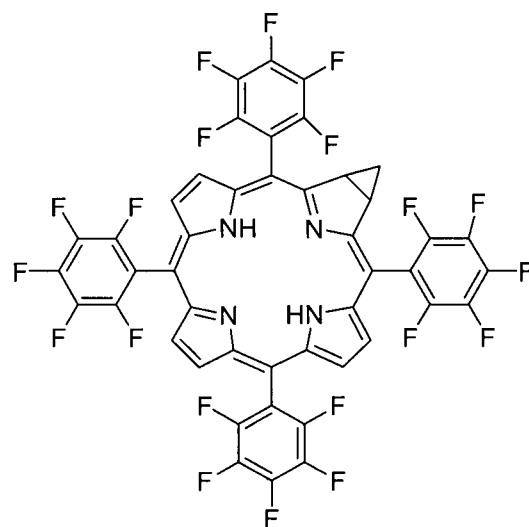
electron deficient pFTPP reacts with non-stabilized carbonyl ylides, while TPP reacts with the electron deficient tetracyano-substituted carbonyl ylide. These results highlight the differences in reactivity of these two porphyrins. The cyano groups of **42** were hydrolyzed with concentrated hydrochloric acid, and then methylated giving **41**. Changes were observed in the UV-Vis spectra as the substituents were modified.

Diazomethane gave the cycloadduct pyrazoline with pFTPP (**45**). Compound **45** was then subjected to heat or light, both of which caused the loss of N_2 giving the cyclopropane **46**. The UV-Vis spectrum of the cyclopropane derivative was

red-shifted as compared to the pyrazoline, possibly by distortion in the porphyrin ring system as a result of the cyclopropane ring.



45



46

Table of Contents

Abstract	ii
Table of Contents	v
List of Figures	viii
List of Schemes	x
List of Tables	xiii
Nomenclature	xiv
List of Abbreviations	xvi
Acknowledgements	xviii
Chapter One Introduction	1
1.1 Tetrapyrrolic Macrocycles	1
1.1.1 Introduction.....	1
1.1.2 Structural Characteristics	4
1.1.3 Reactivity.....	8
1.1.4 Optical Absorption Spectra of Porphyrins.....	10
1.1.5 Synthesis of Porphyrins	13
1.2 Photodynamic Therapy	19
1.2.1 Introduction.....	19
1.2.2 Production of a Useful Photosensitizer.....	21
1.2.3 Mechanism of Photosensitization	22
1.2.4 Singlet Oxygen Production	24
1.2.5 Porphyrin Related Photosensitizers.	27

1.2.5.1 Core Modified Water Soluble Porphyrins	27
1.2.5.2 BPDMA	29
1.2.5.3 Zinc Tetra-ruthenated Porphyrin	31
1.3 1,3-Dipolar Cycloadditions	32
1.3.1 Introduction	32
1.3.2 Short History of 1,3-Dipoles	34
1.3.2.1 Diazomethane	37
1.3.2.2 Azides	37
1.3.2.3 Ozone	38
1.3.2.4 Nitrile Oxides	39
1.3.3 Mechanism and Reactivity of 1,3-Dipoles	40
1.3.3.1 General Description of Mechanism	40
1.3.4 Methods of 1,3-Dipolar Cycloaddition	55
1.3.4.1 Diazoalkanes	55
1.3.4.2 Azomethine Ylides	59
1.3.4.3 Carbonyl Ylides	61
1.3.4.4 Thiocarbonyl Ylides	62
1.3.4.5 Nitrile Ylides	64
Chapter Two Results and Discussion	65
2.1 Introduction	65
2.1.1 Synthesis of Chlorins from Porphyrins	66
2.1.1.1 Natural Sources	66
2.1.1.2 Diels-Alder Reactions	66

2.1.1.3 Osmium Tetroxide Oxidation	69
2.1.1.4 1,3-Dipolar Cycloadditions.....	69
2.2 Results	70
2.2.1 Azomethine Ylides	71
2.2.2 Carbonyl Ylides.....	78
2.2.2.1 Tetracyanoethylene Oxide	78
2.2.2.2 Non-stabilized Carbonyl Ylide	89
2.2.3 Diazoalkanes	86
2.2.3.1 Diazomethane	86
2.2.3.2 (Trimethylsilyl)diazomethane.....	92
2.2.4 Nitrile Oxides	93
2.2.5 Ozone.....	96
2.2.6 Thiocarbonyl Ylides	97
2.2.7 Nitrile Imines	98
2.2.8 Azides	99
2.2.9 Azaallyl Anions	100
Chapter 3 Conclusions and Suggestions for Further Work.....	102
Chapter 4 Experimental	104
4.1 Instrumentation and Materials.....	104
4.2 General Procedures and Data.....	105
Chapter 5 References	116

List of Figures

Figure 1-1	Tetrapyrrolic Macrocycles	1
Figure 1-2	Structure of Chlorophyll and Heme	2
Figure 1-3	Structure of Poly(vinylidene dichloride)-cobalt-porphyrin	3
Figure 1-4	Chelate Appended Porphyrins	4
Figure 1-5	Aromatic (4n+2) Pathway of Porphyrin	5
Figure 1-6	Tetraphenylporphyrin (6) and Octaethylporphyrin (7)	7
Figure 1-7	Representative Porphyrin Spectra	11
Figure 1-8	UV-Visible Spectra of Metalloporphyrins	12
Figure 1-9	UV-Visible Spectra of Chlorin and Bacteriochlorin	13
Figure 1-10	Absorption Intensity of Human Tissue	21
Figure 1-11	Modified Jablonski Diagram of a Photosensitizer	25
Figure 1-12	Singlet State of Molecular Oxygen	26
Figure 1-13	Core Modified Porphyrin Photosensitizers	28
Figure 1-14	μ -{ <i>Meso</i> -5-10-15-20-tetra(4-pyridyl)porphyrin}-tetrakis-{bis- (bipyridine)chlororuthenium(II)} (26)	32
Figure 1-15	Resonance Structures of 1,3-Dipoles	33
Figure 1-15a	Possible 1,3-Dipoles	35
Figure 1-16	Activation Energy Diagram of Early and Late Transition State (T.S.) ..	41
Figure 1-17	Symmetry Allowed Interactions of Type One 1,3-Dipolar Cycloadditions	44
Figure 1-18	Change in Molecular Orbital Energy Upon Substitution	45

Figure 1-19	Symmetry Allowed Interactions of Type Three 1,3-Dipolar Cycloadditions	48
Figure 1-20	Symmetry Allowed Interactions of Type Two 1,3-Dipolar Cycloadditions	49
Figure 1-21	Complex Used for Molecular Orbital Calculations	54
Figure 1-22	Diazomethane Reactions with Electron Rich and Electron Poor Dipolarophiles.....	56
Figure 1-23	Correlation of the Rates of Reaction of Diazomethane and Diphenyldiazomethane	58
Figure 2-1	Selected Chlorins Tested as PDT Agents	65
Figure 2-2	Results of α, α' di(trimethylsilylmethyl)amine Reaction with pFTPP and AgF	73
Figure 2-3	UV-Vis Spectra of 36a , 37a , and 38a	77
Figure 2-4	Product of Acid Hydrolysis and Methylation of 40	81
Figure 2-5	Structure of Compound 40	82
Figure 2-6	n-Confused Porphyrin.....	82
Figure 2-7	UV-Vis Spectra of 40 , 40a , and 41	83
Figure 2-8	UV-Vis Spectra of 45 , 46	91
Figure 2-9	Cyclopropane "Mixed Orbitals"	91
Figure 2-10	Trimethylsilylazide Cycloaddition Product	100

List of Schemes

Scheme 1-1	Electrophilic Substitution of the Porphyrin System.....	6
Scheme 1-2	Electrophilic Aromatic Substitution	6
Scheme 1-3	Reactions of the Cross-Conjugated Double Bonds of Porphyrins.....	10
Scheme 1-4	Synthesis of Uro'gen III	15
Scheme 1-5	Synthesis of Tetraphenylporphyrin (6).....	16
Scheme 1-6	Synthesis of Octaethylporphyrin (7).....	17
Scheme 1-7	Mechanism for the Synthesis of Octaethylporphyrin	17
Scheme 1-8	Porphyrin Synthesis from Dipyrrolic Precursors.....	18
Scheme 1-9	Synthesis of Hematoporphyrin Derivatives	20
Scheme 1-10	Type One Reactions of a Photosensitizer	23
Scheme 1-11	Reactions of Singlet Oxygen	24
Scheme 1-12	Synthesis of BPDMA.....	30
Scheme 1-13	Reactions of the Two Types of 1,3-Dipoles	33
Scheme 1-14	Buchners' Proposed Mechanism of the Reaction between Diazoacetic Acid with Fumaric Acid.....	36
Scheme 1-15	Reaction of Methyl Diazoacetate with Dimethyl Acetylenedicarboxylate.....	36
Scheme 1-16	Reaction of Diazoacetic Acid with Methyl Acrylate.....	36
Scheme 1-17	Structures of Diazomethane and Hydrogen Azide.....	37
Scheme 1-18	Reaction of Phenyl Azide with Dimethyl Acetylenedicarboxylate	38
Scheme 1-19	The Criegee Mechanism for Ozonolysis.....	38

Scheme 1-20	Non-concerted 1,3-Dipolar Cycloaddition Mechanism.....	40
Scheme 1-21	Reaction of Fulminic Acid with Acetylene and Ethylene	42
Scheme 1-22	Mesomeric Betaines.....	52
Scheme 1-23	Metal Catalyzed Reaction of Phenyl Nitrile Oxide and 3-Hydroxy-1-Propene	53
Scheme 1-24	Metal Catalyzed Nitrene Cycloaddition	54
Scheme 1-25	Production of Diazomethane.....	55
Scheme 1-26	Diradical Mechanism of 1,3-Dipolar Cycloaddition of Diazomethane	57
Scheme 1-27	Electrocyclic Ring Opening Formation of Azomethine Ylides.....	59
Scheme 1-28	Synthesis of Non-Stabilized Azomethine Ylides.....	59
Scheme 1-29	Inverse Electron Demand Azomethine Ylide 1,3-Dipolar Cycloaddition.	60
Scheme 1-30	Reaction of 2-Azaaryl Anion with Anionophile	61
Scheme 1-31	Electrocyclic Ring Opening to form a Carbonyl Ylide	62
Scheme 1-32	Reduction of di-Chloromethylether to form an Unstabilized Carbonyl Ylide.....	62
Scheme 1-33	Methods of Generating Non-stabilized Thiocarbonyl Ylides.....	63
Scheme 1-34	Formation of Nitrile Ylides.....	64
Scheme 2-1	Reaction of Benzoquinonedimethane with TPP	67
Scheme 2-2	Diels-Alder Reactions with Protoporphyrin IX	68
Scheme 2-3	Dihydroxylation of TPP	69
Scheme 2-4	Reaction of Tetraarylporphyrins with Azomethine Ylide	70
Scheme 2-5	Mechanism of Azomethine Ylide Formation	74

Scheme 2-6	Original Assumed Product of TCNEO/TPP Reaction	79
Scheme 2-7	Unstabilized Carbonyl Ylide Reaction with pFTPP to form 44	84
Scheme 2-8	Mechanism of Diazomethane Methylation (X = O, S, or N).....	86
Scheme 2-9	Cyclopropanation of TPP	87
Scheme 2-10	Reaction of Diazomethane with pFTPP.....	88
Scheme 2-11	Cyclopropane Formation from Pyrazoline.....	90
Scheme 2-12	Methods of Nitrile Oxide Formation	95
Scheme 2-13	Predicted Products of Porphyrin Ozonolysis	96
Scheme 2-14	Synthesis of Mesomeric Betaine 47	99
Scheme 2-15	Formation of Azaallyl Anions.....	101

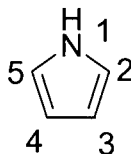
List of Tables

Table 1-1	Singlet Oxygen Quantum Yields	27
Table 1-2	UV-Vis Spectra Showing the Wavelengths of Maximal Absorption of (2) and (3) Compared to the Porphyrin Analogue.....	29
Table 1-3	Frontier Molecular Orbital Energies of Parent 1,3-Dipoles (Type One)...	46
Table 1-4	Relative Rate Constants of Reactions Between Diazomethane and Various Dipolarophiles.....	47
Table 1-5	Frontier Molecular Orbital Energies of Parent 1,3-Dipoles (Type Three)	49
Table 1-6	Molecular Orbital Energies of Type Three 1,3-Dipoles	50
Table 1-7	Relative Rate Constants of 1,3-Dipolar Cycloadditions with Phenyl Azide.....	51

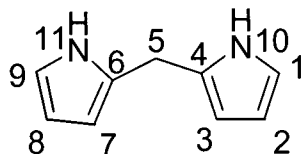
Nomenclature

Monopyrrolic Systems

The pyrrolic skeleton is numbered starting from the nitrogen atom as shown. Positions 2 and 5 are commonly referred to as the “ α ” and 3 and 4 as the “ β ” positions.

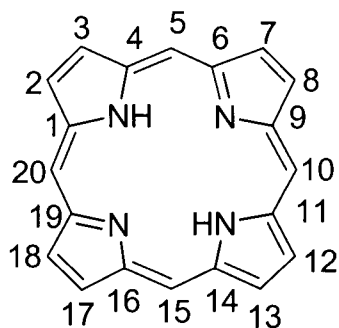


Dipyrromethanes are numbered as shown below. Positions 1 and 9 are referred to as the “ α ” positions, while positions 2, 3, 4, and 8 are the “ β ” positions. Position 5 is called the “*meso*” position.



Porphyrins and Related Systems

The “ α ” positions are those at carbons 1,4,6,9,11,14,16, and 19. The “ β ” positions are those at carbons 2,3,7,8,12,13,17, and 18 and positions 5,10,15, and 20 are referred to as the “meso” positions



List of Abbreviations

AgF	silver fluoride
aq.	aqueous
BPD	benzoporphyrin derivative
BPDMA	benzoporphyrin derivative monoacid ring A
CV	cyclic voltammograms
d	doublet
dd	doublet of doublets
DBU	1,8-diazabicyclo[5.4.0.]undec-7-ene
DDQ	2,3-dichloro-5,6-dicyano-1,4-benzoquinone
DMAD	dimethylacetylene dicarboxylate
DMF	dimethyl formamide
DMSO	dimethylsulfoxide
DNA	deoxyribonucleic acid
DPP	5,15-diphenylporphyrin
EI	electron impact
EDG	electron donating group
EWG	electron withdrawing group
FMO	frontier molecular orbital
HOMO	highest occupied molecular orbital
HpD	hematoporphyrin derivative
HRMS	high resolution mass spectrometry
Hz	Hertz

LiAlH ₄	lithium aluminum hydride
LRMS	low resolution mass spectrometry
LUMO	lowest unoccupied molecular orbital
m	multiplet
MS	mass spectrometry
NCS	n-chlorosuccinimide
NMR	nuclear magnetic resonance
β -NO ₂ -TPP	2-nitro-5,10,15,20-tetraphenylporphyrin
OEP	2,3,7,8,12,13,17,18-octaethylporphyrin
PDT	photodynamic therapy
pFTPP	tetrakis(pentafluorophenyl)porphyrin
q	quartet
qu	quintet
s	singlet
t	triplet
TCNEO	tetracyanoethylene oxide
THF	tetrahydrofuran
TLC	thin layer chromatography
TPP	tetraphenylporphyrin
UV-Vis	ultra-violet and visible

Acknowledgements

I would like to thank Dr. David Dolphin for allowing me to explore the field of porphyrin chemistry as I pleased. This freedom allowed me challenge my own limits as a scientist.

I would like to thank the Dolphin group, not only for their support and encouragement, but also for the companionship that made the last two years enjoyable. Thanks especially to Angela M. Desjardins, David Fenwick, Dr. Elizabeth Cheu, and Dr. Alison Thompson, for helping me immeasurably with the writing of this thesis.

I would also like to thank Ethan Sternberg for his guidance during my time at U.B.C.. He allowed me to understand, if only in a small way, the world of porphyrin chemistry.

Chapter One: Introduction

1.1 Tetrapyrrolic Macrocycles

1.1.1 Introduction

This thesis discusses the chemical reactivity of porphyrins and 1,3-dipoles. Porphyrins are members of the tetrapyrrolic macrocycle family. Some of the other members of this family are shown in Figure 1-1.

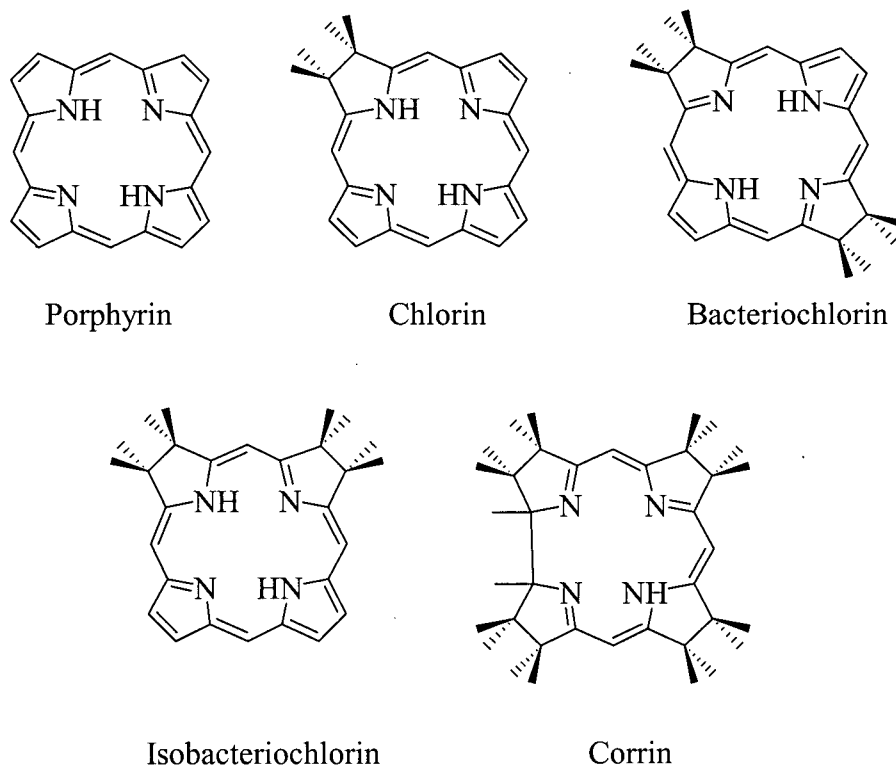


Figure 1-1. Tetrapyrrolic Macrocycle.

All of the species shown in Figure 1-1, with the exception of the corrin, are aromatic. The consequences of this will be discussed in Section 1.1.2.

Tetrapyrrolic macrocycles are abundant in nature. The most common uses of porphyrins and their analogues are related to the fundamental needs of plants and animals. Photosynthesis is the process that is responsible for the presence and

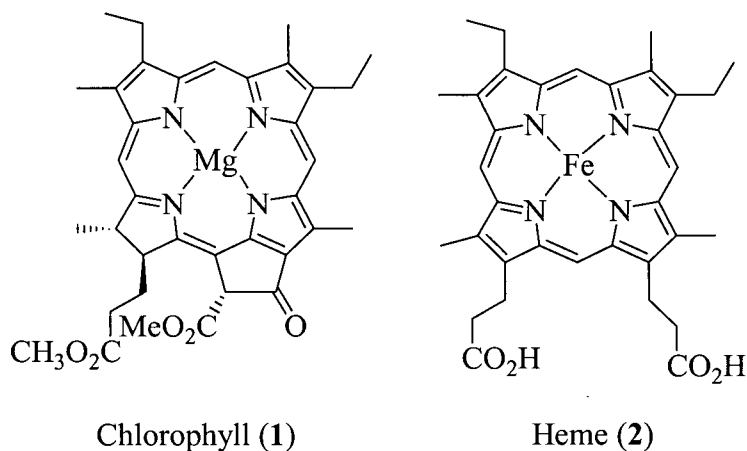


Figure 1-2. Structure of Chlorophyll (1) and Heme (2).

maintenance of oxygen in the atmosphere. Chlorophyll, which is involved in photosynthesis, is a purpurin. Purpurins are chlorins with an exocyclic ring as shown in Figure 1-2 (1), and complex to magnesium giving chlorophyll. Aromatic tetrapyrrolic macrocycles can complex to many different metals (Section 1.1.2). The first step of photosynthesis involves the capture of light by chlorophyll. The light energy is then converted into chemical energy via a cascade of oxidation and reduction processes. Hemoglobin (the prosthetic of which is heme, see Figure 1-2) is used in the transport of oxygen in the human body. In addition, heme forms the prosthetic group for catalases

and peroxidases,¹ which protect humans from species such as superoxide (O_2^-) and peroxide (O_2^{2-}). Nature depends on porphyrins to carry out and control redox processes.

Many important uses for porphyrins have been discovered since the elucidation of their structure almost 80 years ago. One of these is in the use of porphyrins as light capturing molecules to transform light energy into electrical energy.

Another use of porphyrins is in the production of oxygen selective membranes.² The poly(vinylidene dichloride)-cobalt-porphyrin membrane (Figure 1-3) was investigated for its selectivity of oxygen transport over that of nitrogen.² It was found that the oxygen sorption amount is 30 times greater than that for nitrogen.²

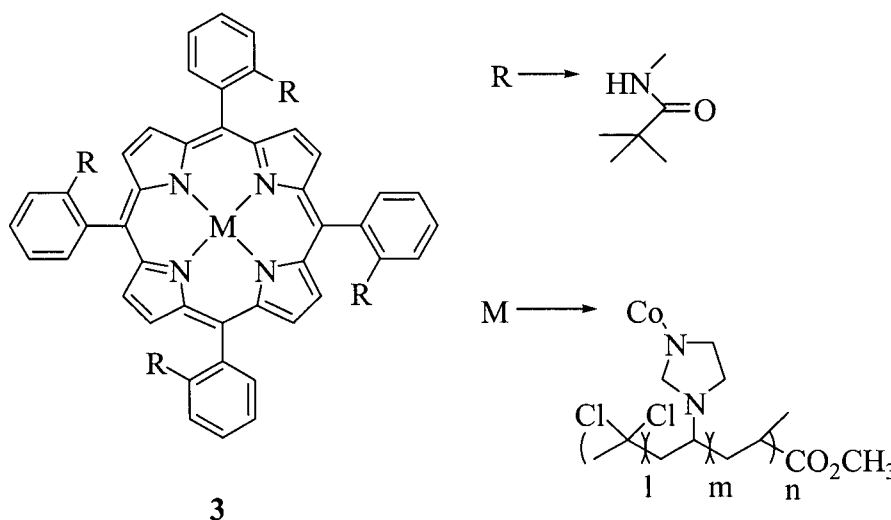


Figure 1-3. Structure of Poly(vinylidene dichloride)-cobalt-porphyrin.

Porphyrins have also been used as reagents to cleave double stranded DNA.³ Tetra-4-(N-methyl)pyridylporphyrin is known to bind to DNA,⁴ therefore compounds 4 and 5 (Figure 1-4) were assessed for their ability to cleave DNA. The two chelate

appended porphyrins were found to induce single and double stranded cleavages respectively of pBR322 plasmid DNA.³

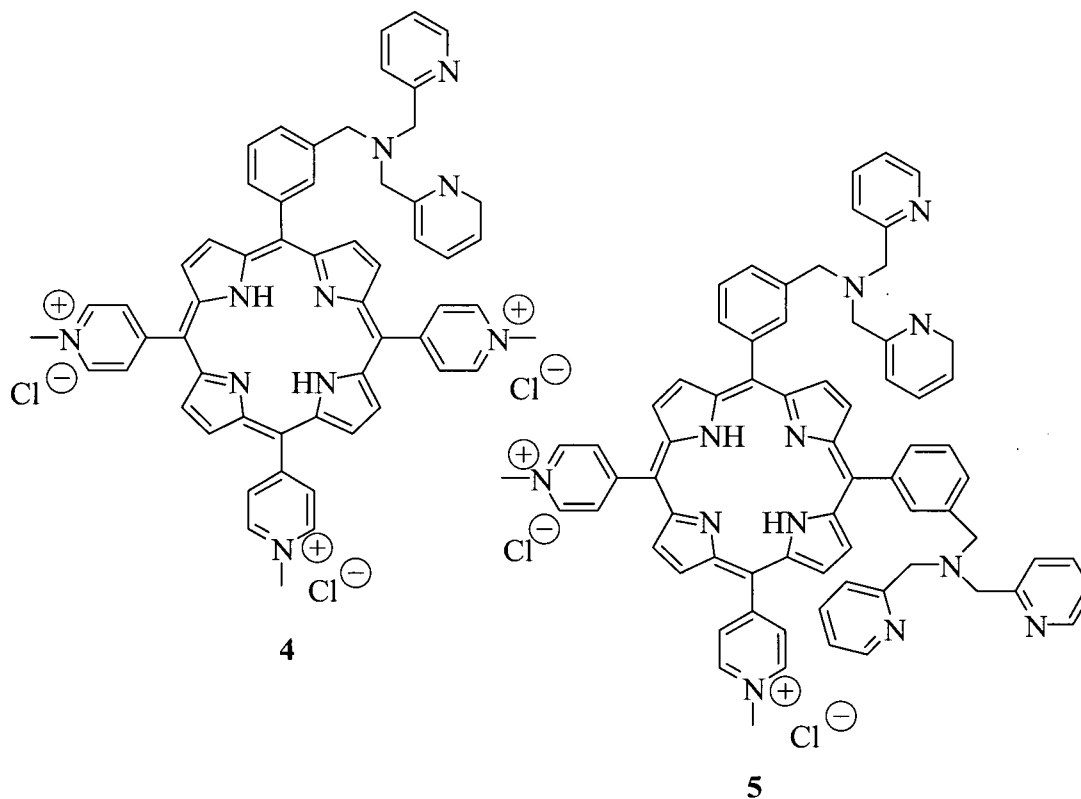


Figure 1-4. Chelate Appended Porphyrins.

Porphyrin cobalt complexes have also been used as nuclear magnetic resonance (N.M.R.) shift reagents.⁵ Applications of porphyrins are becoming more widely developed and applied.

1.1.2 Structural Characteristics

The properties and uses of porphyrins have been investigated for many years, but the exact structure has only been known for a relatively short period of time. Kuster first suggested the structure of a porphyrin to be that of a tetrapyrrole in 1912.⁸ This theory was not widely accepted, as a tetrapyrrolic structure was thought to be too large to be

stable.⁶ In 1929 Fischer, who had originally refuted the tetrapyrrolic structure, completed the total synthesis of heme, and thus Kuster's structure became accepted as the correct one.

Porphyrins are aromatic. This aromaticity defines the unique chemical and physical properties of the porphyrin. The aromatic system consists of 22 π -electrons,

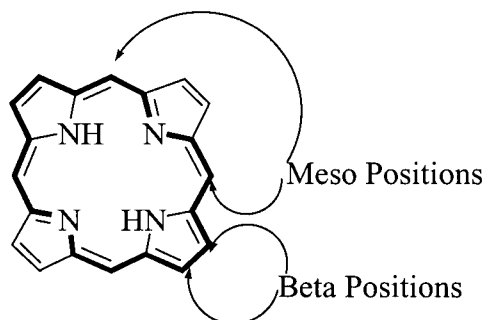
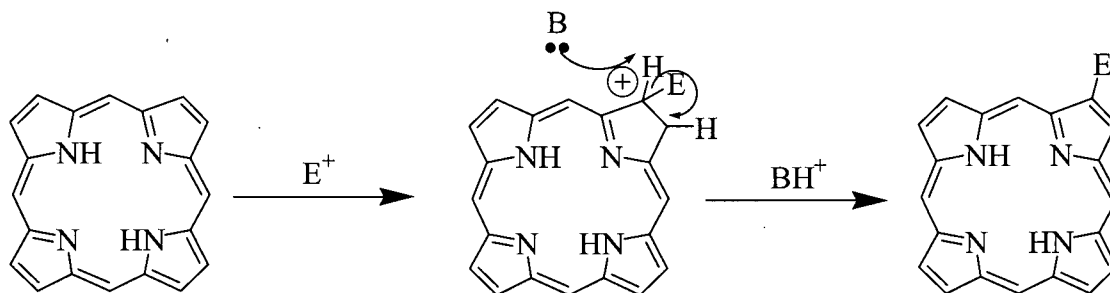


Figure 1-5. Aromatic ($4n+2$) Pathway of Porphyrin.

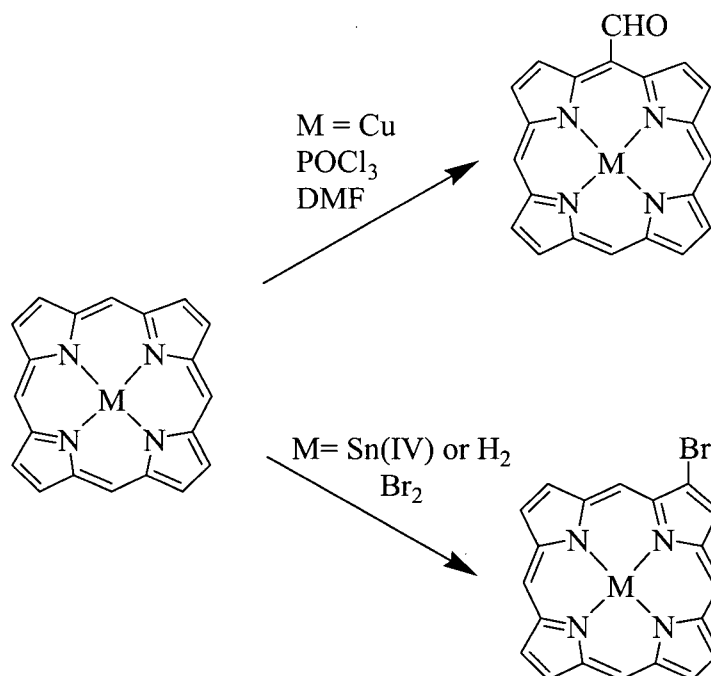
which adheres to the ($4n+2$) rule of Huckel.⁷ This aromaticity can be observed in the N.M.R. spectra of porphyrins. The inner pyrrole protons are shifted significantly upfield, while the *meso* and β -protons (Figure 1-5) are shifted downfield. These effects are caused by the diamagnetic ring current, which can shift the inner pyrrole protons as far upfield as -5 ppm, and the *meso* and β -protons as far downfield as 10 ppm.⁸

The chemical reactions of porphyrins are similar to those of other aromatic systems. Electrophilic (E^+) substitution reactions such as nitration, sulfonation, and acylation of porphyrins all proceed through a cationic intermediate. Subsequently a proton is removed by a base in order to restore aromaticity (Scheme 1-1).

The porphyrin system has two distinct reactive sites, as can be seen from Scheme 1-2. The *meso* and β -positions have different reactivities, and often compete



Scheme 1-1. Electrophilic Substitution of the Porphyrin System.



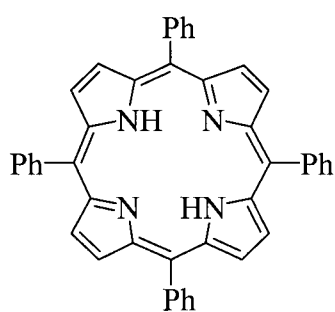
Scheme 1-2. Electrophilic Aromatic Substitution.

during reactions. Reactivity can be directed towards either the *meso* or β -positions through metallation of the inner pyrrole nitrogens of the porphyrin ring. This will be discussed in Section 1.1.3.

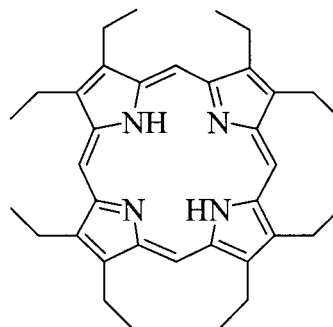
Different metals have been used to metallate the inner pyrrole nitrogens of porphyrins (Section 1.1.1). In fact, almost all of the metals of the periodic table have been used to form complexes with porphyrins.⁹ The size of the ring formed by the four

inner pyrrole nitrogens is such that it will accommodate a variety of metals, although some are too large, and must reside outside the plane of the ring.¹⁰ Metallation occurs by deprotonation of the pyrrole nitrogens. The pK_1 and pK_2 values are both approximately 16, while the pK_3 is 5 and the pK_4 is 2.¹¹ Thus the porphyrin exists formally as its dianion in a metal complex. It also exists as a dication in strong acid.¹³ It is important to note that the protons on the inner pyrrole nitrogens are not localized on any two nitrogen atoms, but equally on all four. This is due to the fact that porphyrins exist equally a two tautomers.

One of the most striking and useful structural features of a porphyrin is the amazing structural diversity that has been attained while maintaining the key features of light absorption and photosensitivity. This structural diversity becomes obvious by comparing the structures of natural (Figure 1-2) and synthetic porphyrins (Figure 1-6).



Tetraphenylporphyrin (6)



Octaethylporphyrin (7)

Figure 1-6. Structure of Tetraphenylporphyrin (6) and Octaethylporphyrin (7).

Diverse functionalization of both TPP and OEP has been achieved. This includes substitution of the phenyl rings and β -positions of TPP (6),¹² as well as the β and *meso*-positions of OEP (7).¹³ The functionalizing of the TPP phenyl rings may occur by using substrates in the synthesis of TPP which give the desired substitution pattern,¹⁷ or by

direct substitution of TPP.¹⁴ OEP can also be synthesized with substituents in the β -position, but mainly functionalization occurs through chemical reaction with the porphyrin ring.¹⁹ These functionalizations enhance the usefulness of porphyrins as briefly discussed in Section 1.1.1.

1.1.3 Reactivity

As mentioned in Section 1.1.2, the chemical reactivity of the free-base porphyrin is due to its aromaticity.¹³ The reactivity of free-base porphyrins is similar to that of other aromatic systems, however several differences do exist. The most notable is the fact that one can easily complex a variety of metals into the core of the porphyrin, and this can have a marked effect on the reactivity at the periphery.

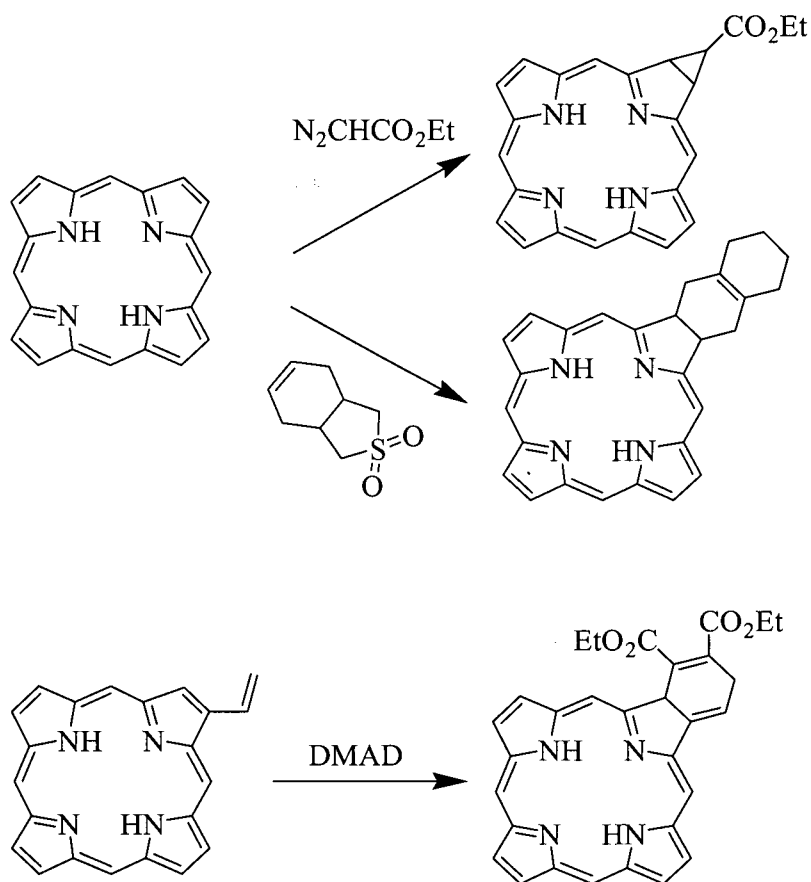
The degree of electronegativity at the porphyrin periphery can be controlled via incorporation of divalent metals. This electronegativity decreases in the order $Mg > Zn > Cu > Ni > Pd$,¹⁵ and the complexes that are formed tend to be more susceptible to electrophilic substitution at the *meso*-positions in the same order. Metals such as Sn(IV) on the other hand, tend to bring substitution to the β -positions. This difference in reactivity can be observed in the electrophilic substitutions shown in Scheme 1-2.¹⁸ The Vilsmeier reaction ($POCl_3$, DMF) is known to formylate preferably at the *meso*-position when the porphyrin is complexed to copper (Cu).¹⁶ Bromination on the other hand occurs preferably at the β -position when the porphyrin is complexed to Sn(IV) or is uncomplexed.²⁶

The porphyrins are not limited to reacting in the common electrophilic aromatic substitution manner that has been discussed thus far. Figure 1-5 shows that there are two double bonds that are conjugated, but are not a part of the aromatic system. In other

words, these two "cross-conjugated" double bonds can be removed without disturbing the aromaticity of the ring. Chlorins and bacteriochlorins are produced, following removal of either one or both of these double bonds, respectively.¹⁷

One example is the reaction of carbenes with OEP. Carbenes, such as those generated from ethyldiazoacetate,¹⁸ tend to form cyclopropane rings by addition to the β -double bonds of porphyrins. Some examples of Diels-Alder reactions have been reported to occur with the cross-conjugated double bonds.¹³ The double bonds can act either as the dienophiles or in concert with vinyl substituents to form the diene (Scheme 1-3).

Substituents also affect the reactivity of the porphyrin ring. As mentioned earlier, porphyrins can be functionalized in many ways, and this can be used to effect changes in the reactivity of the porphyrin. For example, the cross-conjugated double bonds of tetraphenylporphyrins will react only to a small degree with the most reactive dienes in a Diels-Alder reaction (Scheme 1-3).¹⁹ However, if tetrakis(pentafluorophenyl)porphyrin is used then the Diels-Alder reaction occurs much more readily.²¹ A similar phenomenon is observed when porphyrins are reacted with 1,3-dipole.²⁰ This will be discussed in greater detail in Chapter two.



Scheme 1-3. Reactions of the Cross-Conjugated Double Bonds of Porphyrins.

1.1.4 Optical Absorption Spectra of Porphyrins

One of the main properties of porphyrins is their ability to absorb light, and then transform this light energy for another use. Because of this property a great deal of study has been devoted to the light absorption patterns of porphyrins.²¹

There are two main regions of absorption in the UV-visible spectrum of a porphyrin. The first is a very strong absorption between 390 nm-425 nm known as the Soret band, and the second consists of a series of weaker bands between 480 nm-800 nm called the Q-bands.²² The intensity and exact absorption maxima can reveal significant information regarding the structure and nature of the porphyrin system. Usually, there

are four Q-bands for non-metallated porphyrins and two for the metal porphyrin complexes or the form with the inner pyrrole nitrogens protonated.²⁴ Shown in Figure 1-7 are some representative UV-visible spectra of porphyrins. The etio-type spectrum (see Figure 1-7) is seen in porphyrins where the β -substituents are all alkyl groups.²⁴ The rhodo-type spectrum (see Figure 1-7) occur when electron-withdrawing groups are at the β -position³⁰. The oxo-rhodo spectrum (see Figure 1-7) is observed when electron-withdrawing groups are on opposite pyrrole units.³⁰ The phyllo-type spectrum (see Figure 1-7) is observed when some of the β -positions are left unsubstituted, or the *meso*-positions are filled.²⁴

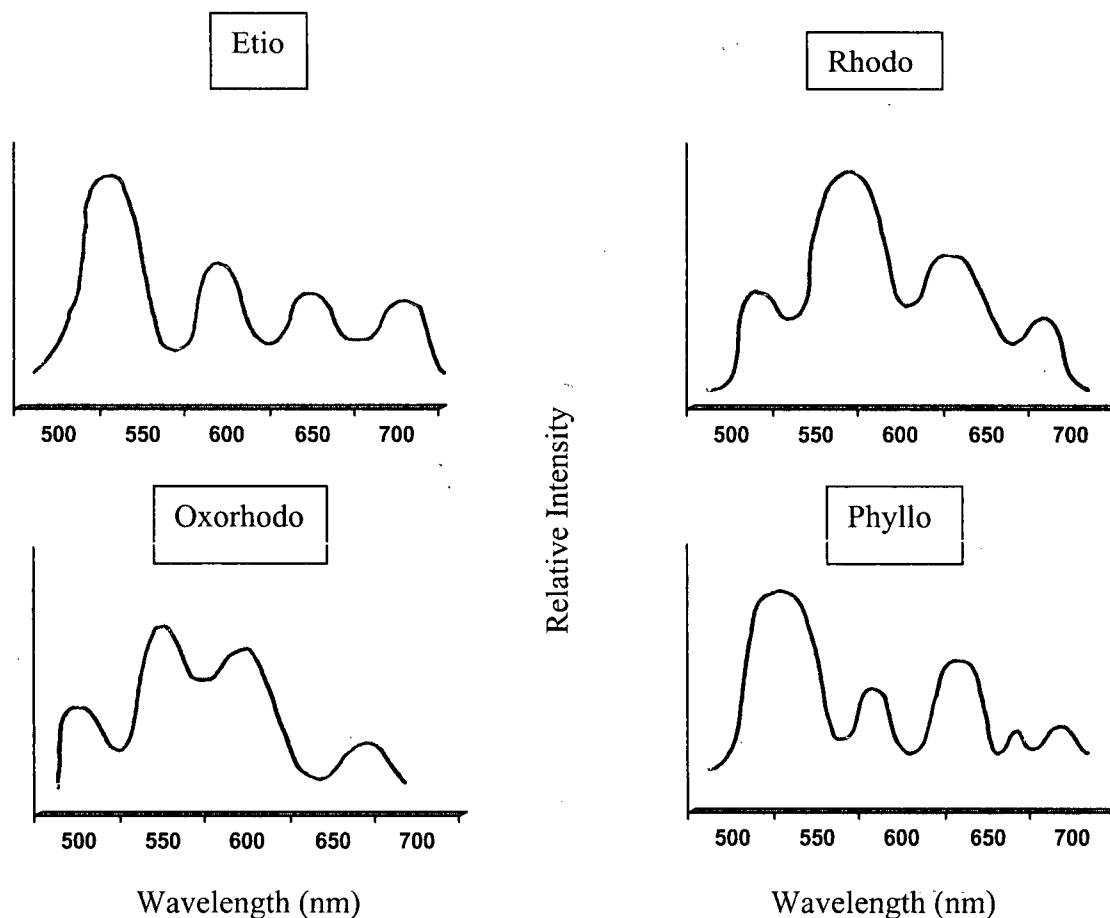


Figure 1-7. Representative Porphyrin Spectra.

The ratio of the intensity of the two Q-bands in a metal porphyrin complex can also reveal useful information.

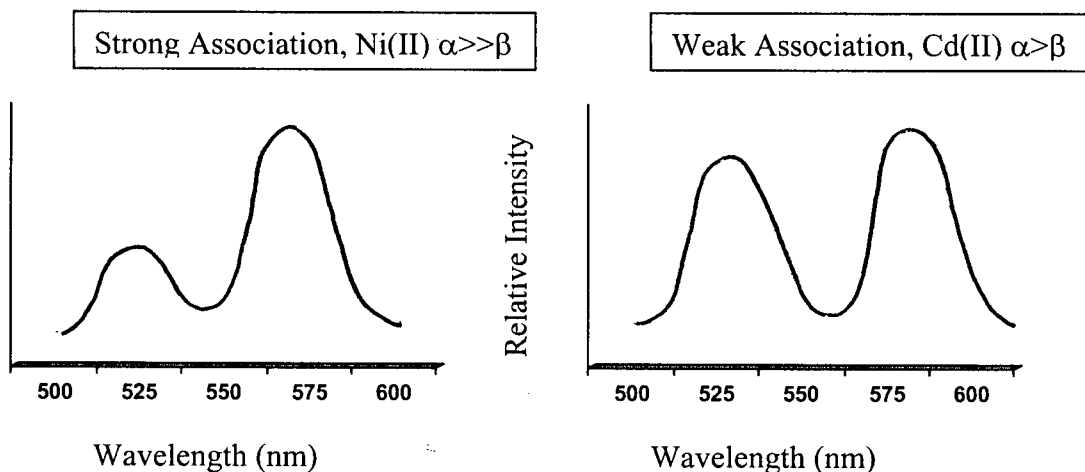


Figure 1-8. UV-Visible Spectra of Metalloporphyrins.

This ratio (Figure 1-8) can be used to qualitatively assess the strength of the metalloporphyrin association.³⁰ If the α -band (the higher intensity band) is much larger than the β -band (the lower intensity one), this shows qualitatively that the metal porphyrin complex is a stable one. The strength of this metal porphyrin interaction refers to how easily this complex may be de-metallated.

Chlorins and bacteriochlorins exhibit UV-visible spectra that are markedly different from those observed for porphyrins. For both types of compounds, the highest wavelength Q-bands are much more intense relative to the Soret band, and shifted to a lower wavelength (red-shifted) than those of the corresponding porphyrin. Two examples are shown in Figure 1-9. An excellent discussion of the theory behind the UV spectra of porphyrins, chlorins and bacteriochlorins is given in "The Porphyrins".²³

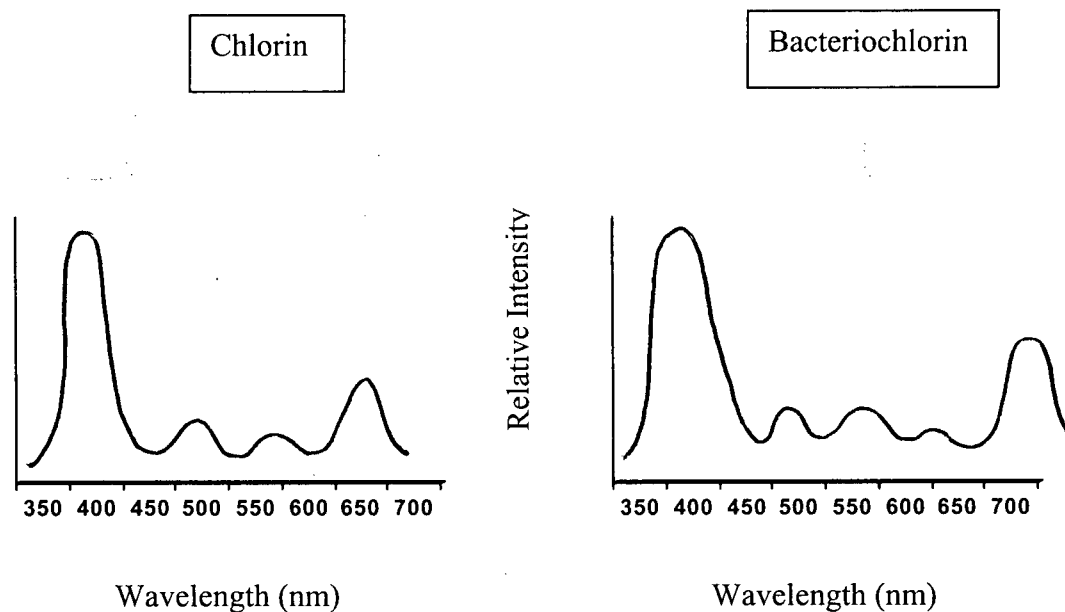


Figure 1-9. UV-Visible Spectra of Chlorin and Bacteriochlorin.

1.1.5 Synthesis of Porphyrins

Porphyrins are produced both by natural and synthetic methods. A single reaction pathway is found for the synthesis of most naturally occurring porphyrins, chlorins and bacteriochlorins found in nature. Methods for synthesizing tetrapyrroles in a laboratory setting are diverse.

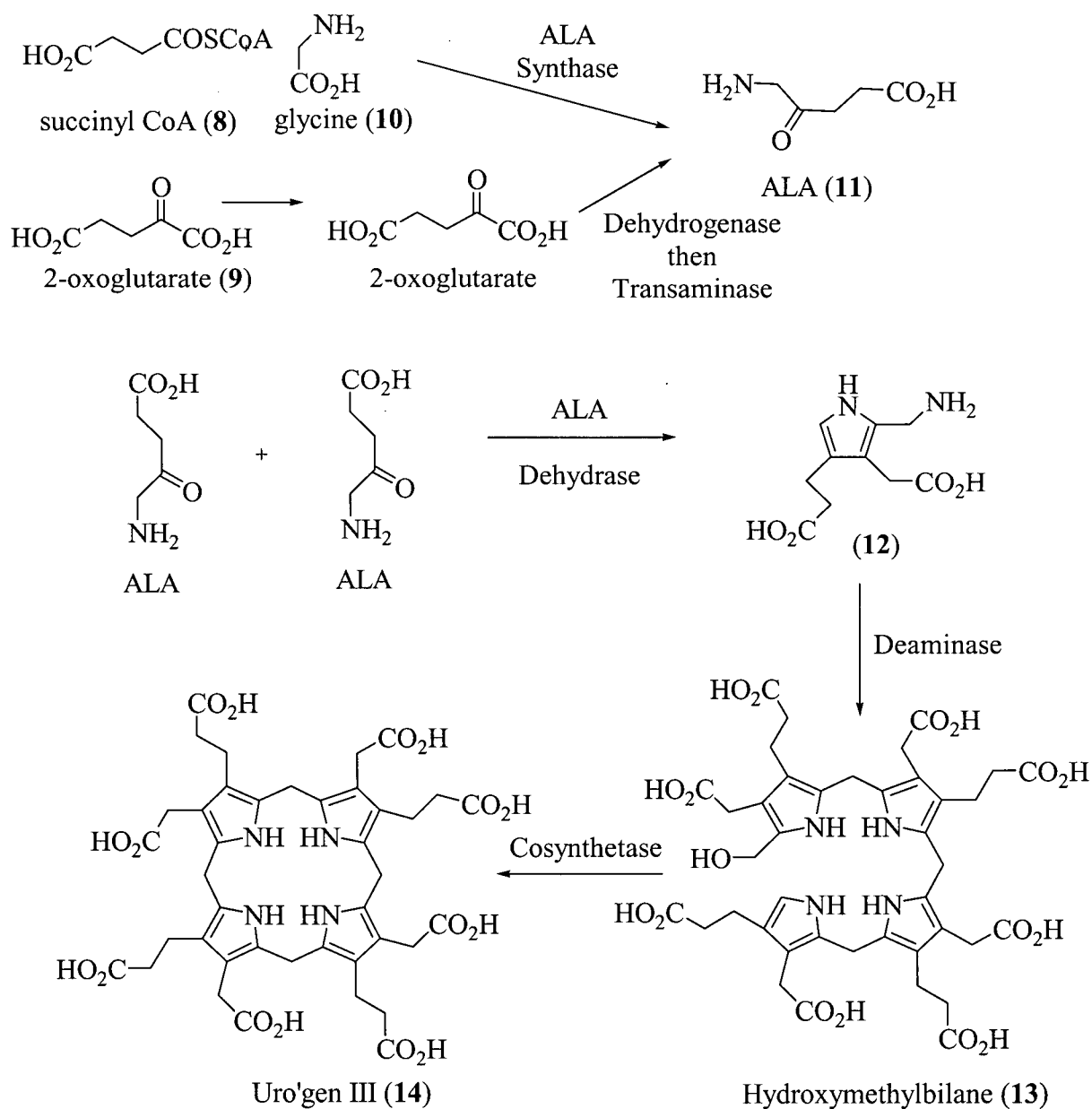
Naturally occurring porphyrins are ultimately synthesized from 5-aminolaevulinic acid (ALA) (11) as shown in Scheme 1-4. ALA self-condenses to form porphobilinogen (PGB) (12), which condenses with four other PGB molecules to form uroporphyrinogen III (uro'gen III) (14). This is accomplished with the help of two enzymes, PGB deaminase and uro'gen cosynthetase.³² Heme, chlorophyll and vitamin B-12 are all produced from uro'gen (III).²⁴ Oxidation of uro'gen (III) to form the porphyrin does not occur until all peripheral manipulations have been accomplished.²⁵ In the case of chlorophyll, the reduction to the chlorin is catalyzed by protochlorophyllide reductase

after all functional group manipulation and metal insertion are complete.²⁶ Vitamin B-12 is functionally a corrin (Figure 1-1), but it has been found that its synthetic pathway also includes uro'gen (III) as an intermediate.²⁷ Uro'gen (III) is found to be a key intermediate in the synthesis of many tetrapyrrolic macrocycles that occur in nature.³⁹

Synthetic porphyrins can be classified into two main groups; those where the β -positions are fully occupied by alkyl groups such as octaethylporphyrin (Figure 1-6), and those where the *meso*-positions are fully occupied such as in tetraphenylporphyrin (Figure 1-6). Both of these species can be synthesized by methods that allow for relatively large-scale reactions with reasonable yields.¹⁵

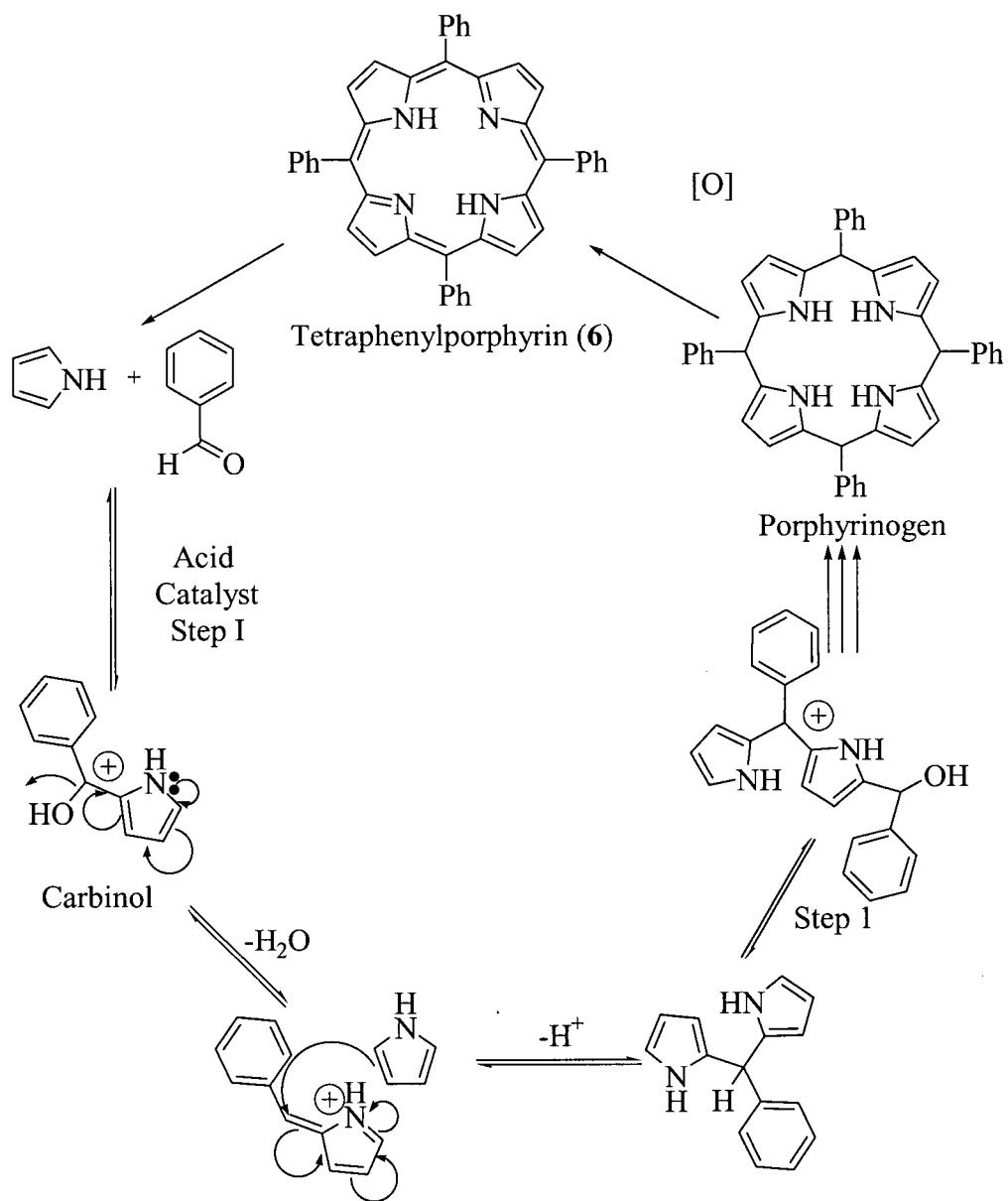
Meso-substituted porphyrins are usually synthesized by the condensation of an alkyl or aryl aldehyde with pyrrole.²⁸ Rothmund first reported that heating benzaldehyde and pyrrole in pyridine under high pressure at 150°C gave the desired porphyrin.²⁹ These conditions were very harsh, and subsequent improvements have been reported. Alder and Longo reported that refluxing the desired pyrrole and benzaldehyde in propionic acid in air (oxygen in the air being used as the oxidant) gave significantly improved results.³⁰ Lindsey reported that using DDQ as an oxidant also improves the yield of the reaction.³⁰

The mechanism of condensation between pyrrole and benzaldehyde is known to proceed via acid catalyzed formation of an arylpyrrole carbinol (Scheme 1-5).³¹ The carbinol then loses water to form the corresponding cation, which then condenses with another pyrrole unit, this process continuing until the porphyrinogen is formed. The porphyrinogen is then oxidized to the porphyrin *in situ*. It is important to note



Scheme 1-4. Synthesis of Uro'gen III.

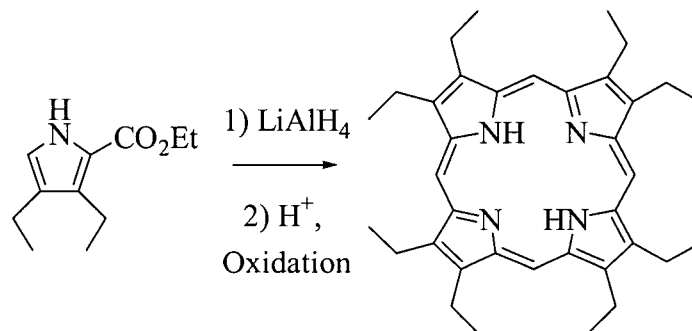
that these are the steps to the desired products, but as there are many other products, there must also be other processes taking place.



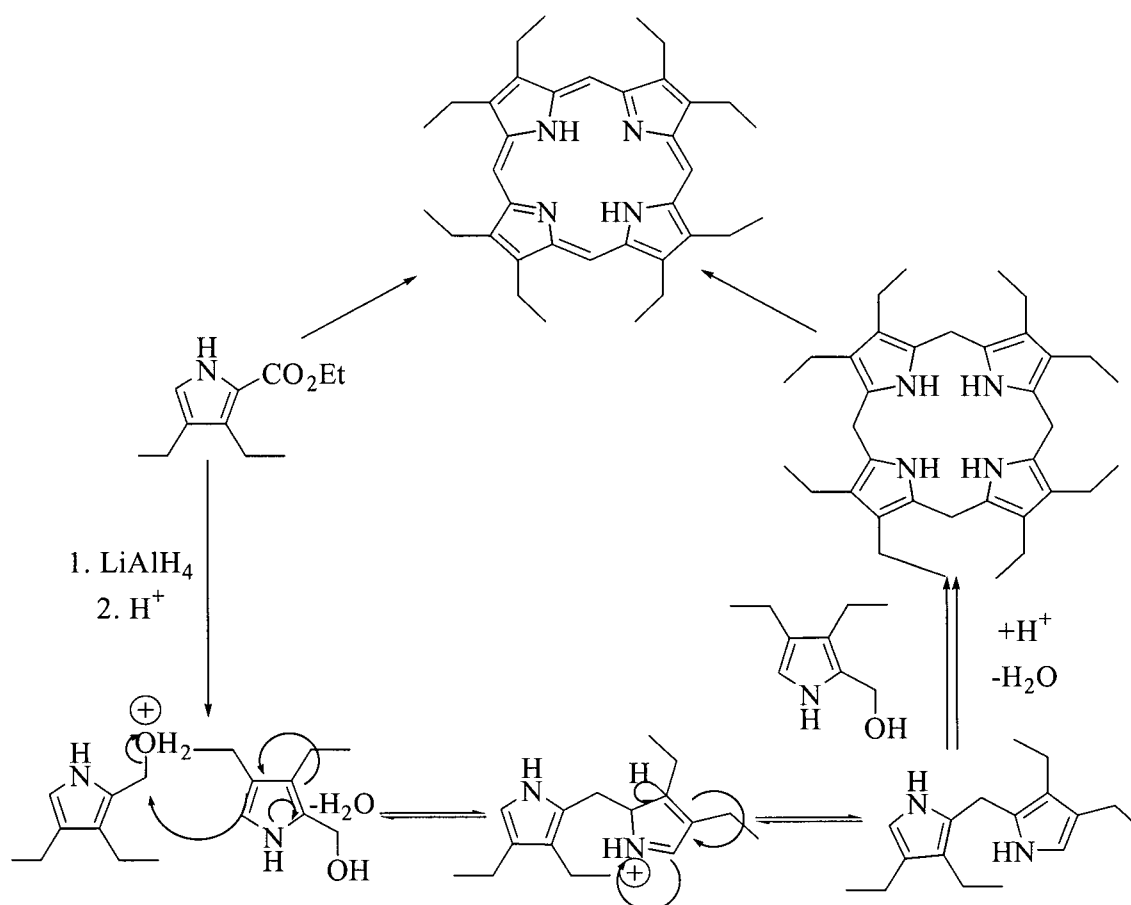
Scheme 1-5. Synthesis of Tetraphenylporphyrin (6).

The most common method for the synthesis of OEP is the reduction and subsequent cyclization of 2-ethoxycarbonyl-3,4-diethylpyrrole (Scheme 1-6).³² The mechanism of this reaction involves the reduction of the ester to an alcohol, followed by a condensation reaction between the alcohol and the pyrrole. This reaction sequence is

repeated until the porphyrinogen is formed, which is then oxidized to the porphyrin (Scheme 1-7).

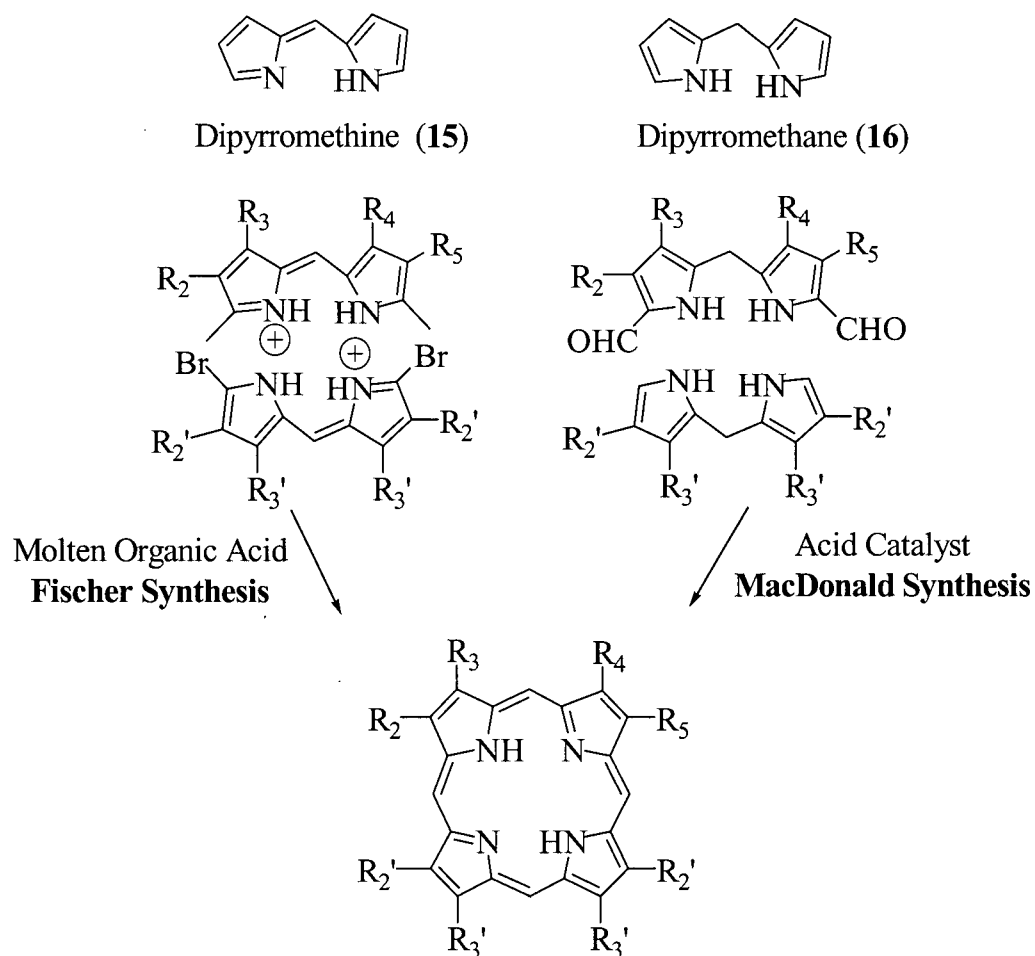


Scheme 1-6. Synthesis of Octaethylporphyrin (7).



Scheme 1-7. Mechanism for the Synthesis of Octaethylporphyrin.

Both methods mentioned above are used to make fully symmetrical porphyrins. There are also methods used to synthesize unsymmetrical analogues. One of these involves the use of the dipyrroles, dipyrromethenes (**15**) and dipyrromethanes (**16**) (Scheme 1-8). Fischer developed many methods for the use of dipyrromethenes as precursors to the porphyrins.³³ The MacDonald reaction involves the acid catalyzed condensation of an α -position di-formyl-substituted dipyrromethane with an α -position non-substituted dipyrromethane (Scheme 1-7).³⁴



Scheme 1-8. Porphyrins Synthesis from Dipyrrolic Precursors.

1.2 Photodynamic Therapy

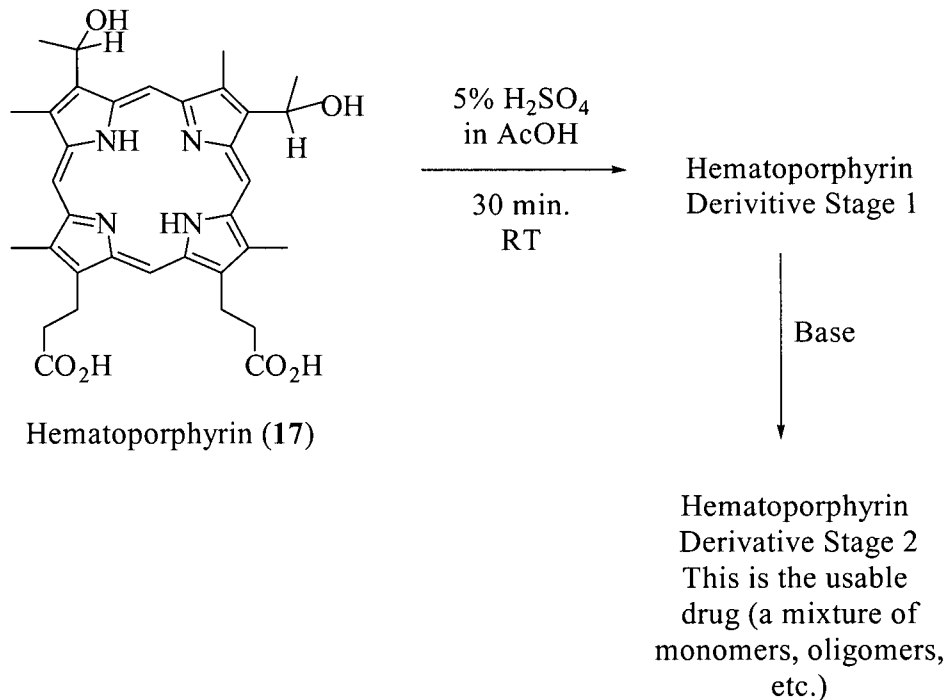
1.2.1 Introduction

Photodynamic therapy (PDT) is a minimally invasive procedure for treatment of diseases that involve rapid cell growth, such as cancer.³⁵ This procedure consists of two steps. First the photosensitizer is administered to the patient. Association of the photosensitizer with lipoproteins then occurs. Since rapidly dividing cells require more lipoproteins than normal cells, the drug will accumulate preferentially in rapidly dividing tissues. A dose of light of a particular wavelength is then administered to the patient's diseased area, activating the drug and thus destroying the tissue. Activation refers to the production of singlet oxygen from molecular triplet oxygen present, which is thought to be the active agent in PDT. Singlet oxygen undergoes many reactions with biological molecules. This will be discussed in more detail in Section 1.2.4. One benefit of this procedure is that the drug is only activated upon exposure to light of a particular wavelength, so only minimal damage occurs in surrounding tissue. The patient must wait for the drug to be metabolized and excreted before exposing themselves to sunlight because of its ability to make the skin sensitive to light.³⁶

The phototoxicity of porphyrins has been known for almost 100 years.⁴⁷ Meyer-Betz injected himself with 200 mg of hematoporphyrin derivative (HpD, Scheme 1-9) in 1913.³⁷ He experienced extreme photosensitivity for many weeks, including lesions on his skin, and other reactions to sunlight. Meyer-Betz was forced to cover every part of his body if he wanted to go outside during daylight. It wasn't until 1924 that Policard found that porphyrins accumulated in malignant tissues.³⁸ This combination of

phototoxicity and preferential accumulation in cancerous tissues, which are two of the fundamental properties of a photodynamic drug, was not fully exploited until 1974, when the first human trials for PDT began.³⁹

HpD, as well as with a purified form called Photofrin (II), have long been the most commonly used PDT agents.⁴⁰ Both of these are a combination of porphyrin monomers, dimers and oligomers that are formed upon the acid hydrolysis of hematoporphyrin (17).⁴¹ Molecules with improved characteristics for use as PDT drugs have since been developed. These will be discussed in detail in Section 1.2.5.



Scheme 1-9. Synthesis of Hematoporphyrin Derivatives.

1.2.2 Production of a Useful Photosensitizer

The characteristics of a useful PDT agent have been defined after many years of researching their properties. There are seven discussed below.⁴²

1. The PDT agent must be a pure compound with a reproducible synthesis.

The purity of the compound was one of the main drawbacks of the first generation of photosensitizers (e.g. Photofrin). They consisted of mixtures of many compounds where the active constituents are not known. It is important to know the exact composition of a drug because impurities may cause side effects that could otherwise be avoided.

2. The PDT agent must be activated at wavelengths between 650 nm-800 nm.

Human tissue is relatively transparent between these wavelengths, while at lower wavelengths it becomes less transparent (Figure 1-10).⁴³ This is important because light must penetrate the tissue before it can sufficiently activate the drug. Another consideration is that there is not sufficient energy present in light above 800 nm to produce the active component in PDT, singlet oxygen (see Section 1.2.4).

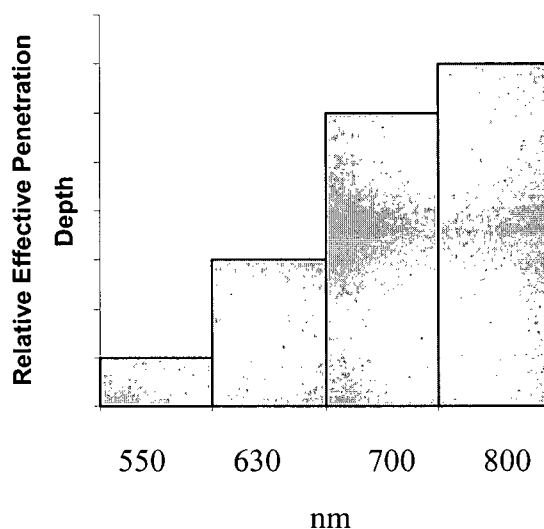


Figure 1-10. Absorption Intensity of Human Tissue.

3. The drug must exhibit minimal dark toxicity.

The advantage of PDT drugs is that they can be introduced generally and activated locally, so that non-diseased tissues are minimally affected. If the drug is active in the absence of light (dark toxicity), then this benefit is lost.

4. The drug must be an efficient photosensitizer.

The drug, when activated, must efficiently generate singlet oxygen (Section 1.2.4). Singlet oxygen is thought to be the active species in PDT, as the therapy is ineffective when done in the absence of oxygen.⁴⁴

5. The drug must localize specifically in diseased tissue.

This goal has not been attained as of yet, although, preferential accumulation in diseased tissue does occur with many PDT agents.⁴⁵

6. The drug must be efficiently metabolized.

If this were not the case, one would have to deal with the same situation as Meyer-Betz.⁴⁷ This was also one of the problems faced by some of the first generation photosensitizers.⁴⁶

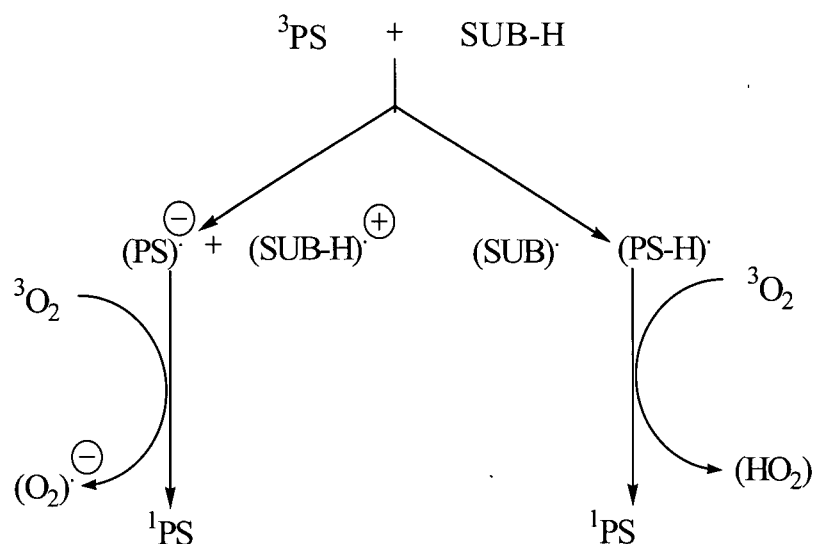
7. The drug must be soluble in the bodies' tissue fluids as to be easily administered and transported to disease areas.

Recently discovered PDT agents will be discussed in Section 1.2.5.

1.2.3 Mechanism of Photosensitization

How can one explain why Meyer-Betz became so sensitive to sunlight after injecting himself with hematoporphyrin derivative? The reason is that this and many other tetrapyrrolic macrocycles are photosensitizers. Photosensitizers (PS) absorb light, which excites the molecule to an excited triplet state (³PS). Tissue damage is caused by

reaction of the excited porphyrin with other molecules in the area (SUB-H) by either type one or type two processes.^{47,62} Type one processes can occur either by either oxidation of, or hydrogen abstraction from a molecule in the vicinity (Scheme 1-10). The



Scheme 1-10. Type One Reactions of a Photosensitizer.

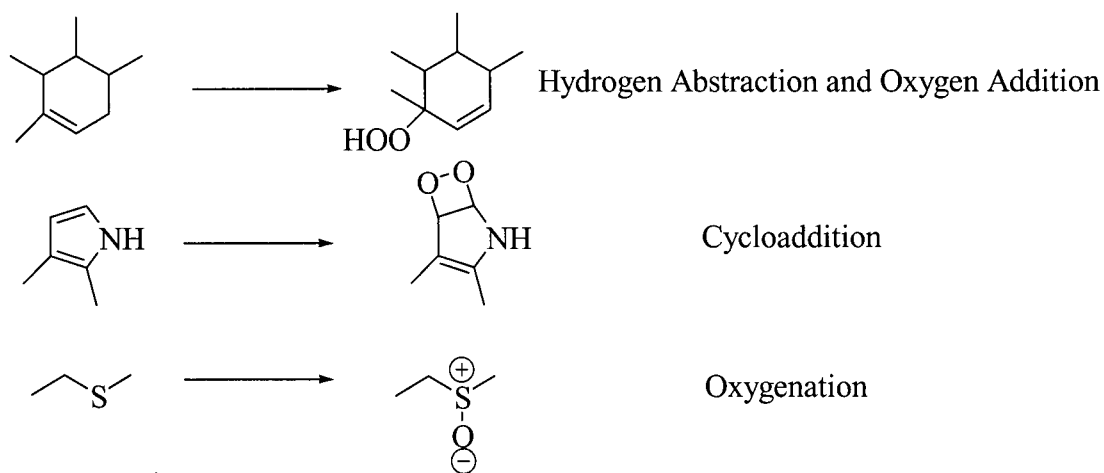
photosensitizer is then able to react with molecular oxygen to form reactive species, which can in turn generate radicals, and start a free chain radical reaction which could cause a great deal of damage in the body.^{61,48} Free radicals formed by hydrogen abstraction, can interact with oxygen to form many different oxidized products, which could in turn initiate free radical chain reactions themselves.^{61,62}

The other method by which photosensitizers can be harmful to tissue is through what is known as a type two reaction.^{61,62} In this process, the excited triplet photosensitizer, interacts directly with oxygen to form singlet oxygen. This is a spin allowed process, and thus is very efficient.^{61,62} Singlet oxygen is able to react with

biological molecules in a variety of ways.^{61,62} Since this process is thought to be the dominant one occurring during PDT, it will be discussed in more detail in Section 1.2.4

1.2.4 Singlet Oxygen Production

After a photosensitizer absorbs light, it can transfer this energy to an oxygen molecule to form singlet oxygen. This occurs by promotion of an electron in the ground state triplet oxygen to an excited state, forming singlet oxygen (Figure 1-11). There are two possible singlet states for oxygen. One is a high energy (37.5 kcal/mol) and short lived ($< 10^{-11}$ s), while the other is lower in energy (22.5 kcal/mol) and longer lived (4 μ s in water).^{61,62} The second state is thought to be the one involved in PDT. This high energy oxygen species can then undergo many reactions with functional groups in proteins, carbohydrates, DNA, etc. Some reactions of singlet oxygen are shown in Scheme 1-11. After a short period of time, these reactions, and similar ones, will cause irreparable damage to a cell.



Scheme 1-11. Reactions of Singlet Oxygen.

The process by which the energy transfers from light to oxygen is only one of many possible processes that can occur in the presence of a photosensitizer (Figure 1-11). The modified Jablonski diagram in Figure 1-11 gives a brief description of this process. The mechanism by which the energy is transferred from the photosensitizer to oxygen is not yet completely understood.

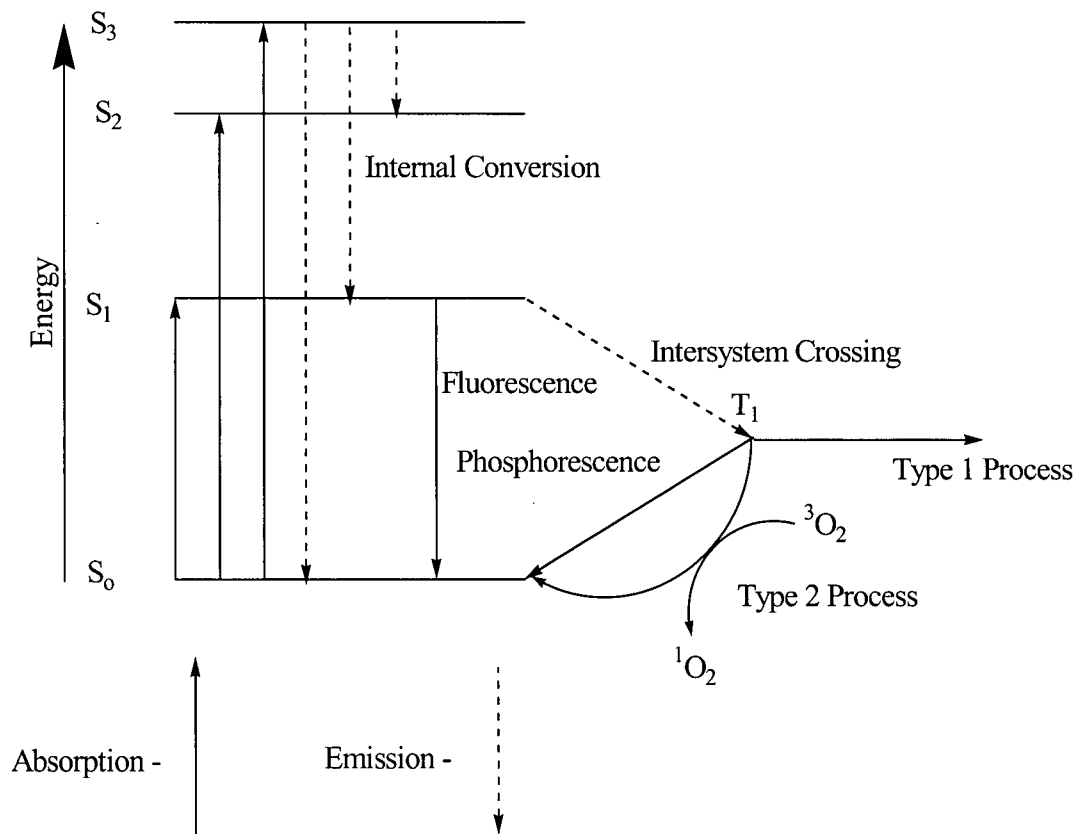


Figure 1-11. Modified Jablonski Diagram of a Photosensitizer.

Figure 1-11 shows a variety of processes that a photosensitizer can undergo once it has become activated. All of these involve the loss of energy to achieve the most stable ground state. Energy can be lost either as heat (internal conversion), or as light (fluorescence). Another option is a spin-forbidden process in which the first excited

triplet state (T_1) is formed (this process also occurs with the loss of heat). The triplet state is much longer lived than that of any singlet state, as all routes to the ground state are spin forbidden. Other possibilities include phosphorescence, type one or type two processes. The singlet state of oxygen is shown in Figure 1-12.

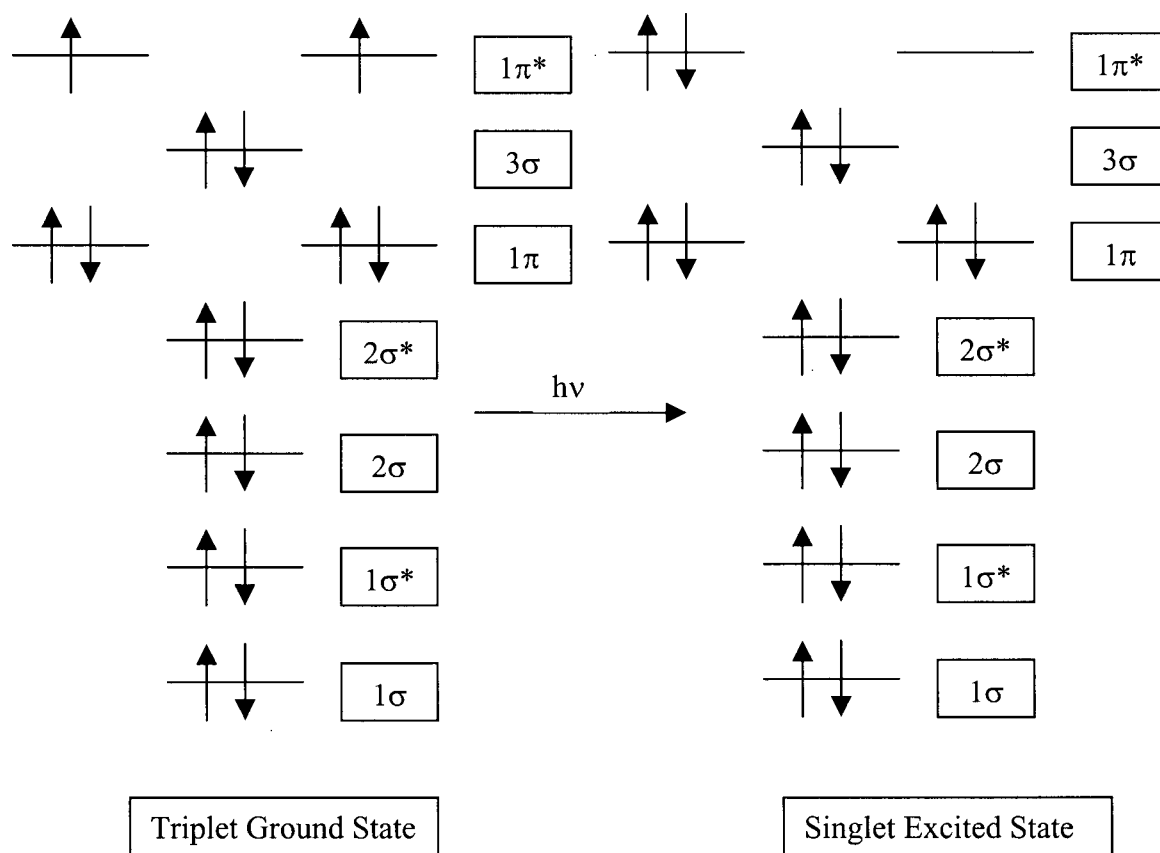


Figure 1-12. Singlet State of Molecular Oxygen.

A photosensitizer must have a long lived triplet state, as well as having the ability to transfer this energy to oxygen before phosphorescence occurs (Figure 1-11). The ability to transfer absorbed energy to oxygen through a non-radiative spin exchange is

quantified as the singlet oxygen quantum yield (Φ_{Δ}).⁴⁹ A few examples are listed in Table 1-1.

Photosensitizer	Solvent	Φ_{Δ} (wavelength)
Hematoporphyrin Derivative (HpD)	CH ₃ OD	0.74 (546+576 nm) ⁵⁰
<i>meso</i> -tetrakis(4- sulfonatophenyl)porphyrin (TPPS)	CH ₃ OD	0.70 (532 nm) ⁶⁰
Benzoporphyrin derivative monoacid ring a (BPDMA)	PB/1 % TX100 (1% octylphenol ethylene oxide condensate (TX 100) and phosphate buffer (PB))	0.79 (692 nm) ⁵¹
Chlorin e ₆	PB	0.75 (660) ⁶²

Table 1-1. Singlet Oxygen Quantum Yields.

1.2.5 Porphyrin Related Photosensitizers

There are a variety of ways to generate photosensitizers which have the qualities deemed necessary as discussed in Section 1.2.2. Photofrin has already been discussed but the more recent and effective compounds will be discussed in Section 1.2.5.

1.2.5.1 Core Modified Water-Soluble Porphyrins

Two of the core modified porphyrins (Figure 1-13) investigated for their photosensitizing ability are 5, 10, 15, 20-tetrakis(4-sulfonatophenyl)-21, 23-dithiaporphyrin (**18**) and 5, 10, 15, 20-tetrakis(4-sulfonatophenyl)-21, 23-

diselenaporphyrin (**19**).⁶⁷ These species were tested in response to the fact that the porphyrin 5, 10, 15, 20-tetrakis(4-sulfonatophenyl)porphyrin (TPPS₄) (Table 1-2) was found to accumulate in tumors almost selectively, but has been reported to be a neurotoxin.⁵² It was hoped that core modification would eliminate this neurotoxicity, while maintaining the photosensitizing properties.

The two core modified porphyrins **18** and **19**, have similar absorption spectra (Table 1-2). Their UV-Vis absorption spectra are analogous to that of a porphyrin, with the exception that the high wavelength Q-bands are significantly red-shifted (shifted to a higher wavelength), as compared to that of a porphyrin (Table 1-2). This is significant as human tissue is more transparent (Figure 1-10) at 695 nm than at the 630 nm absorption maxima of the porphyrin (Table 1-2).⁵³

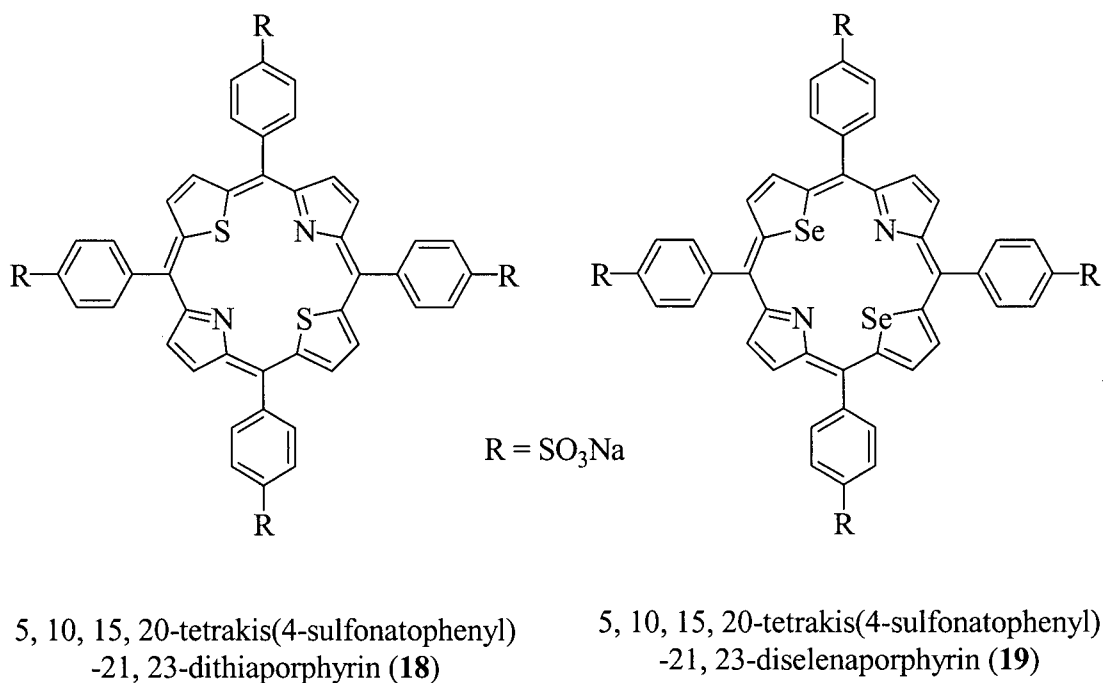


Figure 1-13. Core Modified Porphyrin Photosensitizers.

λ_{\max} nm ($\epsilon \times 10^{-3}$ cm ⁻¹ mol ⁻¹ L) in water					
Compound	Soret	Band IV	Band III	Band II	Band I
TPPS ₄ ⁵⁴	411 (464)	513 (15.5)	549 (7.0)	577 (6.5)	630 (3.9)
18	434 (190)	513 (19.3)	546 (5.5)	633 (2.0)	695 (4.0)
19	434 (221)	513 (22.4)	546 (6.2)	631 (2.2)	695 (4.5)

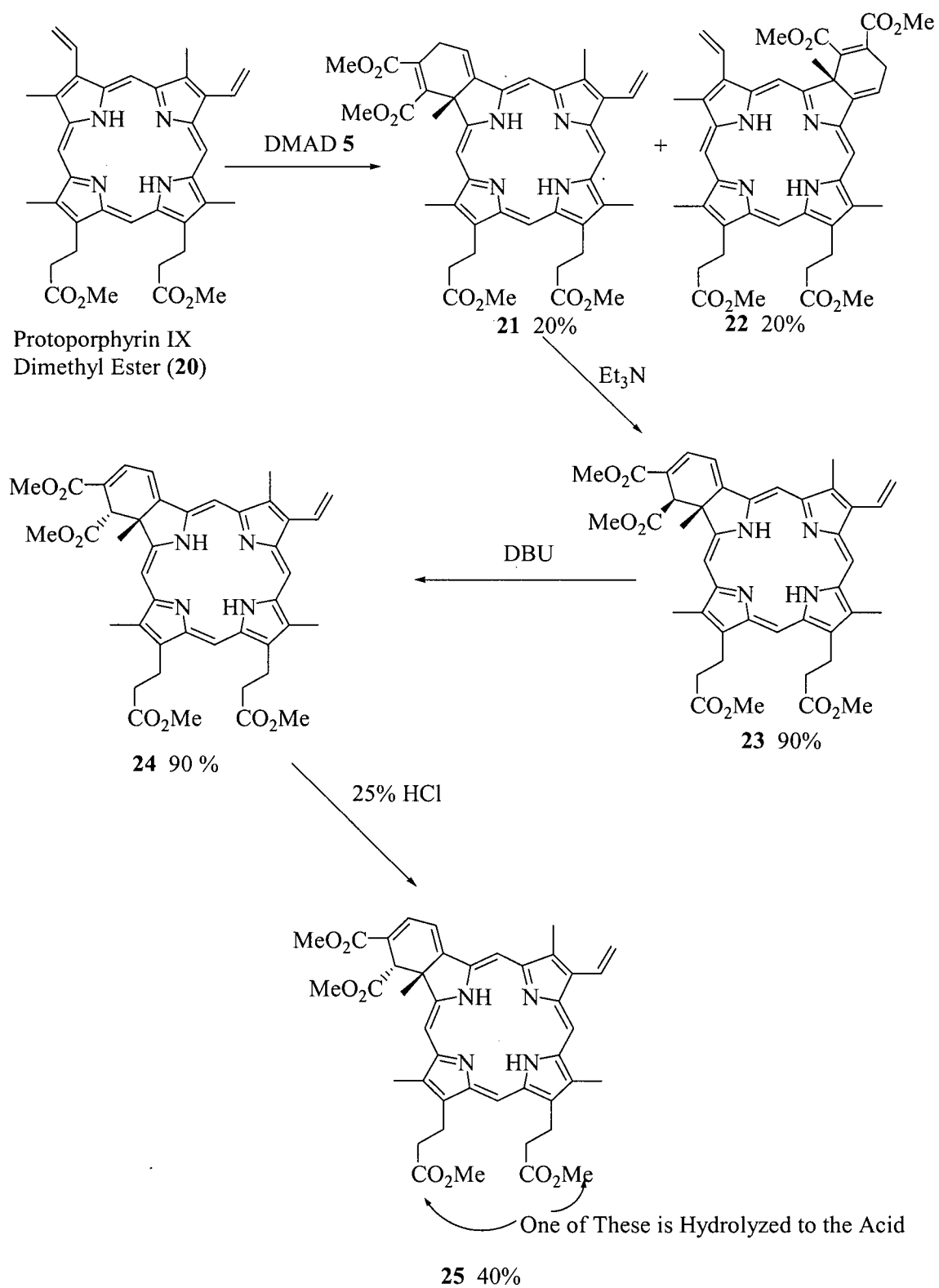
Table 1-2. UV-Vis Spectra Showing the Wavelengths of Maximal Absorption of (18) and (19) Compared to TPPS₄.

It was found that **18** causes significant tumor damage and no alterations to the skin,⁵⁵ in fact **18** was found to be a more effective tumor photosensitizer than chlorin e₆ (Figure 2-1), which has been used as a PDT agent for many years. No neurotoxicity was observed upon administration of **18** when PDT effective doses of were administered.⁵⁵ Compound **19** was not an effective photosensitizer.

1.2.5.2 BPDMA

The Diels-Alder reaction of protoporphyrin IX dimethyl ester (**20**) with dimethyl acetylenedicarboxylate gives a 1,4 diene benzoporphyrin adduct (**21**).⁵⁶ The 1,4-diene benzoporphyrin adduct, under strongly basic conditions, rearranges giving the conjugated 1,3-diene (**23**). The ester group on the carbon adjacent to that of the angular methyl is then isomerized with diazabicyclo[5.4.0]undec-7-ene (DBU) to form **24**. The final step is hydrolysis of the methyl esters giving BPDMA (**25**) (Scheme 1-12).⁵⁷

The purpose of forming the chlorin is to increase the intensity of absorption at long wavelengths. The most intensely absorbing Q-band in the UV-Vis spectrum of the 1,4-diene (**21**) is 666 nm, while the maxima for the 1,3-diene (**23**) is 688 nm.^{58, 77} This absorption is in the optimal range for tissue penetration (Figure 1-10).



Scheme 1-12. Synthesis of BPDMA.

Even with comparable electronic spectra, not all of the 1,3-diene analogues are equally efficient photosensitizers. **24** is not active, and **25** is five times more active than the diacid.^{76,77} Additionally, **25** is metabolized and excreted within 72 h,^{76,77} and has a high singlet oxygen quantum yield (0.78 in homogeneous solution, 0.46 *in vivo*).^{76,58} This drug has recently been approved in the United States for use in treating AMD (age-related macular degeneration).

The structure of **25** lends itself to the possibility of chemical modification so as to take advantage of the chlorin chromophore, while changing the physical properties of the drug. The free acid group can be functionalized in many ways to produce a wide variety of photosensitizers with different physical properties.

1.2.5.3 Zinc Tetraruthenated Porphyrin

Synthesis of novel "site specific photosensitizers" has been pursued.⁵⁹ PDT agents, to date, are not site-specific and cause cessation of cellular activity via damage to the entire cell. This can be undesirable because it is difficult to know what area of the cell the drug is acting on. Ideally, site-specific PDT agents will be more effective as only targeted cellular processes would be effected. μ -{*meso*-5-10-15-20-Tetra(4-pyridyl)porphyrin}-tetrakis-{bis-(bipyridine) chlororuthenium(II)} (**26**) has been found to associate strongly with DNA.⁶⁰ In the presence of DNA and oxygen **26**, efficiently photo-catalyzes the oxidation of 2'-deoxyguanosine.⁶¹ This reaction yields 8-oxo-2'-deoxyguanosine and 4-hydroxy-8-oxo-dihydro-2'-deoxyguanosine.⁷⁷ These are the products of a type two reaction where singlet oxygen was delivered specifically to the 2'-deoxyguanosine residue. Thus, *in vitro*, this is one example of a photosensitizer that reacts specifically with 2'-deoxyguanosine.

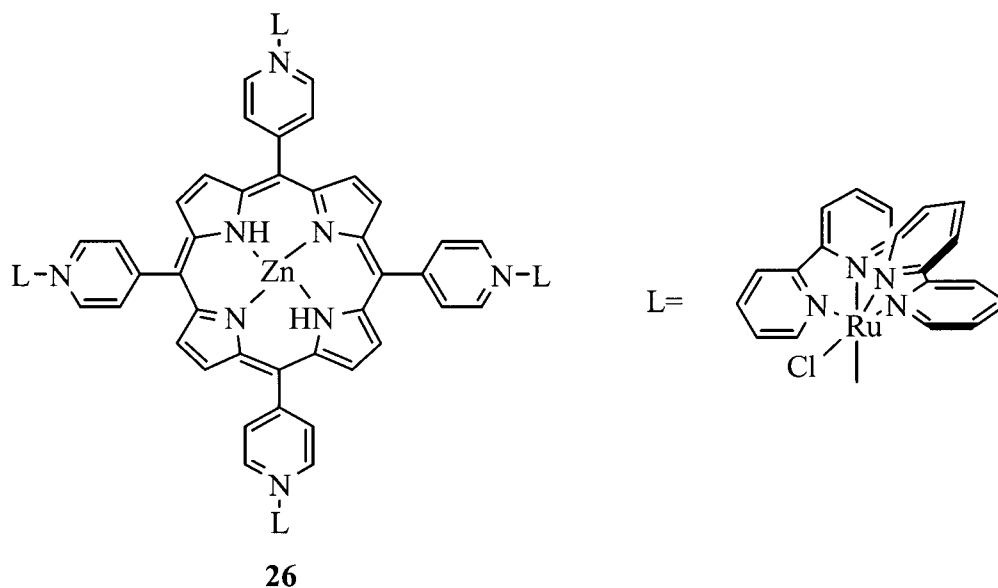


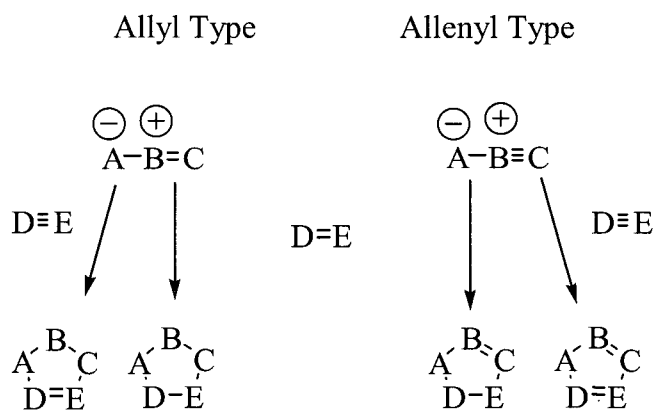
Figure 1-14. μ -{meso-5-10-15-20-Tetra(4-pyridyl)porphyrin}-tetrakis-{bis-(bipyridine)chlororuthenium(II)} (26).

1.3 1,3-Dipolar Cycloadditions

1.3.1 Introduction

The reaction between a “dipole” and a “dipolarophile” is a 1,3-dipolar cycloaddition (Scheme 1-13). The dipolarophile includes a π -bond, while the dipole includes at least three atoms with four electrons in three consecutive p-orbitals. These p-orbitals overlap to produce an allyl anion molecular orbital that is the reactive part of the molecule. A dipole, consists of a positively charged central heteroatom (usually oxygen or nitrogen, but can be sulfur or phosphorus) which compensates for the negative charge that is distributed evenly on the two terminal atoms. This results in a species with no net charge.⁶¹ Figure 1-15 depicts some of the resonance structures of allyl and allenyl type 1,3-dipoles. It is possible to show the positive and negative charges localized at the termini (Figure 1-15). This represents the “ambivalence” in the dipole.⁷⁸ Ambivalence

refers to the fact that the termini can be represented either as nucleophilic or electrophilic, depending on which resonance structure is observed.



Scheme 1-13. Reactions of the Two Types of 1,3-Dipoles.

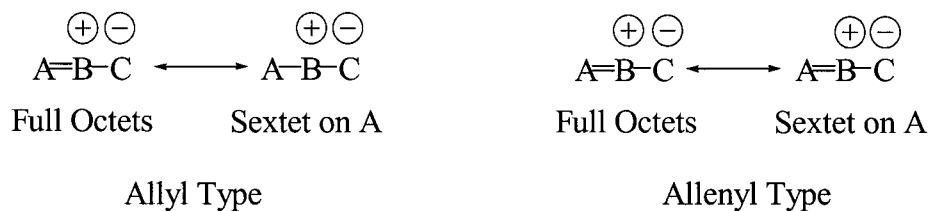


Figure 1-15. Resonance Structures of 1,3-Dipoles.

As shown in Scheme 1-13, the dipole can be that of a propargylic – allenyl, or an allylic form. The difference is that the allenyl type has an extra π -orbital perpendicular to the plane of the allyl anion molecular orbital.⁸² The central atom can be that of either group V or VI (e.g. nitrogen or oxygen) in the allyl type, but only of group

V (e.g. nitrogen) in the allenyl type. This is because only group V atoms are positively charged in their quaternary state.⁶¹

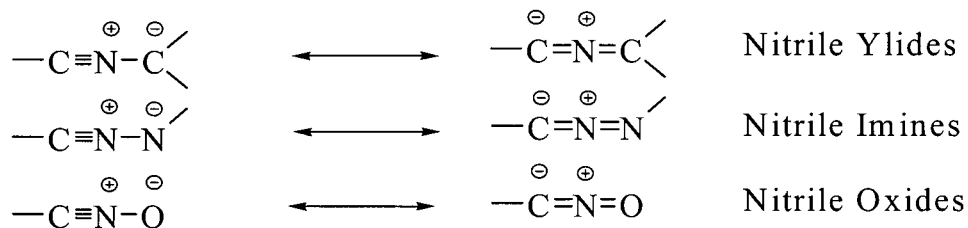
Keeping the description and requirements for the structure of 1,3-dipoles in mind, while also restricting oneself to discussing the first row elements only, a table of possible 1,3-dipoles can be formulated (Figure 1-15a). Even with the restriction of only using the first row elements, the possibilities are quite numerous (Figure 1-15a), and if one were to include higher row elements such as sulfur and phosphorus the diversity of this chemistry, becomes even more apparent.

1.3.2 A Short History of 1,3-Dipoles

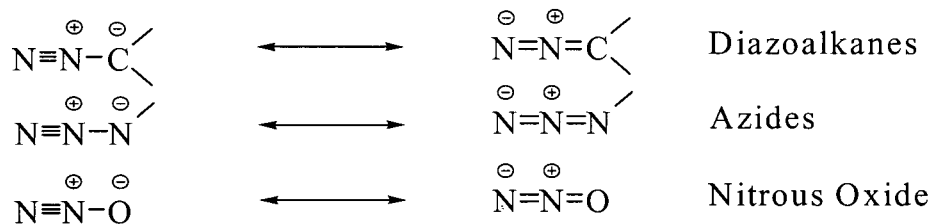
1,3-Dipoles as a species have been known since 1883,⁶² but up until 1958, when the classification shown in Figure 1-15a was conceived, only five cycloadditions with 1,3-dipoles had been described.⁶¹ The original 1,3-dipolar cycloaddition reaction was reported from the family of diazoalkanes.⁷⁹

Propargyl-Allenyl Type

Nitrilium Betaines

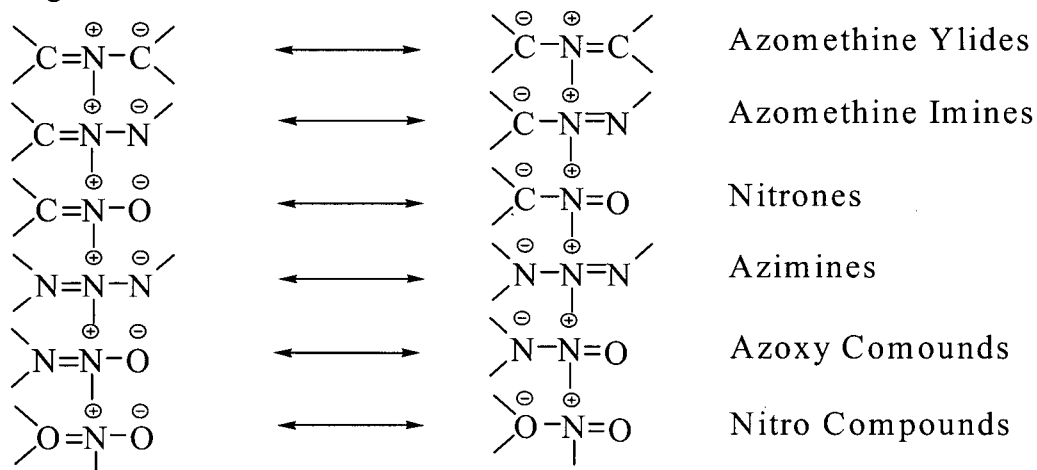


Diazonium Betaines



Allyl Type

Nitrogen as Central Atom



Oxygen as Central Atom

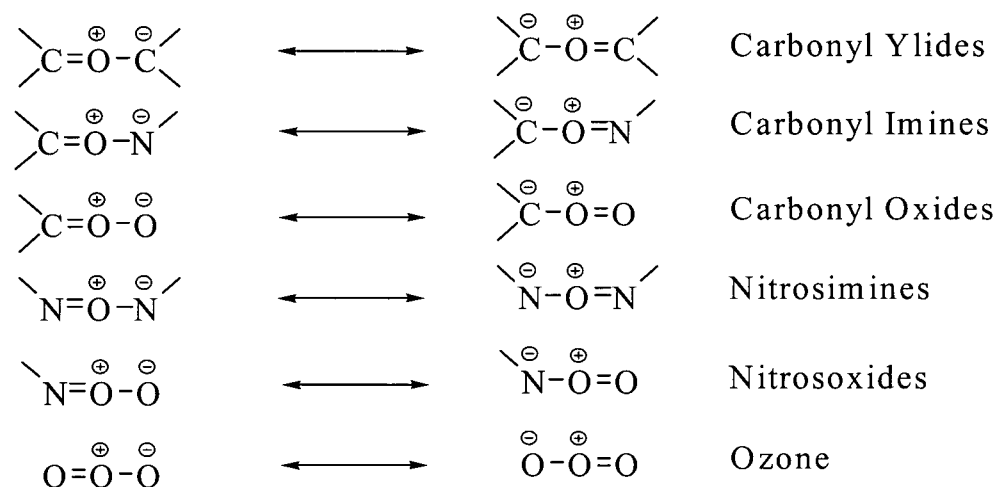
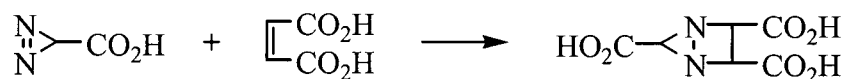


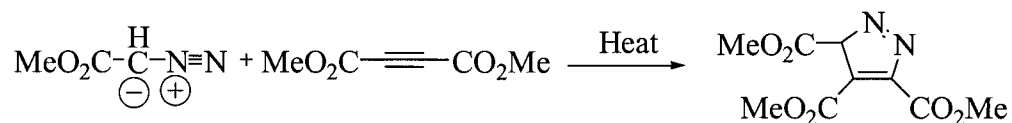
Figure 1-15a. Possible 1,3-Dipoles.

Eduard Buchner was reported to be the first person to accomplish a 1,3-dipole reaction.⁶³ Buchner reacted ethyl diazoacetate with unsaturated carboxylic esters which gave a cycloadduct and N₂ was expelled upon heating this cycloadduct (Scheme 1-14).⁸⁶



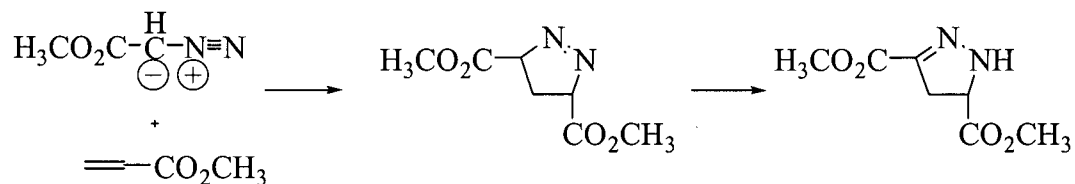
Scheme 1-14. Buchners' Proposed Mechanism of the Reaction Between Diazoacetic Acid and Fumaric Acid.

Buchner then reacted methyl diazoacetate with dimethyl acetylenedicarboxylate (DMAD) (Scheme 1-15), however no N₂ was expelled upon heating the resultant cycloadduct. Buchner realized in 1893 that the product was the pyrazole (Scheme 1-15).⁶⁴



Scheme 1-15. Reaction of Methyl Diazoacetate and Dimethyl Acetylenedicarboxylate.

Buchner then proceeded to react methyl diazoacetate with methyl acrylate, and this yielded a 2-pyrazoline, which had been formed in a rearrangement from the initially formed 1-pyrazoline (Scheme 1-16).



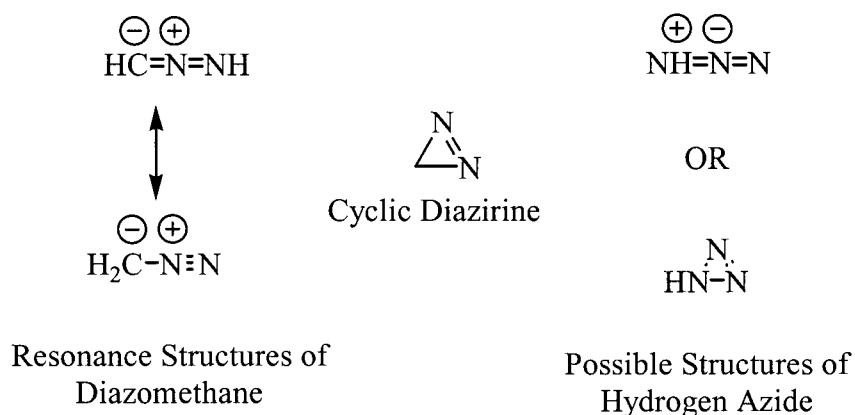
Scheme 1-16. Reaction of Diazoacetic Acid with Methyl Acrylate.

1.3.2.1 Diazomethane

Von Pechmann synthesized diazomethane in 1894.⁶¹ Pechmann reacted diazomethane with dimethyl fumarate⁶⁵ and dimethyl maleate,⁶⁶ but assigned the incorrect structures. The structure of diazomethane, being linear or cyclic, was determined the 1930's using electron diffraction data.⁶⁹ The colourless cyclic diazine (Scheme 1-17) was synthesized in 1960, and as diazomethane is a yellow gas, this confirmed the structure of diazomethane as linear and not cyclic.⁶⁷

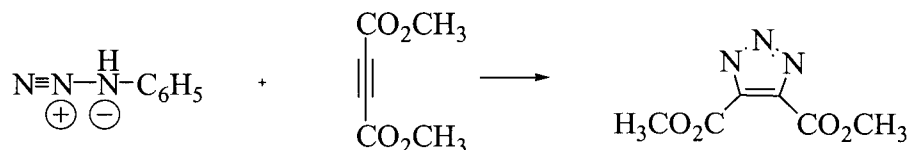
1.3.2.2 Azides

Azides have a history that is closely related to that of the diazoalkanes. Although not yet proven, much of the structural evidence points towards a linear, as opposed to cyclic structure,¹³ as for the aliphatic diazo compounds (Scheme 1-17).⁶⁸ Unlike the structure for diazomethane, the cyclic structure for the azide has not been ruled out (Scheme 1-17). The bulk of the structural evidence comes from the reactivity of the azide⁶⁹ and ¹⁵N labeling experiments as reported by Clausius and Weisser.⁷⁰



Scheme 1-17. Structures of Diazomethane and Hydrogen Azide.

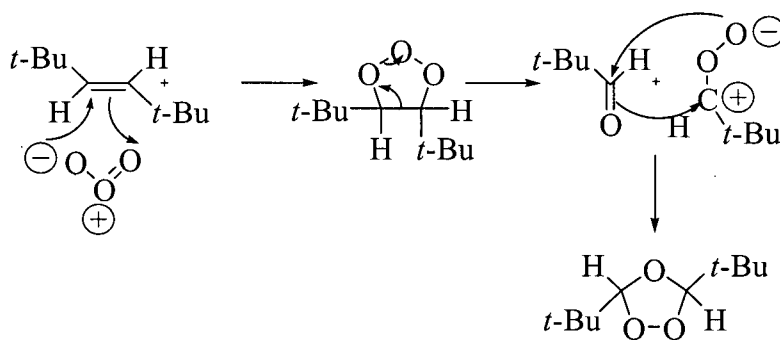
Michael was the first to report the reaction of phenyl azide with dimethyl acetylenedicarboxylic acid ester, and realized that this reaction was closely related to Buchners' reaction (Scheme 1-18).⁷¹



Scheme 1-18. Reaction of Phenyl Azide with Dimethyl Acetylenedicarboxylate.

1.3.2.3 Ozone

Ozone can be used as a reagent for the cleavage of double bonds.⁷² The mechanism of the reaction between ozone and a double bond has been a source of a great deal of controversy. Criegee in 1953 did much work towards elucidating this mechanism, and theorized that it involved a 1,3-dipolar cycloaddition, a 1,3-dipolar cycloreversion, and a 1,3-cycloaddition sequence (Scheme 1-19).^{73,61} The 1,2,3-trioxane structure of the intermediate ozonide was established in 1966 by Bailey *et al.* using tert-butyl groups and establishing their equivalence using NMR.⁷⁴



Scheme 1-19. The Criegee Mechanism for Ozonolysis.

Still debates continued over the identity of the intermediates in the reactions of ozone. The carbonyl oxide was initially thought to be the zwitterionic intermediate (Scheme 1-19). The correct structure of the intermediate was finally established as the carbonyl oxide capable of syn, anti – isomerism in 1975.⁷⁵ This structure is analogous to that of the azomethine oxide, which was originally reported in 1918.⁶¹ The mechanism of ozonolysis is still contentious. In a recent paper the occurrence of a 1,3-dipole reaction in the ozonolysis mechanism was refuted by Schank et al.⁷⁶

1.3.2.4 Nitrile Oxides

The history of nitrile oxides follows the discovery of formonitrile oxide and benzonitrile oxide. Gay-Lussac and Liebig first reported the former, while Werner and Buss first synthesized benzonitrile oxide in 1894.⁷⁷ Nitrile oxides have been found over the years to be one of the most reactive of the 1,3-dipoles, and not only react with a variety of dipoles and heterodipolarophiles, but also dimerizes to form furoxans.⁷⁸ This competing dimerization was found to be slowed considerably by 2,6-disubstitution on the aromatic ring of the benzonitrile oxide,⁷⁹ and with this di-substitution, many of these 1,3-dipoles are stable even at *r.t.*.

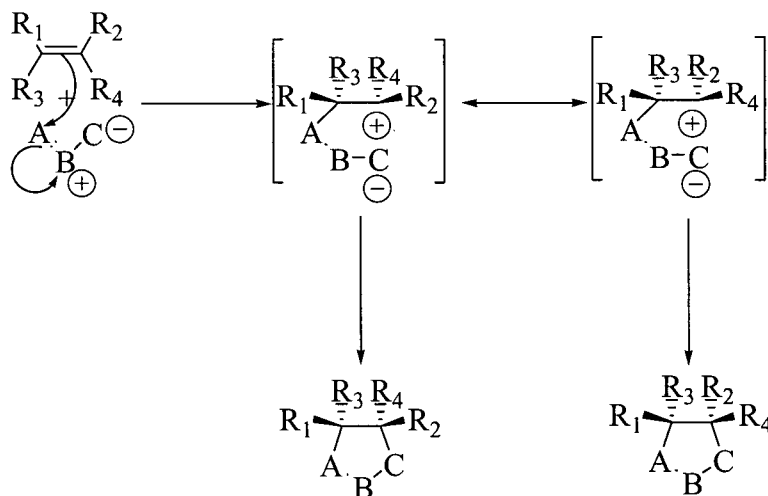
The number of uses of nitrile oxides in 1,3-dipolar cycloaddition chemistry is rapidly growing. One use is a method to introduce isoxazole or 2-isoxazolines into a molecule with good control over its regio- and stereochemistry. Often nitrile oxides are used in natural product synthesis.⁸⁰ In many instances no other reactions could be used to form the isoxazole or 2-isoxazoline.

1.3.3 Mechanism and Reactivity of 1,3-Dipoles

Section 1.3.3 of the thesis will describe both the mechanism of the 3 + 2 cycloaddition of 1,3-dipoles and the theory behind the observed reactivity.

1.3.3.1 General Description of Mechanism

The main controversy surrounding the mechanism of 1,3-dipolar cycloadditions is whether or not these reactions are concerted. The mechanism of reaction of a 1,3-dipole reaction is generally thought of as a suprafacial cycloaddition of the 3 p_z orbitals from the dipole to the 2 p_z orbitals of the dipolarophile. Woodward-Hoffman rules predict that cycloadditions will be thermally allowed if it proceeds by a concerted mechanism. A concerted mechanism provides rationale for the observed stereoselectivity of these 1,3-dipolar reactions.⁸¹ In other words, *cis*-1,2-disubstituted dipolarophiles give *cis*-substituted pentacycles, and *trans*-1,2-disubstituted dipolarophiles give *trans*-substituted



Scheme 1-20. Non-concerted 1,3-Dipolar Cycloaddition Mechanism.

pentacycles.¹⁰³ A few exceptions do exist and were observed because of the lack of stereoselectivity observed in the product (Scheme 1-20). Examples of these will be discussed in Sections 1.3.4.1-1.3.4.5. The mechanism of 1,3-dipolar cycloadditions is not synchronous.⁸² This means that the degree to which each of the new bonds are formed in the transition state is not the same.

1,3-Dipolar cycloadditions are said to proceed via "early transition states".⁶¹ Thus the transition state occurs early along the reaction coordinate of an activation energy diagram (Figure 1-16). This has the effect of making the transition state "reactant

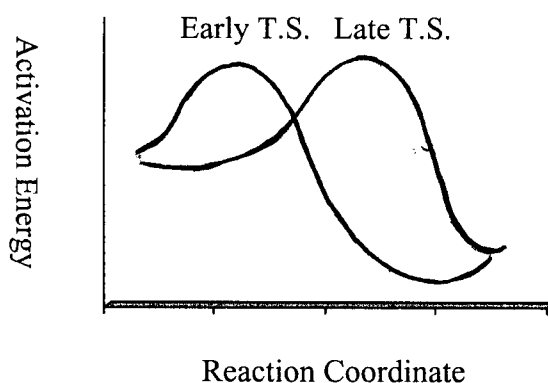
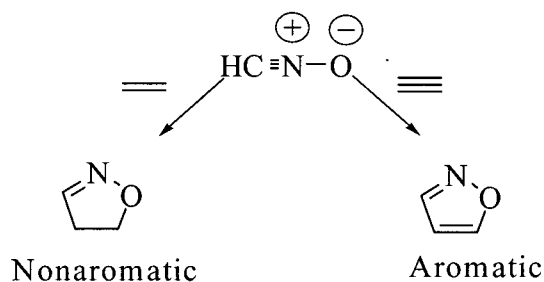


Figure 1-16. Activation Energy Diagram of Early and Late Transition State (T.S.) like",⁸³ while a late transition state is referred to as "product like". The Hammond postulate,¹⁰⁷ states that the transition state structure will be more similar in structure to the species that is energetically closer to it.

The calculation of the energies of reaction between fulminic acid and ethylene and acetylene provides some evidence of the early transition state.⁸⁴ The heat of reaction is much lower for the isoxazole than it is for the 2-isoxaline as determined by *ab-initio* calculations.⁸⁵ This is rationalized, as the aromatic system isoxazole is more stable



Scheme 1-21. Reaction of Fulminic Acid with Acetylene and Ethylene.

than the non-aromatic 2-isoxaline (Scheme 1-21).¹¹⁵ The calculated activation energies for both the reactions are similar.¹¹⁵ This would suggest, according to the Hammond postulate, that the transition state of isoxazole does not benefit from the aromatic stabilizing effect as much as would be expected if the reaction had a late transition state.¹³¹

Early transition states of 1,3-dipole reactions are observed as advantageous in the Perturbation Molecular Orbital (PMO) theory. The PMO theory states that as two molecules approach one another, mutual perturbation consists of three terms;⁸⁶

1. Closed shell repulsion stems from the interaction of filled orbitals.
2. Coulombic forces can be repulsive or attractive depending on the polarities of the reactant pair.
3. The “second order perturbation term” consists of attractive interactions between all the occupied and unoccupied MOs of the reactants as long as these orbitals are of the correct symmetry.

PMO theory is most often used to compare reaction sequences and since terms one and two are considered constant within a series, only the second order perturbation term needs to be considered.⁶¹

This process can be further simplified when one considers that the highest occupied molecular orbital (HOMO) and lowest unoccupied molecular orbital (LUMO) of the reacting species have the lowest energy separation, and should therefore contribute most to the second order perturbation term.¹¹² This enables one to consider solely the frontier molecular orbitals (FMO) when discussing the differences in activities in a series of reactions. The energies of these orbitals, as well as their orbital coefficients, are determined from various theoretical methods.⁶¹ Transition states can be extrapolated from the first differential reaction element as early transition states (Figure 1-16) allow prediction of reactivity for a wide range of processes.¹¹⁸

Sustmann used FMO description to categorize 1,3-dipolar cycloadditions into three groups, type one, two and three reactions.⁸⁷ These assignments are based on the predominant FMO interaction.

Type one reactions are characterized by the LUMO of the dipolarophile interacting with the HOMO of the dipole.¹²⁰ This is also referred to as an "HO controlled" reaction (Figure 1-17). Figure 1-17 shows the symmetry allowed molecular orbital interactions. Figure 1-17 also shows the lowest energy (solid arrow) and higher energy symmetry allowed interactions (dotted arrow). The lowest energy gap represents the interaction that is most likely to lead to a reaction, in this case an HO controlled interaction.

An HO controlled reaction will be accelerated by an electron donating group (edg) on the 1,3-dipole, and an electron withdrawing group (ewg) on the dipolarophile. The reason is that as electrons are donated into the HOMO of the dipole it becomes less

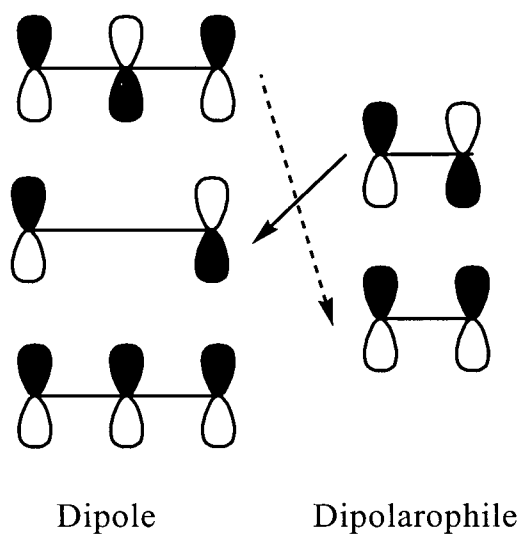


Figure 1-17. Symmetry Allowed Interactions of Type One 1,3-Dipolar Cycloadditions.

stable, and rises in energy towards the LUMO of the dipolarophile. On the other hand, ewgs on the dipolarophile will lower the energy of the LUMO towards the HOMO of the dipole.

The HOMO and LUMO energies of the dipolarophiles can be varied by adding electron withdrawing or donating substituents. Figure 1-18 shows how the energies of the MOs are affected by different substituents. The cases where the HOMO energy is increased will be the most useful for type one dipoles.

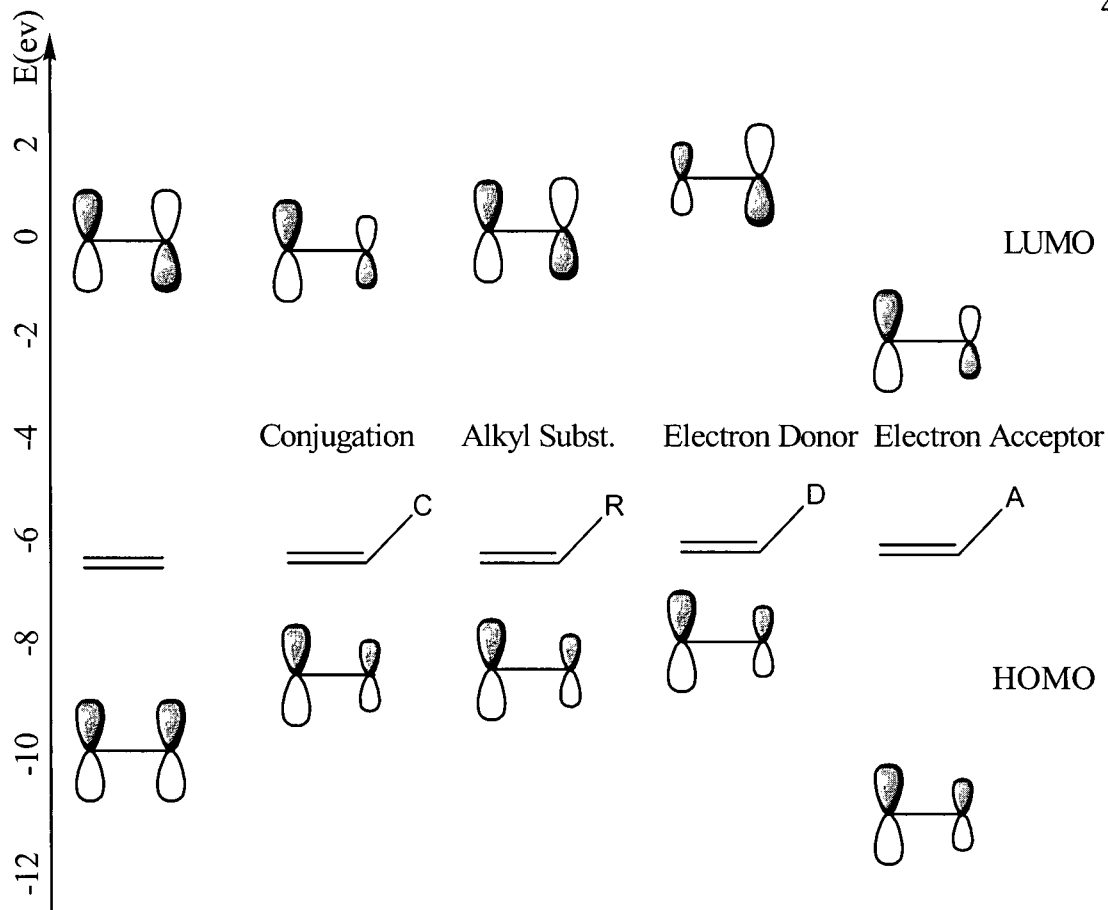


Figure 1-18. Change in Molecular Orbital Energy Upon Substitution.

The energies (see Fig 1-18) of the HOMO's are calculated from the ionization potentials, while the LUMO's were estimated by Houk.⁸⁸ The sizes of the lobes reflect calculated atomic orbital coefficients. These coefficients are determined by the orbital interaction responsible for the reaction. As seen in Figure 1-18, substituents not only exert an effect on the energy of the orbitals, but also on atomic orbital coefficients. These coefficients have been reported to effect the regiochemistry of a 1,3-dipolar cycloaddition,⁶¹ as the atom of the dipole with the largest molecular orbital coefficient associates with the atom of the dipolarophile also with the largest orbital coefficient.

1,3-Dipole	$\epsilon(\text{eV})$ HOMO	Method	$\epsilon(\text{eV})$ LUMO	Method
H ₂ CNCH ₂ Nitrile Ylide	-7.7	Estimate	0.9	Estimate
NNCH ₂ Diazomethane	-9.0	Photoelectron Spectroscopy	1.8	Estimate
H ₂ CNHCH ₂ Azomethine Ylide	-6.9	CNDO/2 Calculation ⁸⁹	1.4	CNDO/2 Calculation ¹¹⁸
H ₂ CNHNH Azomethine Imine	-8.6	Estimate	0.3	Estimate
H ₂ CCOCH ₂ Carbonyl Ylide	-7.1	Estimate	0.4	Estimate
H ₂ CONH Carbonyl Imine	-8.6	Estimate	-0.2	Estimate

Table 1-3. Frontier Molecular Orbital Energies of Parent 1,3-Dipoles (Type One).

The FMO energies of typical type one 1,3-dipoles are listed in Table 1-3.⁶¹ The energy of their HOMO's (estimated from experimental ionization potentials)⁹⁰ are high enough that the interaction with the LUMO of the dipolarophile with the HOMO of the

dipole is the dominant one. These dipoles are often referred to as nucleophilic because of their preference to react with electron deficient dipolarophiles. Some of these species will be discussed individually in Section 1.3.4.

Examples of type one reactivity are shown in Table 1-4.

Monosubstituted Ethylene, $RCH=CH_2$		1-Substituted Butadienes $CH_2=CR-CH=CH_2$	
R = $CO_2C_2H_5$	11200	R = CO_2CH_3	2570
C_6H_5	43	C_6H_5	21
H	20	H	10.7
$CH=CH_2$	10.7	CH_3	2.43
C_4H_9	.44	OCH_3	1.34
OC_4H_9	.01	$N(C_2H_5)_2$.06
Olefinic Carboxylic Esters		β -Substituted Styrenes, $RCH=CH-Ph$	
Ethyl Acrylate	112000	R = H	44.5
Methyl Methacrylate	6270	C_6H_5	1.01
Methyl Crotonate	641	$CH(CH_3)_2$.29
Methyl Cinnamate	264	$N(CH_2)_4$.03

Table 1-4. Relative Rate Constants of Reactions Between Diazomethane and Various Dipolarophiles.

This table shows the relative rate constants of reactions between diazomethane, and a host of dipolarophiles.⁹¹ Diazomethane is shown to react more quickly with electron deficient rather than electron rich or neutral dipolarophiles.

Type three 1,3-dipoles react in a manner opposite to that of the type one 1,3-dipoles. In these cases the LUMO of the dipole react with the HOMO of the dipolarophile, or in a "LU controlled" manner (Figure 1-19). In other words, the HOMO of the dipole is of such low energy that the interaction between the LUMO of the dipole and HOMO of the dipolarophile is the dominant one.⁶¹ Thus edges on the dipolarophile and ewgs on the dipole will accelerate the reaction.

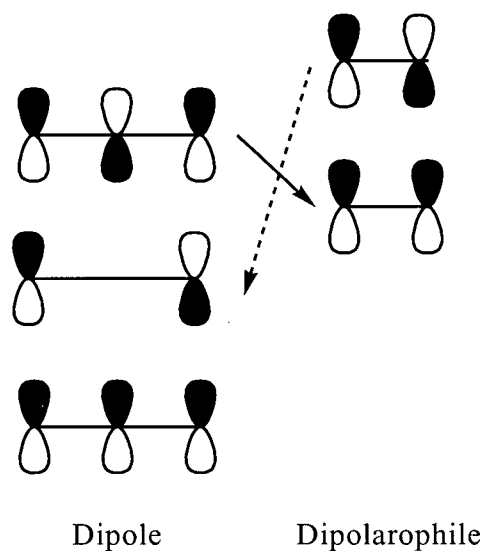


Figure 1-19. Symmetry Allowed Interactions of Type Three 1,3-Dipolar Cycloadditions.

These dipoles are referred to as electrophilic because they tend to react more efficiently with electron rich dipolarophiles. Parent 1,3-dipoles that react in a LU controlled manner are listed in Table 1-5.¹¹⁵

1,3-Dipole	ϵ (eV) HOMO	Method	ϵ (eV) LUMO	Method
NNO Azoxy	-12.9	Photoelectron Spectroscopy	-1.1	Estimate
OOO Ozone	-13.5	Photoelectron Spectroscopy	-2.2	Negative of Electron Affinity

Table 1-5. Frontier Molecular Orbital Energies of Parent 1,3-Dipoles (Type Three).

The final group of 1,3-dipoles is made up of those dipoles that react neither by LU or HO controlled reactions (Figure 1-20). These are type two 1,3-dipoles. The energies

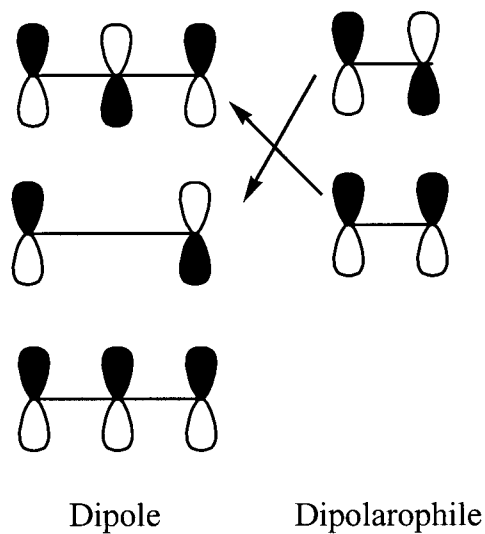


Figure 1-20. Symmetry Allowed Interactions of Type Two 1,3-Dipolar Cycloadditions.

Of these HOMO's and LUMO's are intermediate to those of type one and three 1,3-dipolar cycloadditions (Table 1-6).

Adding either an edg or ewg to the dipole or dipolarophile can accelerate these reactions. Type two molecular orbital energies are shown in Table 1-6.¹¹⁵ The focus is on making either the HO or LU interaction predominate. This will lower the energy difference between one of the interactions, thus increasing the reaction rate. A good example of type two reactivity is shown with phenyl azide (Table 1-7).⁹² Table 1-7 shows “parabolic” reactivity. Reactivity like this is common among type two dipoles. Dipolarophiles that are very electron deficient (*i.e.* DMAD) react well with phenyl azide, while dipolarophiles that are electron rich (*i.e.* pyrrolidincyclopentene) also react well with phenyl azide, and to a much greater degree. “Non-activated” (*i.e.* cyclohexene) dipolarophiles do not react well. This is an example of substituting the dipolarophile to control reactivity.

1,3-Dipole	ϵ (eV)	Method	ϵ (eV)	Method
HCNNH Nitrile Imines	-9.2	Estimate	0.1	Estimate
HCNO Nitrile Oxides	-10.8	Photoelectron Spectroscopy	-0.5	Estimate
NNNH Azides	-10.7	Photoelectron Spectroscopy	0.1	Estimate
H ₂ CNHO	-9.7	Estimate	-0.5	Estimate
H ₂ COO	-10.3	Estimate	-0.9	Estimate

Table 1-6. Molecular Orbital Energies of Type Three 1,3-Dipoles.

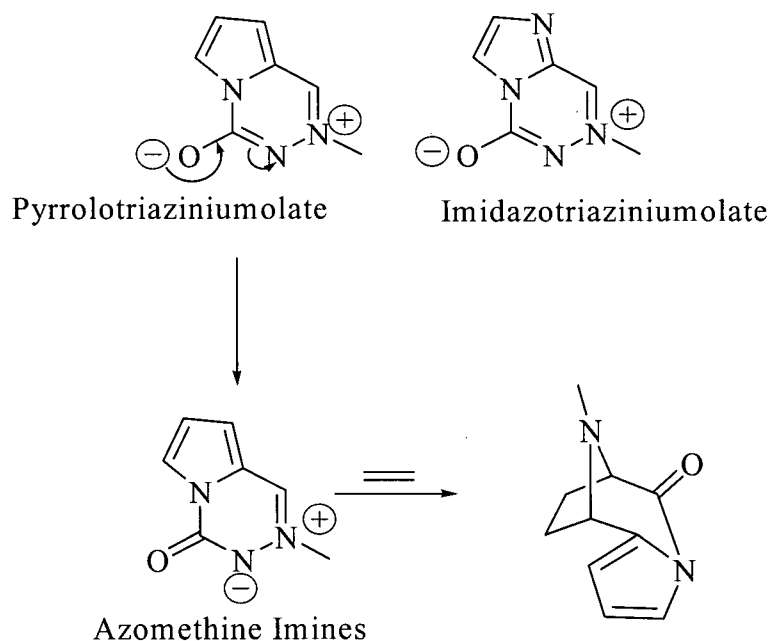
Monosubstituted Ethylenes CH ₂ =CHR		Electron-Poor Ethylenes	
R = CO ₂ C ₂ H ₅	9.85	Diethyl fumarate	8.36
CN	1.07	Maleic anhydride	7.20
C ₆ H ₅	.40	n-Phenylmaleimide	27.6
C ₅ H ₁₁	.24	Methyl methacrylate	.72
OC ₄ H ₉	.40	Ethyl crotonate	.27
Electron Rich Ethylenes		Cycloalkanes	
Butyl vinyl ether	.40	Cyclopentene	1.86
Ethoxycyclopentene	.49	Cyclohexene	.033
1-Morpholinocyclopentene	2580	Bicyclo(2.2.2)octene	.90
1-Pyrrolidinocyclohexene	9930	Norbornene	188
1-Pyrrolidinocyclopentene	115000	Norbornadiene	194
Acetylenic Dipolarophiles			
Dimethyl acetylenedicarboxylate	25.4		
Methyl Propiolate	10.4		
Phenylacetylene	.29		

Table 1-7. Relative Rate Constants of 1,3-Dipolar Cycloadditions with Phenyl Azide.

Another way of controlling reactivity is by adding substituents that will change the energies of the molecular orbitals of the dipoles.^{93,94} This process accomplishes the

same goals as modification of the dipolarophiles in the phenyl azide reactions shown in Table 1-7.

Azomethine ylides are typical type one, nucleophilic dipoles. Section 1.3.4.2 describes an example of electron deficient azomethine ylides that react more efficiently with electron rich dipolarophiles. Another example of this "inverse electron demand" is the mesomeric betaines containing pyrrolo- or imidazo-triaziniumolate system (Scheme 1-22).⁹⁵ These molecules react functionally as azomethine imines, a typical type one dipole. In this case though, the reactions are more facile with electron rich dipolarophiles.³⁴



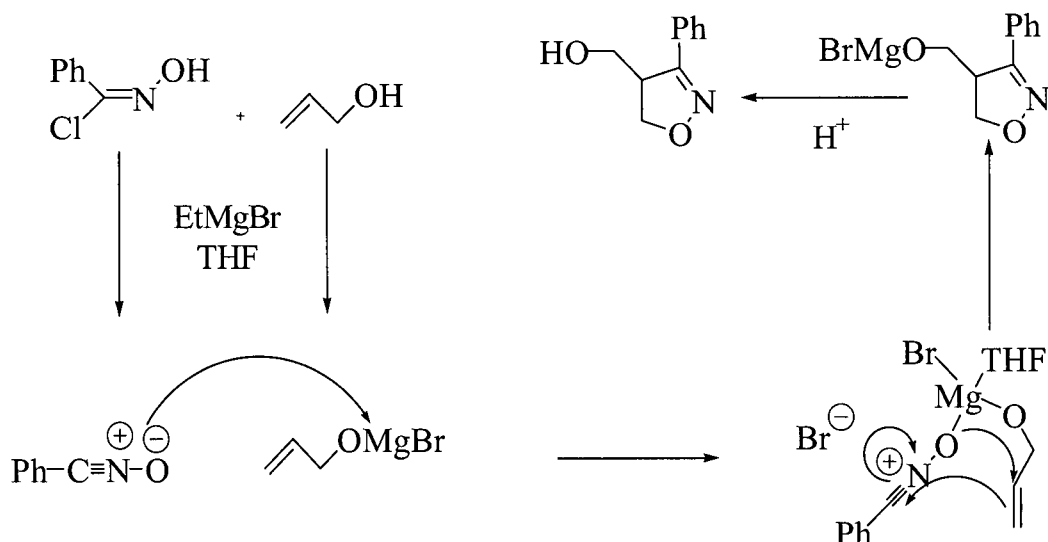
Scheme 1-22. Mesomeric Betaines.

The explanation for this change in reactivity comes from the energies of the molecular orbitals. The calculated HOMO-LUMO gap is smaller for the LUMO of the dipole HOMO of the electron rich dipolarophile (enamine) than the HOMO of the dipole

LUMO of the electron deficient dipolarophile (DMAD). This causes the increase in the rate of the reaction.¹⁰⁸

Another method of controlling the reactivity of 1,3-dipoles outside of substituent manipulation is the use of transition metals. Metals generally coordinate on the dipole or dipolarophile thus, changing the orbital energies. Transition metals are also often used in conjunction with chiral ligands in order to induce stereoselectivity,⁹⁶ but this aspect will not be presented here. Two examples that will be discussed are magnesium alkoxides reacting with nitrile oxides and transition metal catalysis of nitron cycloadditions.

Nitrile oxides are considered to be type two dipoles, and will react if there is an "activated" dipolarophile present. In cases where the dipolarophile is internal and non-activated, the yields of these reactions are low, as nitrile oxides dimerize giving



Scheme 1-23. Metal Catalyzed Reaction of Phenyl Nitrile Oxide and 3-Hydroxy-1-Propene.

furoxans.⁹⁷ The magnesium catalyzed process shown in Scheme 1-23, was compared to that of the non-catalyzed, triethylamine promoted reaction. The non-catalyzed reaction, had a relative rate of 0.09, while the relative rate of the magnesium catalyzed process was

14.⁹⁸ This is an increase in rate of over 100 times. The rationale for the rate increase is based on molecular orbital calculations. The calculations were based on the complex shown in Figure 1-21, which approximates the complex shown in Scheme 1-23, with the exception of H₂O replacing THF and Cl replacing Br.

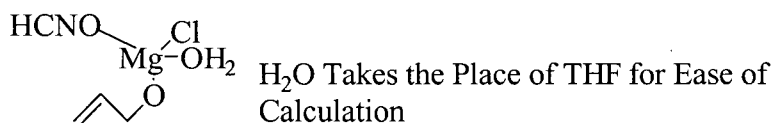
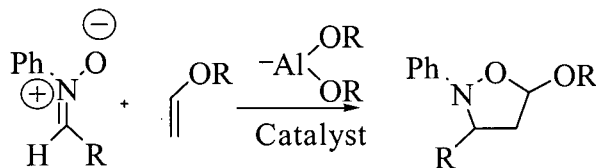


Figure 1-21. Complex Used for Molecular Orbital Calculations.

The energies of the FMO's change dramatically with the addition of metal, so much so that the process becomes a type three reaction (LU controlled). The complex formation, according to *ab initio* calculations, induced an increase of the HOMO-LUMO energies of the dipolarophile from -0.396 and 0.176 hartree to -0.349 and 0.188 Hartree, respectively.¹¹¹ The energies of the dipole decreased .107 and .048 Hartree for the HOMO and LUMO respectively. This was enough to change the reaction from HO controlled to LU controlled. The energy gap of the LU controlled reaction went from 0.572 to 0.477 Hartree, while the HO controlled process is much higher in energy, 0.671 Hartree.¹⁶⁰

A second example involves the reaction of a nitron with an electron rich dipolarophile (Scheme 1-24).⁹⁹ This reaction, normally HO controlled



Scheme 1-24. Metal Catalyzed Nitron Cycloaddition.

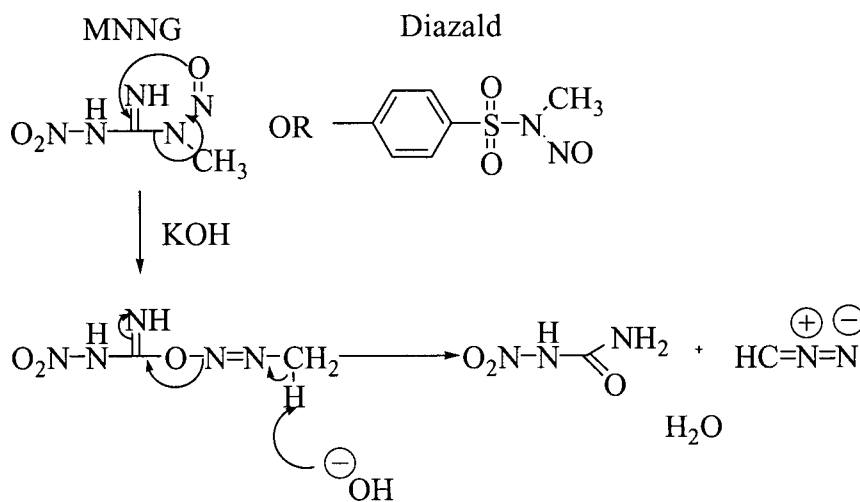
became a LU controlled process via inverse-electron demand by the addition of a chiral aluminum catalyst.¹⁶¹ No kinetic studies have yet been reported on this procedure, but the reaction was more efficient with electron rich dipolarophiles, and it was observed that regio- and diastereoselectivity increased upon the addition of the catalyst.¹⁰⁰

1.3.4 Methods of 1,3-Dipolar Cycloaddition

Many of the 1,3-dipoles used today in organic synthesis are very reactive species, and must be generated *in situ*. What follows is a short collection of the methods used for generating 1,3-dipoles, along with a discussion of the mechanisms that are specific to each species. An emphasis will be on those 1,3-dipoles that appear in this thesis.

1.3.4.1 Diazoalkanes

The simplest diazoalkane, diazomethane, is usually generated by the reaction of a base with *n*-methyl *n*-nitroso amines (Scheme 1-25). This reaction generates the yellow gas in a solution of ether where it can be safely handled and used in further reactions.¹⁰¹



MNNG = 1-methyl-3-nitro-1-nitrosoguanidine

Scheme 1-25. Production of Diazomethane.

Analogues of diazomethane are also widely used in cycloaddition chemistry. These include phenyldiazomethane,¹⁰² trimethylsilyldiazomethane,¹⁰² and ethyldiazoacetate¹⁰² which are all more or less stable at r.t., and can be directly reacted with dipolarophiles.

The mechanism of the diazomethane 1,3-dipolar cycloaddition has been a source of controversy for many years. To this day, there are results that are difficult to explain with even the most sophisticated theory.

The original disagreement came in the late 1970's and early 1980's. Huisgen,¹⁰³ was the first person to systematically look at the reactivities of many of the 1,3-dipoles. Firestone disagreed however, about the concertedness of the 1,3-dipolar cycloadditions of

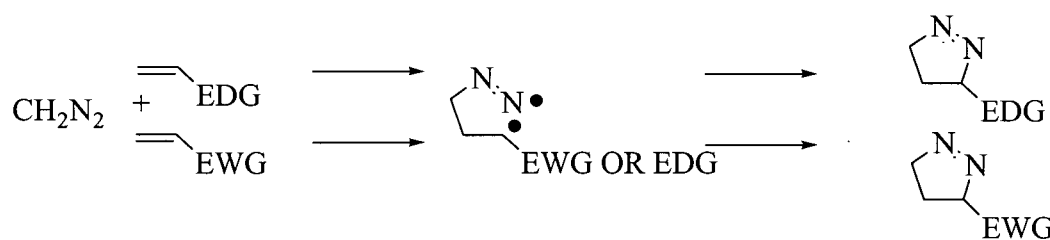
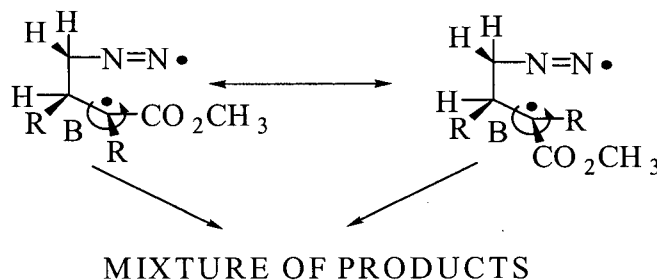


Figure 1-22. Diazomethane Reactions with Electron Rich and Poor Dipolarophiles.

diazomethane that Huisgen initially reported on.¹⁰⁴ Huisgen had done a great deal of work involving 1,3-dipolar reactions, and maintained that the reaction mechanism was a concerted process. In 1976, Firestone suggested that the diazomethane reaction underwent a non-concerted process, where the intermediate was a diradical (Figure 1-22).¹³⁴ The discussion was based on the fact that diazomethane reacts with both electron rich and poor dipolarophiles to give the 1-pyrazoline. The diradical mechanism, according to Firestone would result in the observed results, while a concerted, but not

synchronous mechanism would result in opposite orientations for electron rich and poor dipolarophiles in the resultant product.¹⁴⁰ This stems from the fact that the diradical intermediate will be stabilized more efficiently if the radical is next to an activating group. The concerted process is governed by FMO theory, and this predicts the reaction will be most efficient with electron poor dipolarophiles. Huisgen in 1977 reported that the reaction is stereospecific and this is an insurmountable obstacle for the diradical mechanism as the ring closure must be faster than rotation around bond B as shown in Scheme 1-26.¹⁰⁵



Scheme 1-26 Diradical Mechanism for 1,3-Dipolar Cycloaddition with Diazomethane

Huisgen reported evidence that supported a di-radical mechanism that would give products of mixed stereochemistry.¹⁰⁶ Rastelli *et al.*¹⁰⁷ using a slightly modified form of FMO calculations at a high level of theory, and assuming that only concerted mechanisms were possible, they were able to predict the formation of only the 1-pyrazoline for both ewgs and edgs.¹⁰⁸

The mechanism of reaction of aliphatic diazo compounds is not appreciably affected by steric bulk. A graph showing the reaction rates of diazomethane and diphenyldiazomethane is shown in Figure 1-23. There is good correlation between the reactivity of the two dipoles, which differ in structure by 2 phenyl groups. This suggests that not only do the reactions go through the same mechanism, but that the phenyl groups

have no appreciable effect on reactivity.¹⁰⁹ The reason for the minimal effect that the phenyl groups have on reactivity is the early transition state of the 1,3-dipolar cycloadditions. In this case, the bonds of the product are not formed to a significant extent in the transition state, thus steric effects do not play a role in the kinetics of the reaction.

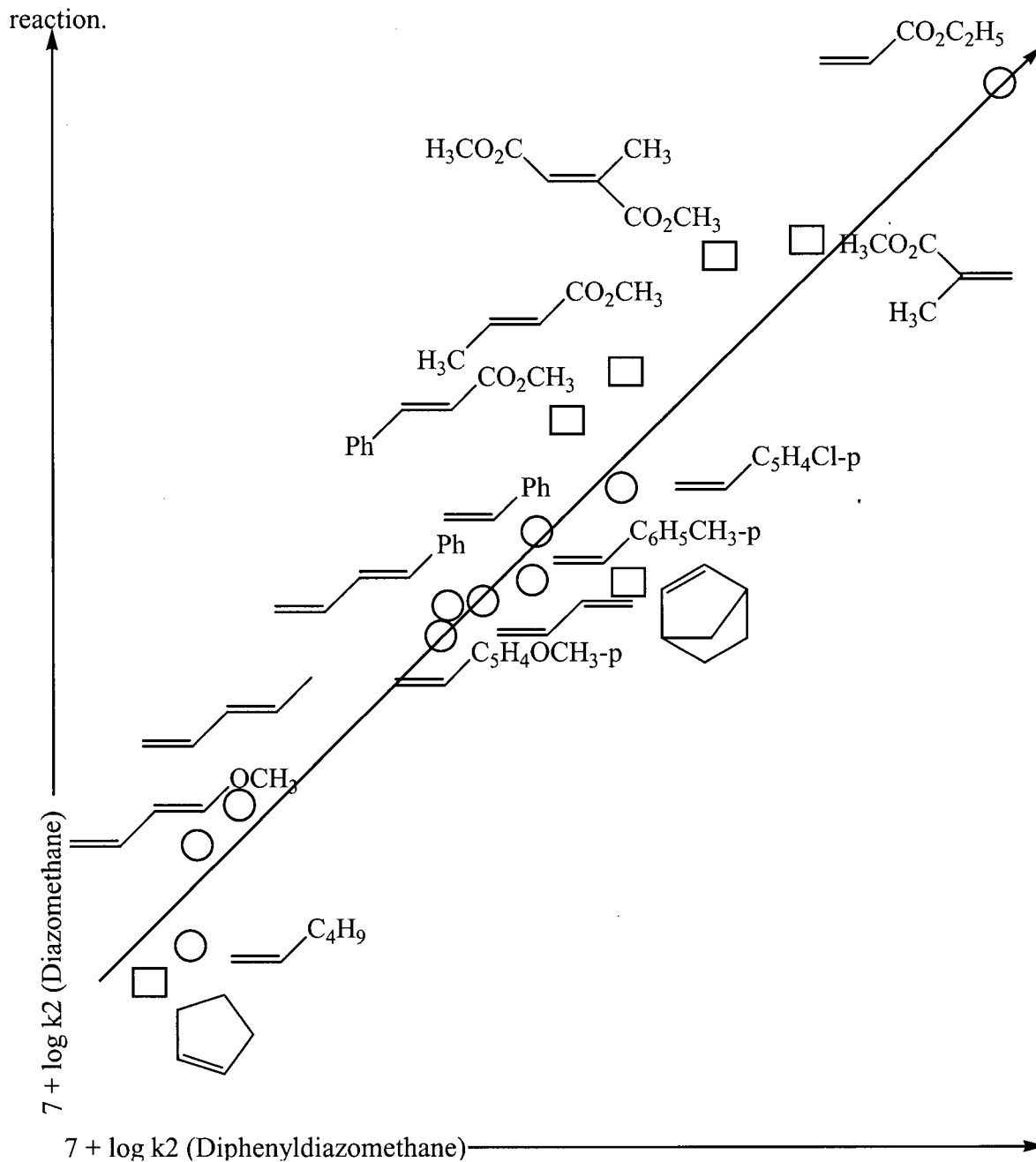
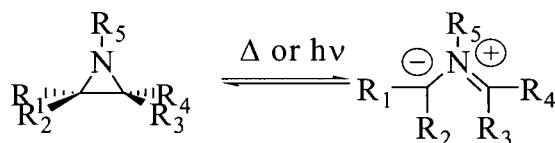


Figure 1-23. Correlation of the Rates of Reaction of Diazomethane and Diphenyldiazomethane.

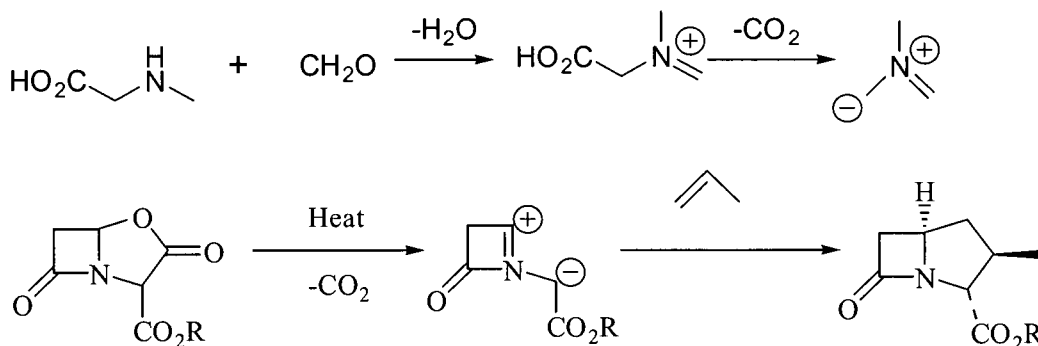
1.3.4.2 Azomethine Ylides

One of the most common ways to generate azomethine ylides is the electrocyclic ring opening of aziridines (Scheme 1-27).¹¹⁰



Scheme 1-27. Electrocyclic Ring Opening Formation of Azomethine Ylides.

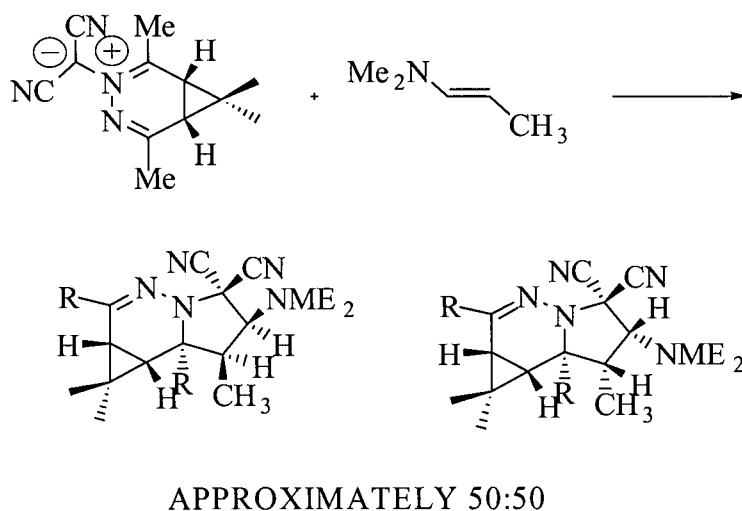
Other methods include the formation of an imine between an *n*-alkyl amino acid and an aldehyde, followed by decarboxylation to form an un-stabilized ylide and decarboxylation of β -lactams (Scheme 1-28).¹¹¹ The cycloaddition of such a species is used to form a pyrrolidine, and has been used synthetically in the stereoselective synthesis of β -lactams.¹¹²



Scheme 1-28. Synthesis of Non-Stabilized Azomethine Ylides.

The mechanism of azomethine ylide 1,3-dipolar cycloaddition is concerted, and some reactions are characterized by stereospecificity of the products.¹¹³ There are examples of this reaction where the products obtained are non-stereospecific.

The most recent example of a non-stereospecific azomethine ylide 1,3-dipolar cycloaddition was investigated by Bohm *et al.*¹¹⁴ This paper describes the reaction of an electron deficient azomethine ylide with an electron rich dipolarophile in a LU controlled process. Azomethine ylides are generally type one, nucleophilic dipoles, but this can be changed with the addition of electron withdrawing groups. The reaction as shown in Scheme 1-29 has good conversion, but the selectivity is poor. Almost equal amounts of the cis and trans products are formed. This suggests a non-concerted mechanism (Scheme 1-20).¹⁵¹

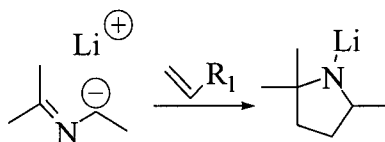


Scheme 1-29. Inverse Electron Demand Azomethine Ylide 1,3-Dipolar Cycloaddition.

Kinetic studies were performed on these electron deficient azomethine ylides of the type shown in Scheme 1-29.¹¹⁵ These studies showed that the ylides reacted more efficiently with electron rich dipolarophiles than with electron poor. This is what would be expected from a LU controlled 1,3-dipolar cycloaddition.¹³⁰ AM1 calculations of the MO's confirmed the reason for this reactivity. The HOMO/LUMO energies of the parent

azomethine ylide from Table-1 are -6.9 eV/ 1.4 eV. The energies for the electron deficient azomethine ylide are -7.77 eV/ -1.54 eV. The energy of the LUMO of the ylide is 3 eV less for the electron deficient species, while the HOMO is 0.8 eV less. The lowering of the LUMO causes the reaction to be LU controlled, and accounts for the ylide reacting with electron rich dipolarophiles more efficiently than electron poor. This may also provide an explanation for a non-concerted mechanism.¹⁵²

In cases where the reaction of an azomethine ylide is not possible, or does not yield the desired products, a new method for 3+2-cycloaddition can be used. The reaction of a 2-azaallyl anion forms a pyrrolidine, but this 2-azaallyl anion reacts with electron rich dipolarophiles, instead of electron poor. This makes the 2-azaallyl anions a complimentary method to the azomethine ylides (Scheme 1-30).¹¹⁶



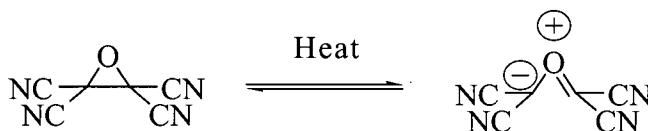
Scheme 1-30. Reaction of 2-Azaallyl Anion with Anionophile.

The reactions of the 2-azaallyl anions are designated as concerted $[\pi 4s + \pi 2s]$, mechanism. These generally proceed with conservation of stereochemistry.¹³¹ It is interesting to note that the products of the reaction can be quenched with an electrophile giving *n*-substituted pyrrolidines.

1.3.4.3 Carbonyl Ylides

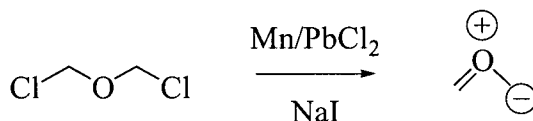
Stabilized and non-stabilized carbonyl ylides can be generated for reactions with dipolarophiles. Stabilized carbonyl ylides can be generated by first order thermal

electrocyclic ring opening (Scheme 1-31) via the cleavage of the carbon-carbon bond of electron deficient epoxides.¹¹⁷ These species are known to react mainly with electron rich systems.



Scheme 1-31. Electrocyclic Ring Opening to form a Carbonyl Ylide.

Non-stabilized carbonyl ylides can also be generated through different methods.¹¹⁸ One example is the two-electron oxidation of a di-chloromethylether using Mn/PbCl₂ and NaI.¹¹⁹

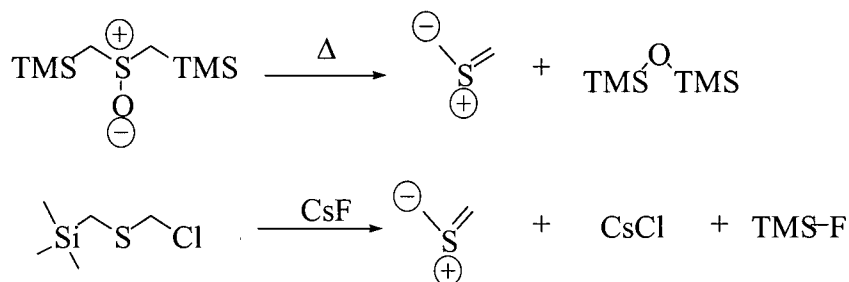


Scheme 1-32. Reduction of di-Chloromethylether to form an Unstabilized Carbonyl Ylide.

Non-stabilized carbonyl ylides react with both electron poor dipolarophiles and electron rich.¹⁶⁰ This is not expected as the parent carbonyl ylide is a type one dipole. The reaction proceeds in a concerted manner, and yields stereoselective products.¹²⁰

1.3.4.4 Thiocarbonyl ylides

Unstabilized thiocarbonyl ylides can be generated by thermal decomposition of di(methyltrimethylsilyl)sulfoxide to the thiocarbonyl ylide,¹²¹ or by the desilylation of chloromethyl trimethylsilylmethyl sulfide.¹²²



Scheme 1-33. Methods of Generating Unstabilized Thiocarbonyl Ylides.

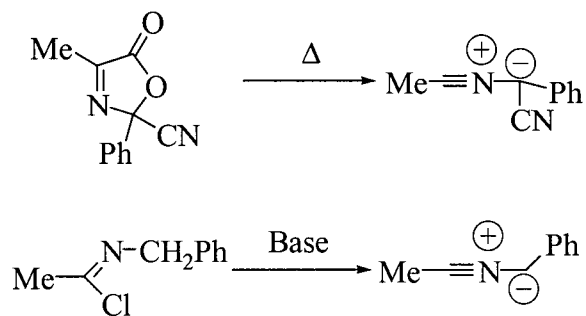
These reactions of the non-stabilized ylides are useful. They undergo ready cycloaddition with electron poor dipolarophiles, and react via a concerted mechanism. This was observed from the fact that the stereochemistry in the dipolarophile is conserved during reaction.¹²³

It has also been noted in some examples that thiocarbonyl ylides undergo non-stereospecific reactions, which is rationalized by a non-concerted mechanism.¹²⁴ Such reactions proceed with an electron rich thiocarbonyl ylide reacting with electron poor dipolarophiles such as dicyanomaleate and dicyanofumarate.¹²⁵

Thiocarbonyl ylides like most 1,3-dipoles react via an early transition state. This can be observed from ab-initio calculations which showed, even though the 1,3-dipolar cycloaddition of the thiocarbonyl ylide was much more exothermic than the thiocarbonyl imine, the transition state energy (activation energy) was higher.¹²⁶ This suggests that the relative energy of the product that is formed has very little effect on the energy of the transition state, and thus it must occur early. This is in line with what was discussed earlier about the transition state of these reactions.

1.3.4.5 Nitrile Ylides

There are several different ways to generate a nitrile ylide, but the most common are the thermal extrusion of carbon dioxide,¹²⁷ and dehydrohalogenation (Scheme 1-34).¹²⁸



Scheme 1-34. Formation of Nitrile Ylides.

The reaction has all the characteristics of the other 1,3-dipoles, except that there are no surprises with this one. These reactions occur strictly diastereospecifically.¹²⁹ The nitrile ylides is considered to be one of the most nucleophilic, and will react very quickly with electron deficient dipolarophiles (the reaction is HO controlled). In fact, its reactivity profile is similar to that of diphenyldiazomethane.¹³⁰

Recently, metallo-nitrile ylides have been investigated, and are another example of metal coordination changing the landscape of the MO's, in that these dipoles react with electron rich dipolarophiles,¹³¹ as did both the nitrile oxides (Scheme 1-23) and nitrones (Scheme 1-24).

The above discussion has given a brief overview of the 1,3-dipole cycloaddition chemistry that has been investigated during this thesis. If there are any questions about this chemistry, there are reviews and books to consult.¹³²

Chapter 2: Results and Discussion

2.1 Introduction

One of the most important methods for the production of new photosensitizers is the synthesis of chlorins.¹³ The reason for this is that chlorins absorb light intensely at wavelengths where human tissue is most transparent (Figures 1-9 and 1-10).

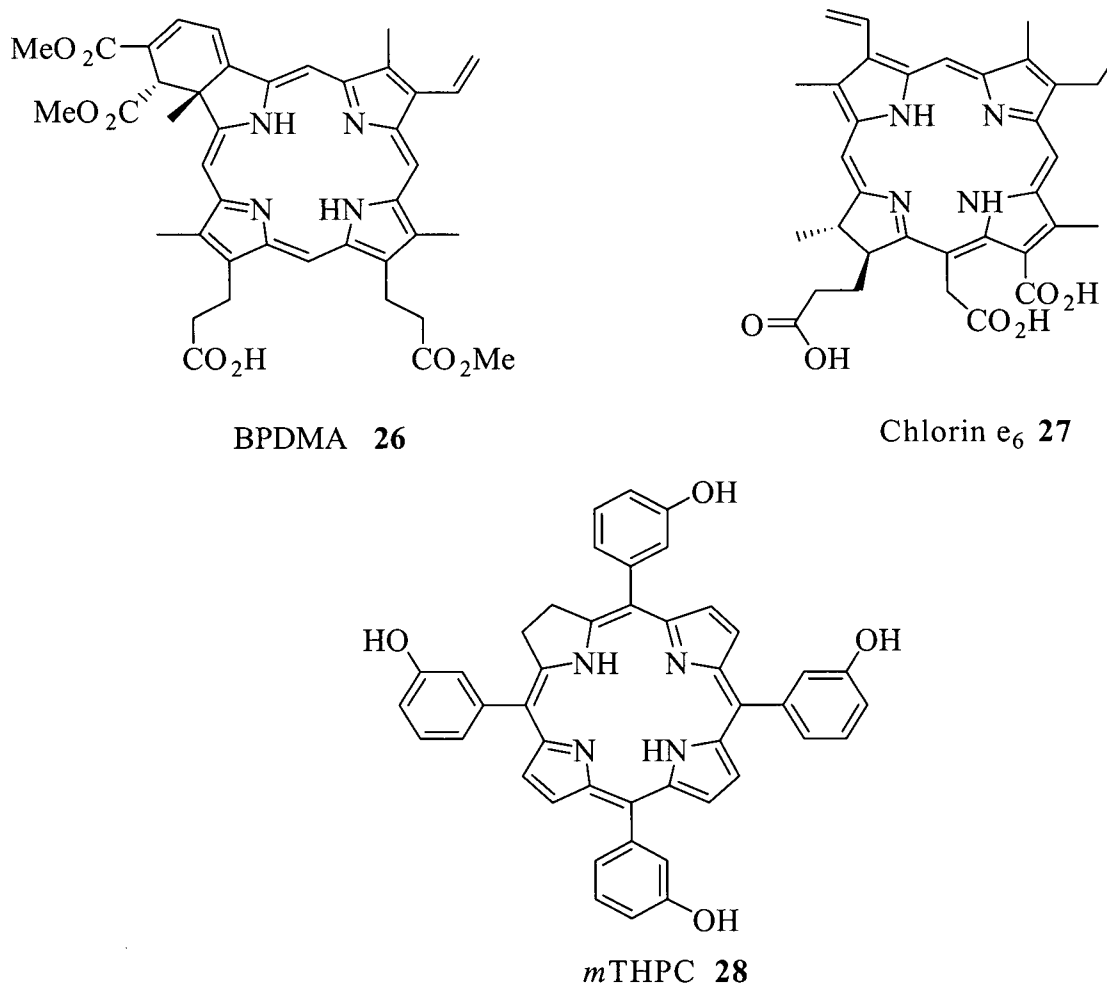


Figure 2-1. Selected Chlorins Tested as PDT Agents.

Chlorins such as BPDMA (26), chlorin e₆¹³³ (27) and *meso*-tetraphenyl(*m*-hydroxyphenyl)chlorin¹³⁴ (*m*THPC, 28) are all useful photosensitizers (see Figure 2-1).

The most apparent method to generate a chlorin is to dihydrogenate a cross-conjugated double bond. This is generally done via a diimide reduction.¹³⁵ The dihydrogenation of porphyrins has been extensively reviewed.¹³⁶ Some other examples of methods to synthesize chlorins will be presented in Section 2.1.1.

2.1.1 Formation of Chlorins from Porphyrins

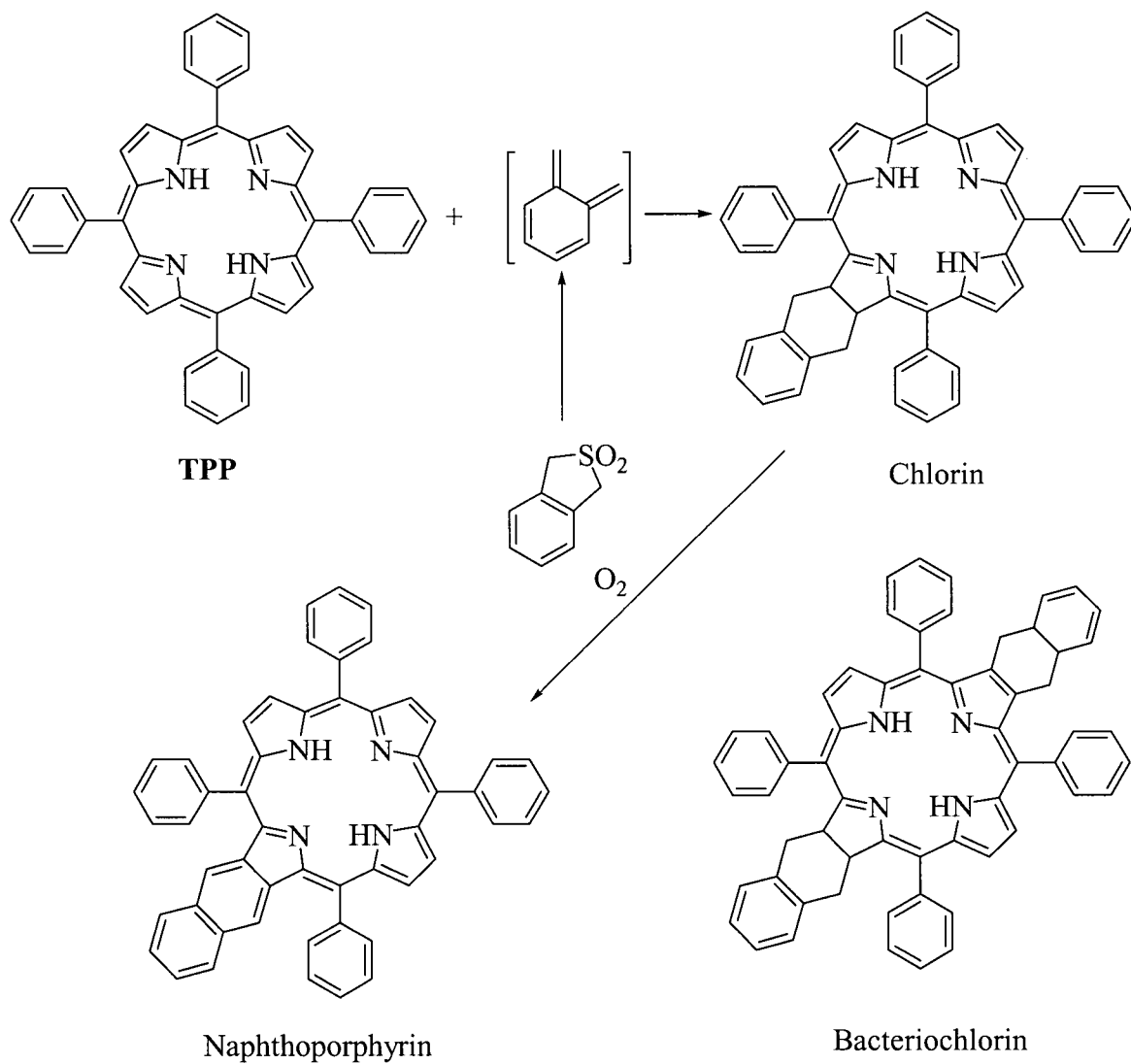
2.1.1.1 Natural Sources

One method for obtaining chlorins for use in PDT is from natural sources. Chlorophyll (Figure 1-2) is a chlorin that occurs abundantly in many plants and in some animals. The main function of chlorophyll is as a photosynthetic agent and chlorophyll can be extracted from leaves and algae by boiling in methanol. Chlorophyll is then purified by column chromatography. The isolation and purification of chlorophylls has been reviewed extensively.¹³⁷

2.1.1.2 Diels-Alder Reactions

A Diels-Alder reaction is a $[4\pi_s + 2\pi_s]$ electrocyclization between a diene and a dienophile. In the case of a porphyrin, the cross-conjugated double bond could act as a dienophile. The cross-conjugated double bond could also act as part of a diene, in concert with a conjugated double bond at the β -position.

Scheme 2-1 shows an example of the cross-conjugated double bond of tetraphenylporphyrin (TPP) reacting as a dienophile. This reaction between TPP and

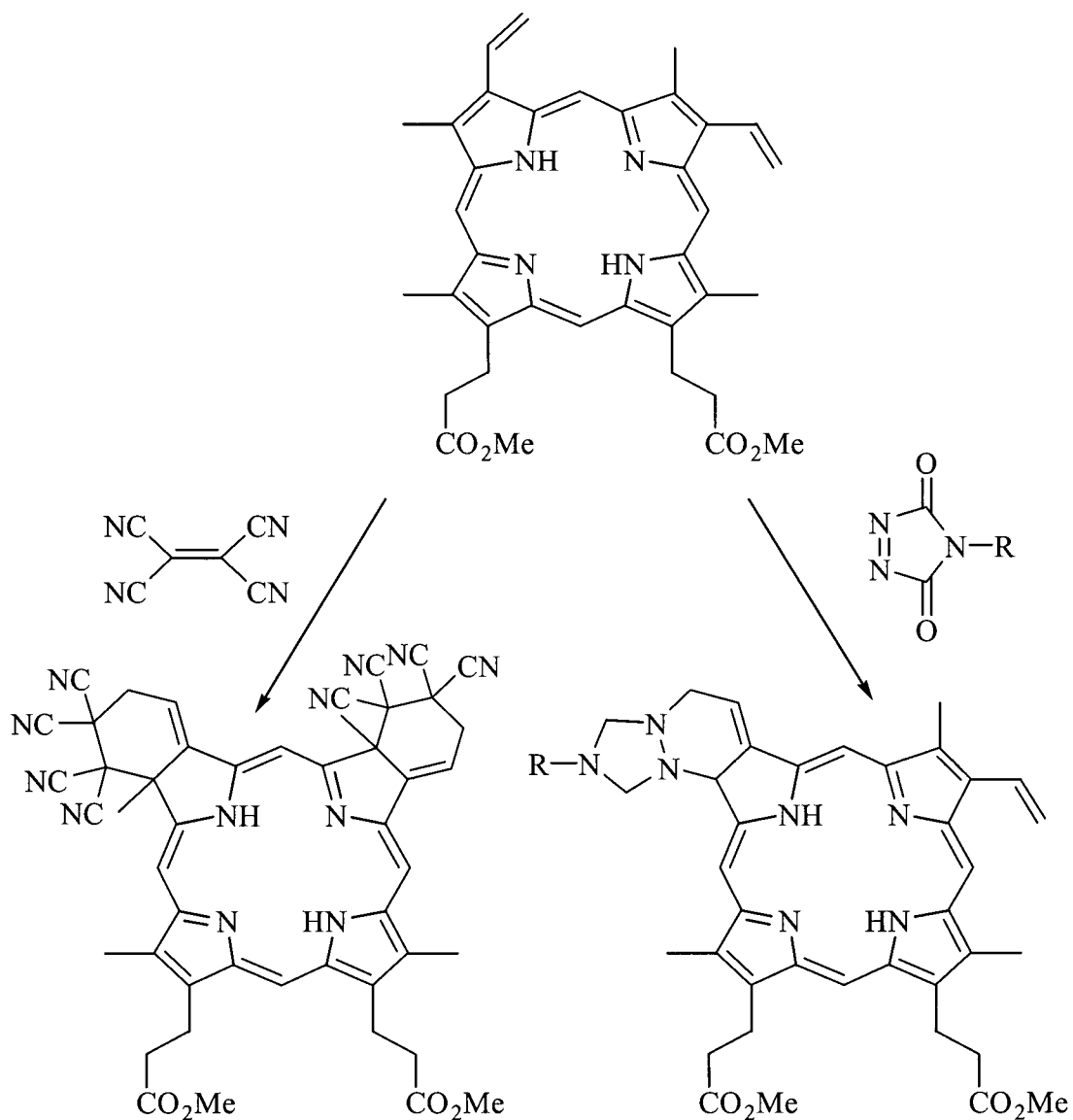


Scheme 2-1. Reaction of Benzoquinonedimethane with TPP.

benzoquinondimethane is the first example of this type of Diels-Alder reaction.¹³⁸ High temperatures are required for the extrusion of SO_{2(g)} from the benzoquinone sulfone, which then reacts as the diene to form the chlorin. Oxidation of the resultant chlorin yields the naphthoporphyrin. Bacteriochlorins would be observed if tetrakis(pentafluorophenyl)porphyrin (pFTPP) was used as the dipolarophile in the

reaction described in Scheme 2-1. This suggests that the cross-conjugated double bonds of the electron deficient porphyrin (pFTPP) are more reactive towards cycloaddition than the double bonds of TPP.¹⁸¹

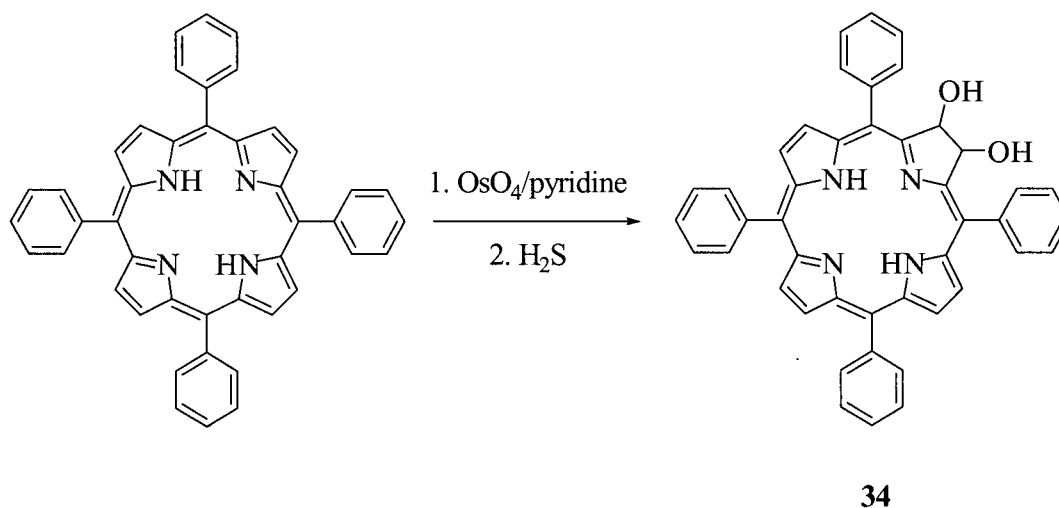
There have also been examples of the cross-conjugated double bonds of porphyrins being used in concert with an exocyclic double bond to form a diene in a Diels-Alder reaction.¹³⁹ Protoporphyrin IX dimethyl ester is a common diene and has been used in reactions with tetracyanoethylene,^{8,9} DMAD,¹⁰ and urazines (Scheme 2-2).¹¹



Scheme 2-2. Diels-Alder Reaction with Protoporphyrin IX.

2.1.2.3 Osmium Tetroxide Oxidation

Osmium tetroxide can be used to dihydroxylate the cross-conjugated double bonds of porphyrins.¹⁴³⁻¹⁴⁵ This procedure involves using a stoichiometric amount of the osmium tetroxide/pyridine complex and reducing the resulting osmate ester with H₂S (Scheme 2-3).¹³

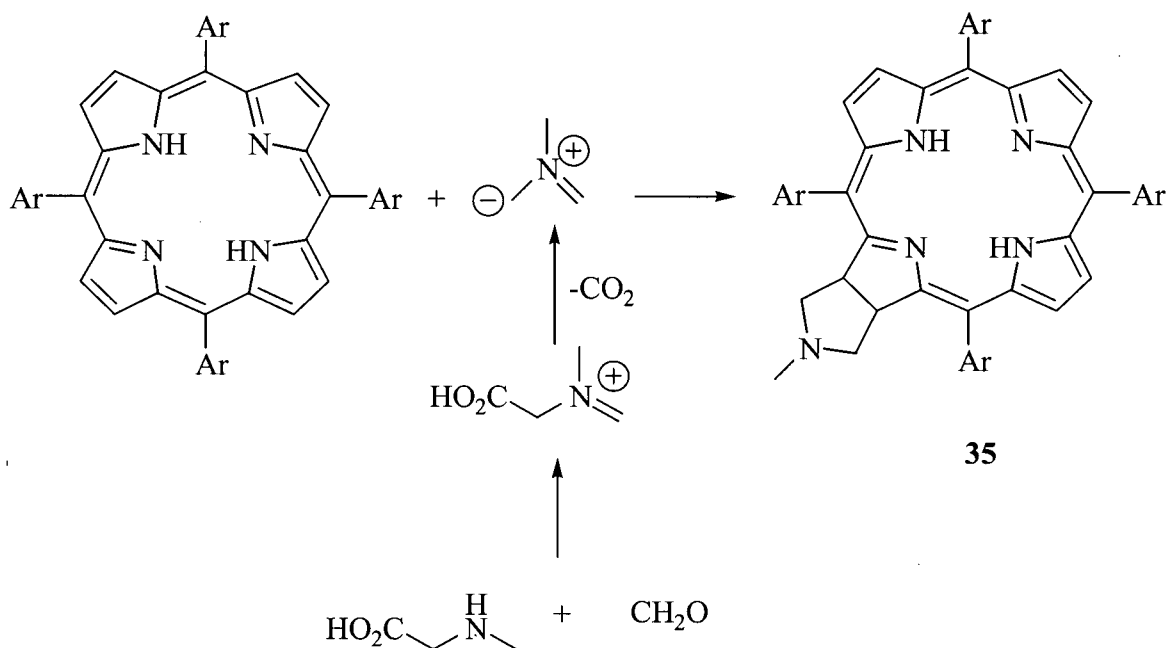


Scheme 2-3. Dihydroxylation of TPP.

2.1.1.4 1,3-Dipolar Cycloadditions

One example in the literature of 1,3-dipolar cycloadditions being used to form chlorins from porphyrins was reported by Cavaleiro *et al.*¹⁹² Cavaleiro reported that reactions between tetraarylporphyrins, namely TPP and pFTPP, and unstabilized azomethine ylides resulted in yields of the chlorin from 10 – 60%.¹⁴⁶ TPP and pFTPP were refluxed with sarcosine and paraformaldehyde. The resulting imine that formed from the reaction between the alpha amino acid and formaldehyde, decarboxylated to

produce the parent azomethine ylide (Scheme 2-4). TPP formed the chlorin in 12 % yield, while pFTPP gave 61 % chlorin and 11 % bacteriochlorin.¹⁹²



Scheme 2-4. Reaction of Tetraarylporphyrins with Azomethine Ylide.

2.2 Results

Sections 2.2.1-2.2.9 provides a synopsis of the work done in the course of this research. Explanations of the results are included.

Different dipolarophiles were used in the course of this research, including pFTPP. This dipolarophile is interesting not only because of its reactivity, but also because of the effect that fluorine substituents can have on the biological activity of a drug.¹⁴⁷ Fluorine and hydrogen atoms have comparable Van der Waals radii, thus may be biologically indistinguishable and yet chemically quite different. Fluorinated compounds can have some interesting biological properties because of this. Fluorine substitution can increase

lipophilicity, and the rate at which biologically active compounds move across lipid membranes.¹⁹⁵

2.2.1 Azomethine Ylides

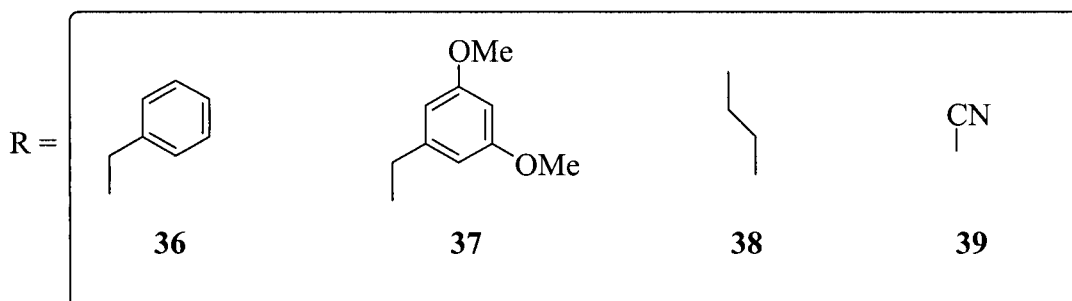
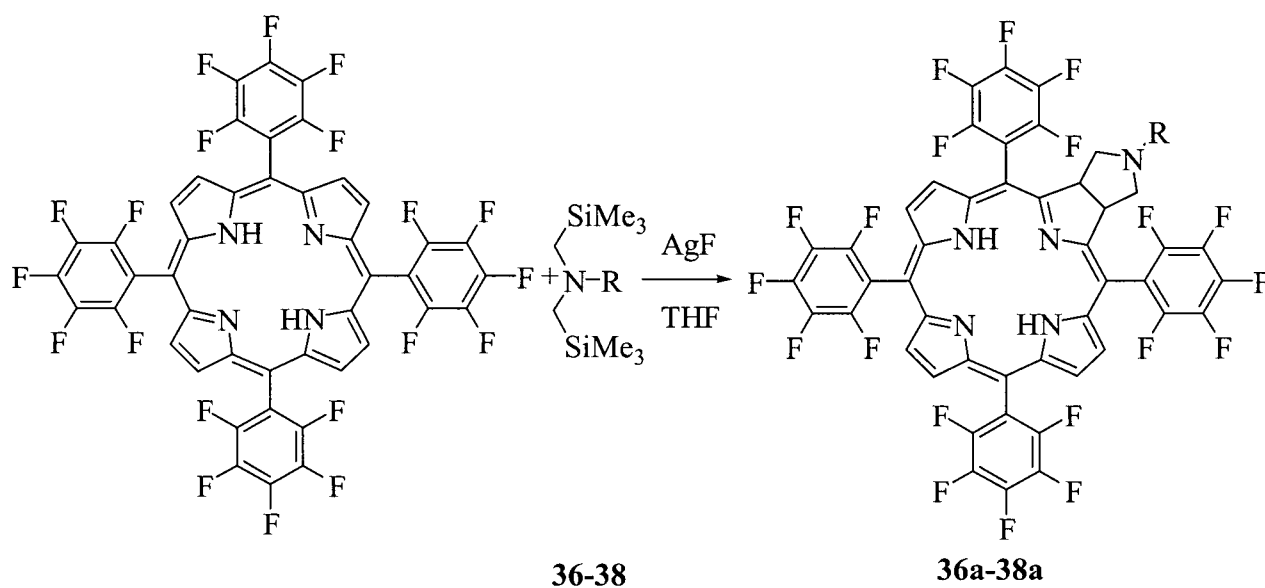
Azomethine ylides were discussed in Section 1.3.4.2. The most general way of synthesizing the unstabilized ylide is through the sequential double desilylation of the α,α' -di(trimethylsilylmethyl)amines (Figure 2-2).¹⁴⁸ This procedure has been used to synthesize cycloadducts using many different dipolarophiles. Most of these dipolarophiles are electron poor double bonds, although there are cases where the reaction has proceeded with heterodipolarophiles.¹⁹⁵ This procedure yields the unstabilized azomethine ylide, meaning there are no substituents on either of the pyrrolidine carbon atoms of the product. This is important in reactions with tetraarylporphyrins, as the aryl rings are rotating, and institute a large steric requirement to any reactions at the β -position.

Since the parent ylide is a typical type one dipole, it was decided that the best results would be obtained with pFTPP and not TPP as the dipolarophile. The electron withdrawing ability of the 20 fluorine atoms of pFTPP makes the cross-conjugated double bonds amenable to a type one reaction (Section 1.3.3). This is coupled with the fact that Cavaleiro *et al.* reported this porphyrin to be responsive in both Diels-Alder¹⁵⁹ and 1,3-dipolar cycloadditions.¹⁶⁴ The reason for this difference in reactivity between pFTPP and TPP can be explained by looking at the HOMO and LUMO energies.¹⁹⁸

Cyclic voltammograms (CV) show the voltages at which porphyrins undergo two one-electron oxidations and two one-electron reductions.¹⁴⁹ These give the energies of the HOMO and the LUMO of the compound.¹⁹⁸ The CV of ZnTPP¹⁹⁹ (Zn being a redox-

inactive metal) shows that the oxidations occur at 0.80 V and 1.16 V, while the reductions occur at -1.33 V and -1.66 V. The first oxidation represents the energy required to remove an electron from the HOMO, thus the energy of the HOMO of ZnTPP is -0.80 eV while the energy of the LUMO is 1.33 eV. The HOMO of pFTPP is -1.37 eV and the LUMO is 0.95 eV. These results show that the energies of both of the sets of molecular orbitals are lower in the case of the fluorinated species, suggesting that pFTPP will react as a type one dipolarophile (see Section 1.3.3.1). The stabilization of the LUMO of the dipolarophile makes the energy difference between the LUMO of the dipolarophile and the HOMO of the dipole smaller. This should have a positive effect of the rate of the reaction.

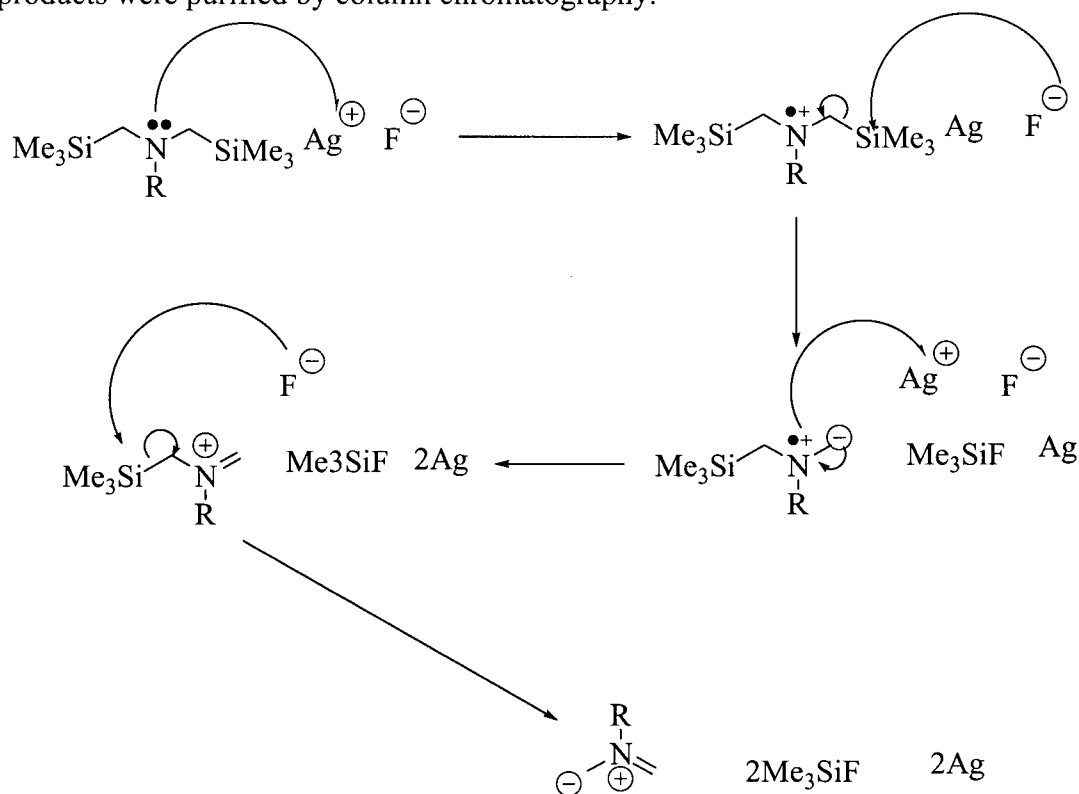
The α,α' -di(trimethylsilylmethyl)amines were prepared according to the procedure as reported in the literature.¹⁶⁶ The amines were refluxed in dry acetonitrile, with two equivalents of chloromethyltrimethylsilane and two equivalents of K_2CO_3 .²⁰¹ The α,α' -di(trimethylsilylmethyl)amine **39** was synthesized from **36** via a Von Braun reaction.¹⁵⁰ Cyanogen bromide was dissolved in dry CH_2Cl_2 and then a solution of **36** in dry CH_2Cl_2 was slowly added.²⁷



α -Silylmethylamine	Equivalents	Time (h)	Yield (%)
36	11	2	58
37	11	1	33
38	11	0.1	67
39	11	24	0

Figure 2-2. Results of α,α' -Di(trimethylsilylmethyl)amine Reaction with pFTPP and AgF.

The 1,3-dipolar cycloadditions were done with a large excess of amine and AgF. The amines (**36-39**) were added as solutions in THF to pFTPP dissolved in THF. AgF was then added to the resultant solution under a stream of N₂ in the dark. The mixture was continuously stirred under N₂ for 0.1-1 h. Once the reaction was complete, the products were purified by column chromatography.



Scheme 2-5. Mechanism of Azomethine Ylide Formation.

During the course of the reaction, it was observed that a silver mirror formed on the inside of the reaction flask. This suggests that the AgF was reduced to metallic silver (Scheme 2-5). This was seen in the reaction of compound **39**, even though no product was obtained (see Figure 2-2).

Compound **36** was reacted as shown in Scheme 2-5 with pFTPP to yield two spots on a silica 60 thin layer chromatographic (tlc) plate. The least polar (R_f 0.7, 60 % CH_2Cl_2 /hexane) green spot gave a characteristic chlorin spectrum (Soret; 405.9 nm, Q-bands; 504, 600 and 654 nm, with 654 nm being the most intense). The N.M.R. data suggest a high degree of symmetry within the compound with only three β -proton peaks observed at 8.70 (2H, d, $J = 4.78$ Hz), 8.48 (2H, s) and 8.38 ppm (2H, d, $J = 4.78$ Hz). The phenyl peaks of the benzyl amine are observed at 7.25 and 7.08 ppm. A multiplet observed in the spectrum which integrated for two protons at 5.17 ppm are assigned to the pyrrolidine protons of the chlorin, while signals of the pyrrolidine protons of the cycloadduct are observed at 3.09 (2H, m) and 2.56 ppm (2H, m). A singlet observed at 3.41 ppm (2H, s) was assigned to the benzylic protons. The mass spectrum of **36a** gave a peak of 1108 m/z, which corresponds to the molecular mass of the desired chlorin, and the high resolution spectrum confirmed the molecular formula of $\text{C}_{53}\text{H}_{20}\text{F}_{20}\text{N}_5$. These data suggest the formation of **36a**.

Compound **37** reacted similarly as **36** to give two spots on silica tlc plate. The most polar of which (R_f 0.7, 20 % EtOAc/hexane) gave a similar chlorin UV-Vis spectrum to that of **36a**. The N.M.R. data showed a high degree of symmetry within the compound with only three β -proton peaks observed at 8.70 (2H, d, $J = 4.78$ Hz), 8.47 (2H, s) and 8.36 ppm (2H, d, $J = 4.78$ Hz). The phenyl peaks of the benzylamine are observed at 6.30 (1H, s) and 6.16 ppm (2H, s). The methoxy group protons are observed at 3.57 ppm (6H, s). The pyrrolidine protons of the chlorin are observed at 5.15 ppm (2H, m), while the pyrrolidine protons of the cycloadduct are observed at 3.34 (2H, m) and 3.10 ppm (2H, m). The mass spectrum of this compound gave a peak at 1168 m/z,

which is the expected mass of the desired product **37a**. High resolution mass spectroscopy confirmed the molecular formula to be $C_{55}H_{25}F_{20}N_5O_2$. These data suggest the formation of **37a**.

Compound **38** reacted similarly as **37** and **36** and gave two products. The less polar of which (R_f 0.7 20 % EtOAc/hexane) gave a similar chlorin spectrum as **37a**. The N.M.R. data showed a high degree of symmetry for the compound, with only three peaks for the β -protons at 8.70 (2H, d, $J = 4.78$ Hz), 8.47 (2H, s) and 8.38 ppm (2H, d, $J = 4.75$ Hz). The signal of the pyrrolidine protons of the chlorin were observed at 5.20 ppm (2H, m) and the pyrrolidine protons of the cycloadduct were observed at 3.15 (2H, m) and 2.51 ppm (2H, m). The alkyl amine protons were observed at 2.24 (2H, d, $J = 7.5$ Hz), 1.30 (2H, m), 1.19 (2H, m) and 0.80 ppm (3H, t, $J = 7.5$ Hz). The mass spectrum of this compound gave a peak at 1074 m/z, which is the mass of desired product. The high resolution mass spectrum confirmed the molecular formula to be $C_{50}H_{23}N_5F_{20}$. These data suggest the formation of **38a**. No isolable products were obtained between **39** and pFTPP.

The structures of the products of these three reactions are shown in Figure 2-2 and are the products of the expected cycloadditions. One main side product was observed in each of these reactions. These were purple compounds which were more polar (R_f 0.6 60 % CH_2Cl_2 /hexane) than the cycloadducts and exhibited non-porphyrin-like UV-Vis spectra. Identification of these compounds has not at this point been completed.

The UV-Vis spectra of all three azomethine cycloaddition products are shown in Figure 2-3. No difference was observed between these three UV-Vis spectra. It might be expected that different substituents would result in a change in the orbital energies, thus

resulting in a difference in the observed spectra, however, this does not seem to be the case.

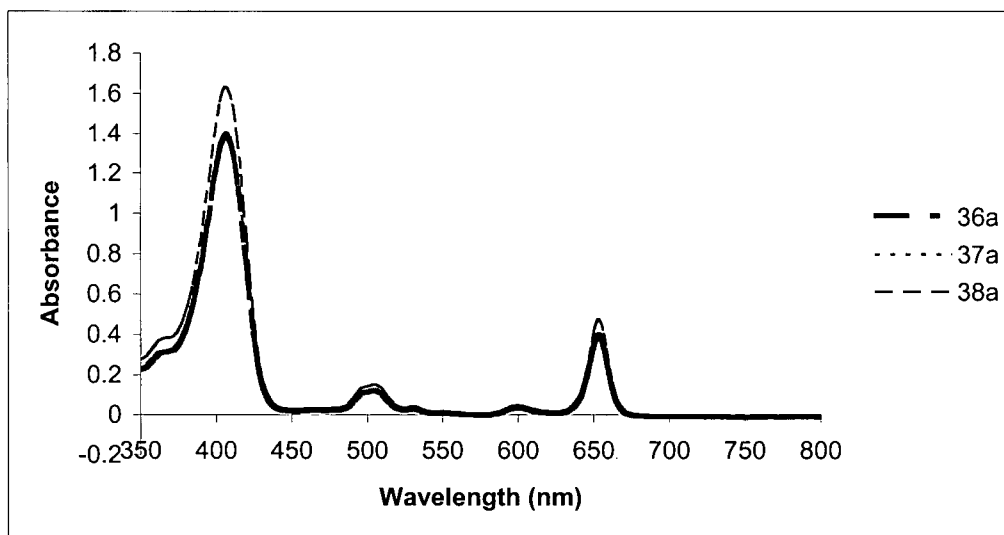


Figure 2-3. UV-Vis Spectra of 36a, 37a and 38a.

The reaction of **36** was also carried out with TPP and cobalt(II)tetraphenylporphyrin (CoTPP). The reaction of **36** with TPP gave only one product. The red spot on a silica tlc plate was less polar than that of the starting material (R_f 0.6, 50% $\text{CH}_2\text{Cl}_2/\text{hexane}$) and had a characteristic metalloporphyrin UV-Vis spectrum. This compound was assumed to be the silver(I) metallated porphyrin and the reaction was discontinued. The reaction with CoTPP gave no product.

Differences in molecular orbital energies may be used to explain the different reactivities observed between dipoles and dipolarophiles. The unstabilized azomethine ylides react very well with electron deficient dipolarophiles (Section 1.3.3). This is observed in the yields of the reactions between **36** - **38** and pFTPP. No reaction was

observed between **39** and pFTPP, even though the initial silver(I) oxidation was observed to occur, implied by the formation of the Ag mirror. This suggested that the azomethine ylide was formed. The electron withdrawing cyano group may alter the energies of the dipole, and possibly cause **39** to become a type two or three dipole. This may be the reason that the non-stabilized azomethine ylide no longer reacts with the electron deficient dipolarophile pFTPP. It was hoped, though, that this change in molecular orbital energies would cause the dipole to react with TPP or CoTPP. Unfortunately, this was not the case, and the cyano N-substituted dipole remained unreactive.

The outcome of the reaction between **36-38** and TPP was not unexpected. The cross-conjugated double bonds of TPP are not as electron deficient as those of pFTPP. This causes them to be not as reactive towards type one dipoles that usually react with electron deficient double bonds.

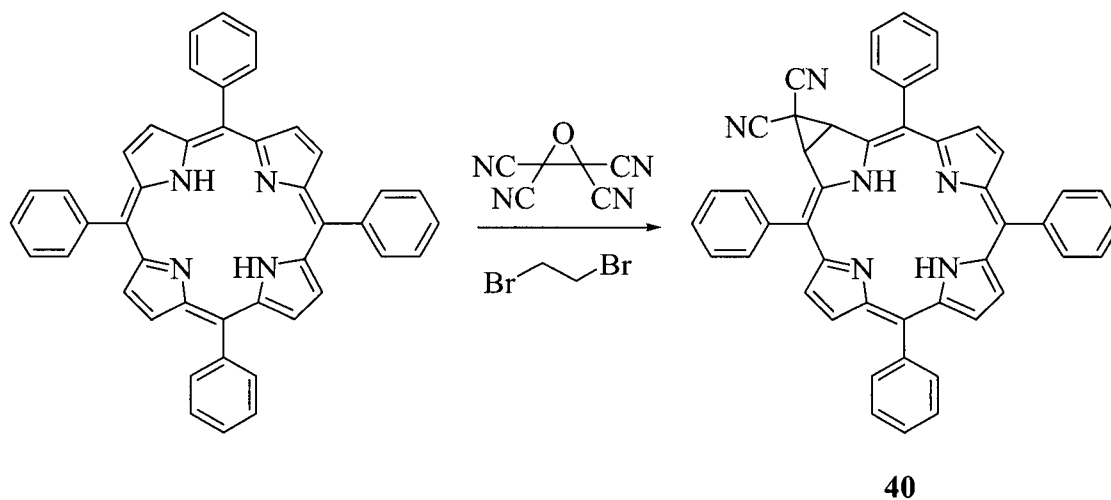
2.2.2 Carbonyl Ylides

Carbonyl ylides are discussed in Section 1.3.4.2. Two different 1,3-dipoles were used in reactions with porphyrin dipolarophiles. Firstly, the electron deficient carbonyl ylide obtained from heating tetracyano⁽⁵⁾ethyleneoxide (Scheme 1-31),¹⁵¹ and secondly, the unstabilized carbonyl ylide obtained from a two electron reduction of α,α' -dichloromethylether (Figure 1-32).¹⁵²

2.2.2.1 Tetracyanoethylene Oxide

In 1965, Linn and Benson found that upon heating tetracyanoethylene oxide (TCNEO) undergoes first order electrocyclic ring opening reactions.¹⁵³ The resulting carbonyl ylide was found to react with olefins, acetylenes and benzene.³⁴ The experimental conditions consisted of refluxing TCNEO with the dipolarophile at 100 °C

for a period between 4-24 h. The reaction proceeds well for many different dipolarophiles, including aromatic systems such as naphthalene and benzene.¹⁷¹ The dicyanocyclopropylchlorin (**40**) was previously assumed to be the product synthesized from the reaction between TCNEO and TPP in this lab.¹⁵⁴



Scheme 2-6. Original Assumed Product of TCNEO/TPP Reaction.

This potential functionalization of the cycloadduct **40** was intriguing. For example, the cyano groups may be hydrolyzed to the carboxylic acids, and then decarboxylation of one of the carboxylic moieties would leave one acid group available for derivitization.

The procedure for hydrolysis was to reflux **40** in conc. HCl for 6 h.¹⁵⁵ This gave a very polar (R_f 0.6 49 % 49 % 2 % acetone/ CH_2Cl_2 /acetic acid) light blue spot on a silica tlc plate. The product **40a** was very insoluble and difficult to purify. The UV-Vis spectrum was characteristic of that of a chlorin (Soret; 418.0 nm, Q-bands; 518.0, 546.0, 596.0 and 645.9 nm, 654.6 nm being the most intense Q-band). Crude **40a** was isolated and reacted further to methylate the acid groups so as the resultant product would be

easier to purify. **40a** was heated in DMSO, in the presence of excess dimethyl sulfate and potassium carbonate.¹⁵⁶ This reaction gave two products, both of which were less polar than **40a**, a more polar product with a characteristic chlorin UV-Vis spectrum (**41**), and a less polar blue spot.

The UV-Vis spectrum of the product isolated from the more polar spot **41** on a tlc plate gave a characteristic chlorin spectrum (Soret; 416 nm, Q-band; 518, 544, 592 and 646.1 nm, 646.1 nm being the most intense of the Q-bands). The N.M.R. data showed a high degree of symmetry in the isolated product, with only 3 β -proton peaks observed at 8.60 (2H, d, $J = 4.89$ Hz), 8.45 (2H, s) and 8.28 ppm (2H, d, $J = 4.89$ Hz). The signals observed for the phenyl protons were between 8.13-7.66 ppm (20H, m), while the signal assigned to the NH protons was at 1.96 ppm (2H, s). The most striking parts of the observed N.M.R. spectrum were the signals assigned to the pyrrolidine protons at 6.02 ppm (2H, s), the THF ring protons assigned to the signal at 4.92 ppm (2H, s) and the methoxy protons assigned to 3.53 ppm (6H, s). The two proton singlet observed at 4.92 ppm was unexpected. The proposed cyclopropane ring structure (Scheme 2-6) would yield an N.M.R. spectrum without the observed singlet at 4.92 ppm. Low resolution mass spectrometry gave the M^+ of this product to be 775 m/z, while high resolution mass spectral data confirmed the molecular formula to be $C_{50}H_{38}N_4O_5$. These suggest a structure as shown in Figure 2-4. These data seem to conflict with the proposed structure of **40**. The dicyanocyclopropanochlorin shown in Scheme 2-6 has also recently been synthesized independently by another method, and again, the spectroscopic data conflict with the data originally obtained from compound **40**.¹⁵⁷

Compound **40** was re-submitted for mass spectrometry. Initially, the mass spectrum was obtained by electron impact (E.I.). This method may make it more difficult to obtain the molecular ion, due to the high energy mass ions produced. LSIMS (liquid secondary ion mass spectrometry) was then chosen as a second attempt to obtain a mass spectrum of the compound. The LSIMS spectrum gave a molecular ion of 759 m/z, which corresponds to the molecular mass of **41**, suggesting the structure of the 1,3-dipolar cycloadduct. The peak that corresponds to the dicyanocyclopropyl cycloadduct ion was not observed in this mass spectrum. It seems that the initial characterization was incorrect.

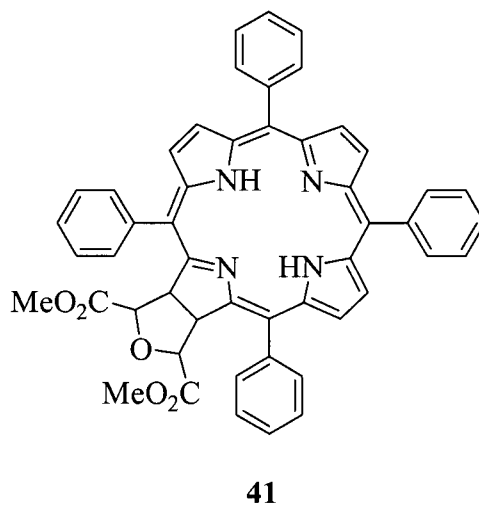


Figure 2-4. Product of Acid Hydrolysis and Methylation of 40.

The structure of **40** proposed with the mass spectral data obtained from this thesis work is as shown in Figure 2-5.

The reaction outlined in Scheme 2-6 was attempted with a variety of dipolarophiles. The reaction of TCNEO with CoTPP was attempted at $-78\text{ }^{\circ}\text{C}$, $100\text{ }^{\circ}\text{C}$, and $0\text{ }^{\circ}\text{C}$. The only product that was recovered from these reactions was a brown, oily

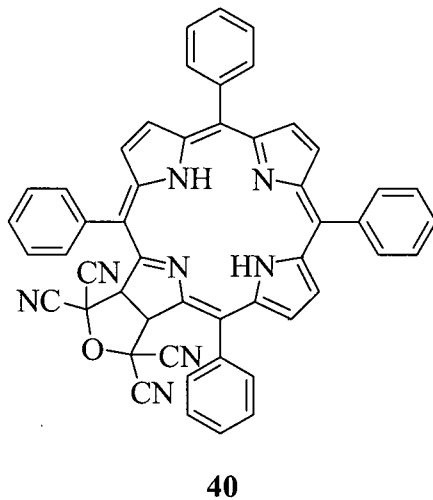


Figure 2-5. Structure of Compound 40.

compound that did not give a UV-Vis spectrum characteristic to that of a porphyrin, and could not be purified. Using polar solvent conditions and silica tlc, a brown smear was observed. No reason could be found for why this decomposition reaction was so vigorous, even at low temperatures. The reaction of NiTPP with TCNEO in toluene gave TPP, and no other discernible compounds. The reaction of n-confused porphyrin **43**

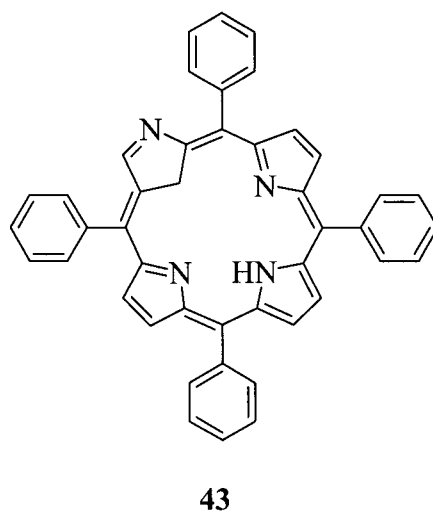


Figure 2-6. n-Confused porphyrin.

(Figure 2-6) gave many different products that in the end could not be purified, but looked interesting for future work. No reaction was observed between TCNEO and pFTPP.

Of the products that were obtained (**40**, **40a** and **41**) it is interesting to note the differences in their UV-Vis spectra.

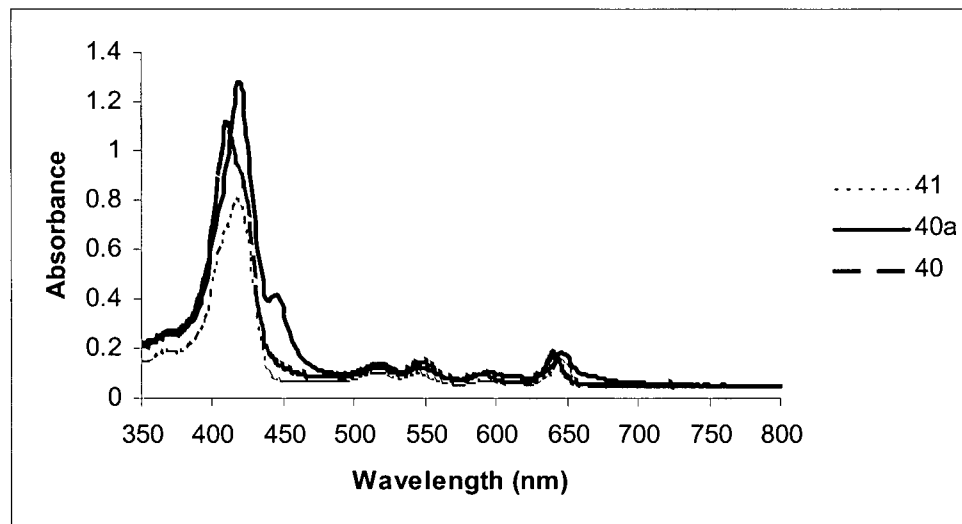
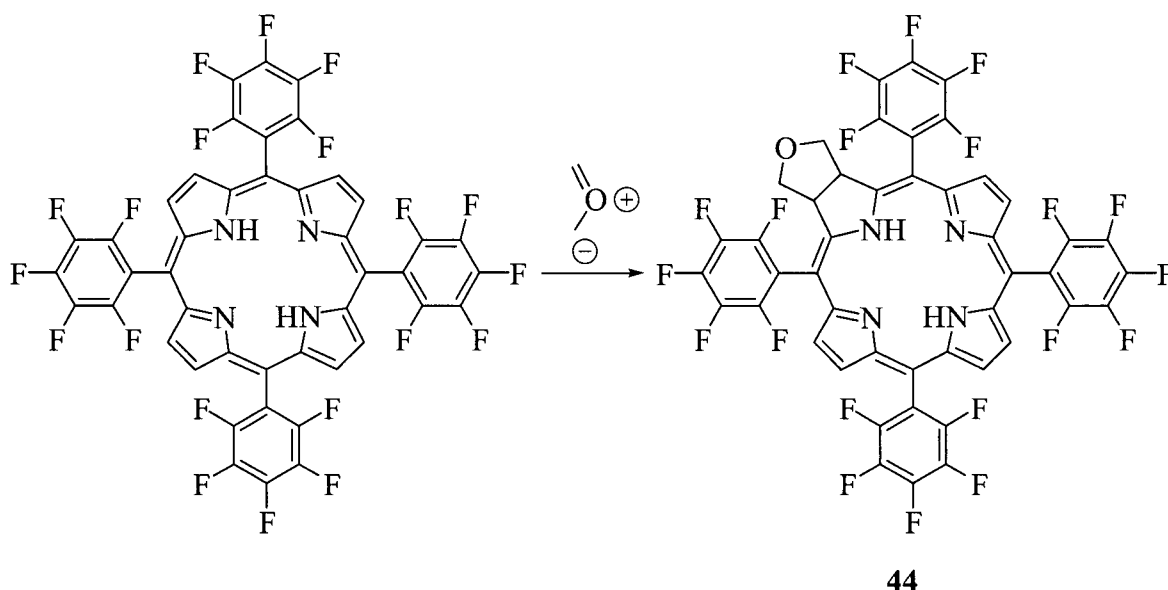


Figure 2-7. UV-Vis Spectra of 40, 40a and 41.

The major difference is seen between the UV-Vis spectra of **40** and **40a**. As the cyano groups are hydrolyzed, and replaced with carboxylic acids, the UV-Vis spectra show a “red-shifting” of the Soret and the Q-bands. This could represent a difference in the electron withdrawing ability of the acid groups as compared to a cyano groups, or the difference in the steric requirements. A change to the acid groups decreases the gaps between the orbitals responsible for the absorption peaks, which would manifest itself in the observed red-shift.

2.2.2.2 Unstabilized Carbonyl Ylide

Unstabilized carbonyl ylides are discussed in Section 1.3.4.3. The reaction used in this experiment to synthesize the ylide was the two electron oxidation of the α,α' -dichloromethylether (Scheme 1-32). This reaction has been used for 1,3-dipolar cycloadditions with many dipolarophiles.¹⁵⁸ This includes electron deficient dipolarophiles such as ester substituted double bonds, and electron rich dipolarophiles such as phenyl sulfide substituted double bonds.¹⁷⁶



Scheme 2-7. Unstabilized Carbonyl Ylide Reaction with pFTPP to form 44.

The only reaction that was successful in this set of experiments was with pFTPP. The reaction yielded two products that were of similar polarity on silica tlc (R_f 0.5 50 % $\text{CH}_2\text{Cl}_2/\text{hexane}$). The UV-Vis spectrum of the less polar compound was typical of a chlorin (Soret; 414 nm, Q-bands; 506, 602 and 656 nm, 656 nm being the most intense Q-band). The N.M.R. spectrum of this product showed a highly symmetrical structure.

The signals for the β -protons are located at 8.70 (2H, d, $J = 4.9$ Hz), 8.47 (2H, s) and 8.38 ppm (2H, d, $J = 4.9$ Hz). The signals of the protons located on the pyrrolidine ring are observed at 5.33 ppm (2H, t, $J = 4.36$ Hz). The peaks representing the THF ring are observed at 4.20 (2H, t, $J = 8.17$ Hz) and 3.92 ppm (2H, dd, $J = 4.36$ Hz and 8.17 Hz). These three sets of protons show correlations to one another in the ^1H COSY spectrum. The mass spectrum of this compound has a parent ion at 1019 m/z, which corresponds to the molecular mass of the desired cycloaddition product, suggesting its formation. The more polar product gave a typically bacteriochlorin spectrum (Soret; 374 nm, Q-bands; 506, 582 and 732 nm, 732 nm being the most intense Q-band) but in the course of purifying this mixture, the bacteriochlorin product could not be obtained in large enough quantities to be fully characterized. Other dipolarophiles used in the reactions with unstabilized carbonyl ylides (Scheme 2-7) were NiTPP, ZnTPP, diphenylporphyrin (DPP), tetra(*p*-nitrophenyl)porphyrin and β -nitro-tetraphenylporphyrin all of which gave no satisfactory results.

The results of the above reactions are good examples of the differences between type one, two and three 1,3-dipolar cycloaddition reactions. The stabilized carbonyl ylide reacted very well with the electron rich cross-conjugated double bond of TPP, while the unstabilized carbonyl ylide did not react at all. pFTPP, on the other hand, reacted very well with the unstabilized carbonyl ylide, but not with the tetracyano-substituted carbonyl ylide. It is presumed that the four cyano groups cause the carbonyl ylide to react more like a type three dipole, which would allow it to react with the relatively electron rich TPP. The electron withdrawing groups lower the LUMO of the dipole to the point at which the dominant interaction becomes the LUMO of the dipole, and the HOMO of the

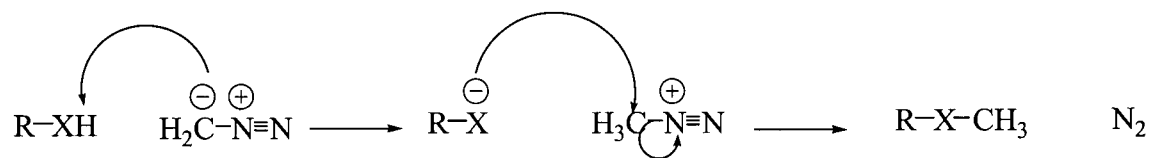
dipolarophile (Section 1.3.3). The unstabilized ylide, reacts as a type one dipole, as one would expect (Section 1.3.3). These reactions provide insight into assessing which dipoles will react with which porphyrin dipolarophile. Electron deficient dipoles seem to react more efficiently with TPP, while the relatively electron rich dipoles react better with pFTPP.

2.2.3 Diazoalkanes

Diazoalkanes were discussed in Section 1.3.4.1. Two diazoalkanes will be discussed in this section, diazomethane and trimethylsilyldiazomethane.

2.2.3.1 Diazomethane

Diazomethane is synthesized by the reaction of n-methyl-n-nitroso amines with a base (Scheme 1.25). Diazomethane has been used in reactions with many different reagents.²¹⁶ Other than the cycloaddition reaction that will be discussed here, diazomethane is also a very efficient methylating agent.¹⁵⁹ Diazomethane first acts as a base to remove the proton from the heteroatom that it will be replacing and then methylates the heteroatom (Scheme 2-8).

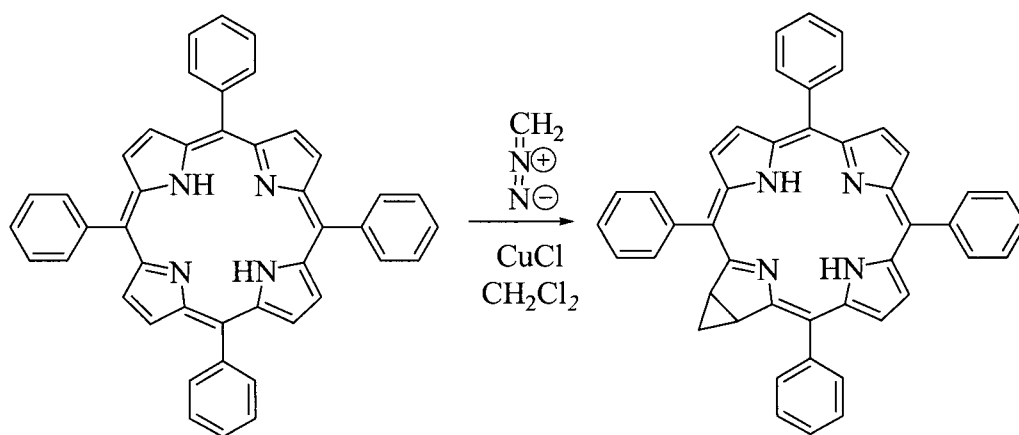


Scheme 2-8. Mechanism of Diazomethane Methylation (X = O, S, or N).

Diazomethane has been used for cycloaddition reactions with a variety of dipolarophiles giving pyrazolines including alkenes (electron rich and poor), dienes, heterodipolarophiles, heterocumulenes and triple bonds.^{160,213} The cycloaddition of diazomethane is a well established synthetic process.

Pyrazolines eliminate N_2 to form cyclopropane rings. The pyrolytic elimination of N_2 covers an activation energy range from a low of 15-20 kcal/mol to a high of 40-45 kcal/mol.²¹⁴ This activation energy difference translates into decomposition temperatures that range from -100°C to 300°C .¹⁶¹ N_2 extrusion can also be achieved photochemically.

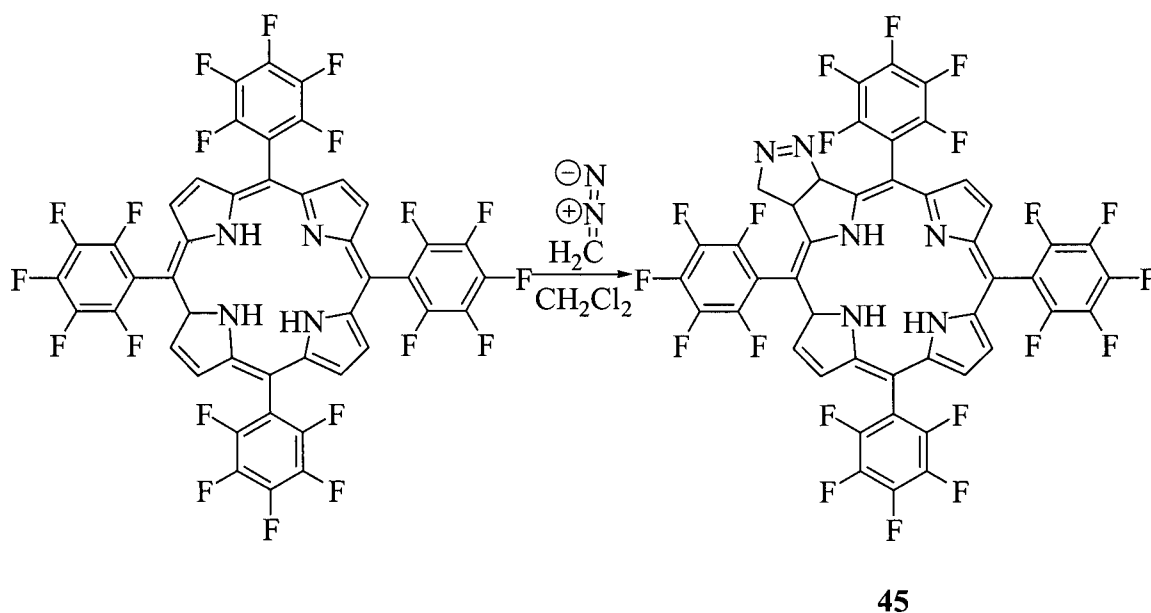
Previous work involving the reaction of porphyrins with diazomethane did not yield the pyrazoline.²¹⁵ Callot *et al.* have reported on reactions between diazomethane and porphyrins using a copper catalyst.¹⁶² Through this method the cyclopropane ring cycloadduct was obtained in 30 % yield (Scheme 2-9).



Scheme 2-9. Cyclopropanation of TPP.

Diazomethane, a type one dipole, reacts much more efficiently with electron poor dipolarophiles, thus a reaction with pFTPP would be more likely to yield the desired cycloadduct. A large excess of diazomethane was added to a CH_2Cl_2 solution of the dipolarophile pFTPP. A more polar (R_f 0.7, 50 % $\text{CH}_2\text{Cl}_2/\text{hexane}$) green spot compared with the less polar spot of the precursor was observed on a silica tlc plate. Upon purification on a silica preparatory tlc plate, the product was found to have a UV-Vis spectrum characteristic to that of a chlorin (Soret; 402 nm, Q-bands; 504, 598, 648 nm,

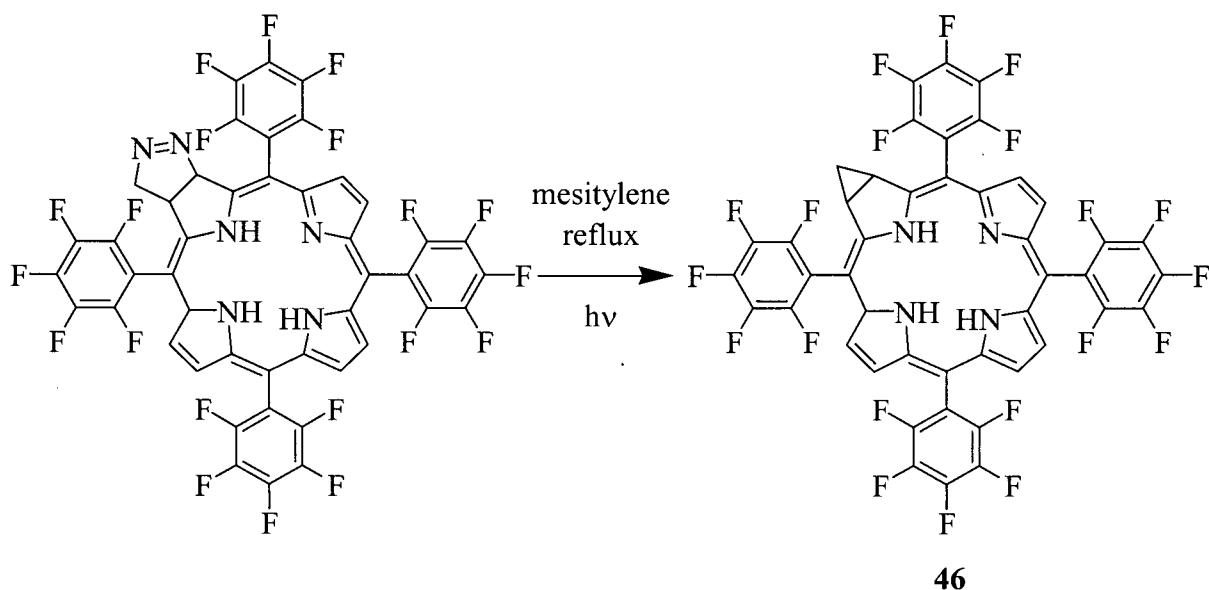
648 nm being the most intense Q-band). The N.M.R. data did not show a symmetrical product as compared to the previous examples. The signals that represent the β -protons are found at 8.80 (1H, d, $J = 4.89$ Hz), 8.77 (1H, d, $J = 4.89$ Hz), 8.61 (1H, d, $J = 4.89$ Hz), 8.53 (2H, s) and 8.44 ppm (1H, d, $J = 4.89$ Hz). The signal observed for one of the pyrrolidine peaks of the chlorin appears at 7.72 ppm (1H, d, $J = 8.8$ Hz). Along with correlation of this proton to the adjacent pyrrolidine proton, this peak also shows a weak ^1H COSY correlation to one of the pyrazoline protons. This signal was assigned to the proton adjacent to the azo-nitrogens. A peak observed at 5.11 ppm (2H, m) was assigned to both the other pyrrolidine proton and a pyrazoline proton. The other pyrazoline proton is found at 4.92 ppm (1H, m). The NH pyrrole proton signals are observed at -2.09 ppm (2H, s). The mass spectrum of the chlorin gave a molecular ion of 988 m/z , which corresponds to the calculated mass of the desired cycloadduct. High-resolution mass spectral analysis confirmed the molecular formula to be $\text{C}_{45}\text{H}_{12}\text{N}_6\text{F}_{20}$, which is the molecular formula of the expected product **45**.



Scheme 2-10. Reaction of Diazomethane with pFTPP.

The reaction shown in Scheme 2-10 has the possibility of producing two enantiomers, as the attack of diazomethane is possible from either side of the plane of the porphyrin ring. The long range coupling between the pyrazoline protons and the pyrrolidine proton adjacent to the azo-nitrogens mentioned on the previous page is due to homo-allylic coupling, which is common in these types of compounds.

Compound 45 is stable at *r.t.* for long periods of time (9 months), however under certain conditions, N₂ will be eliminated. An initial attempt to synthesize the cyclopropane from the pyrazoline (45) consisted of refluxing a toluene solution of the pyrazoline overnight. No observable change was noted on a tlc plate as compared to the starting material. The solvent was then changed to mesitylene, and this solution was refluxed (Scheme 2-11). After 1 h, silica tlc showed no starting material, and only a less polar product (R_f 0.8, 20 % CH₂Cl₂/hexane) that was green on a silica tlc plate. This product had a UV-Vis spectrum characteristic to that of a chlorin (Soret; 410 nm, Q-bands; 508, 606.1 and 662.0 nm, 662.0 nm being the most intense Q-band) and N.M.R. data suggest a symmetrical structure. There are only three signals that correspond to the β-protons at 8.67 (2H, d, J = 4.78 Hz), 8.43 (2H, s) and 8.40 ppm (2H, d, 4.78 Hz). The signals assigned to the cyclopropane are located at 3.90 (2H, dd, J = 4.10 Hz), 1.90 (1H, m) and 0.84 ppm (1H, m). The mass spectrum of this chlorin shows a MH⁺ peak at 988 m/z, and confirms the molecular formula to be C₄₅H₁₂N₄F₂₀ which suggests the cyclopropane adduct 46.



Scheme 2-11. Cyclopropane Formation from Pyrazoline.

The same product **46** is formed when a dilute sample of **45** (1 mg in 2 mL of toluene d_6) is placed in sunlight for 1 h. Both photochemical and thermal reactions are clean, forming only the cyclopropane cycloadduct.

The UV-Vis spectra of the pyrazoline and the cyclopropyl group chlorins are quite different (Figure 2-8). The peaks observed in the spectrum of the cyclopropyl chlorin are red-shifted as compared with that of the spectrum of the pyrazoline chlorin. The reason for this is not well understood. One reason could be that the cyclopropane ring is highly strained (Figure 2-9).

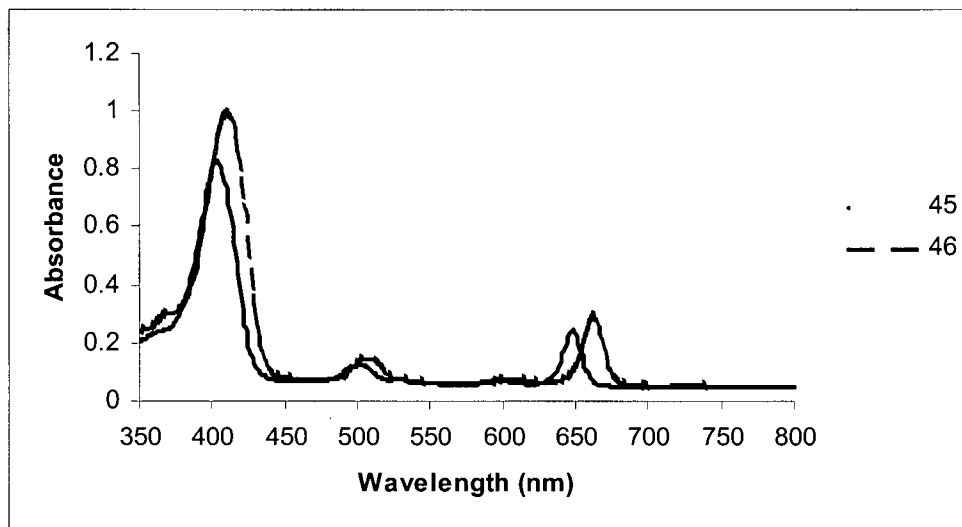


Figure 2-8. UV-Vis Spectra of 45 and 46.

This strain causes what would normally be considered to be sp^3 orbitals in an aliphatic compound, to resemble sp^2 orbitals. These “intermediate orbitals” (Figure 2-9) may then be able to conjugate to the porphyrin ring, in much the same way a double bond would. This resultant conjugation may shift the absorption bands to higher wavelengths. Another reason could be the strained cyclopropyl ring may distort the porphyrin ring, and through this causes a change in the electronic spectra.

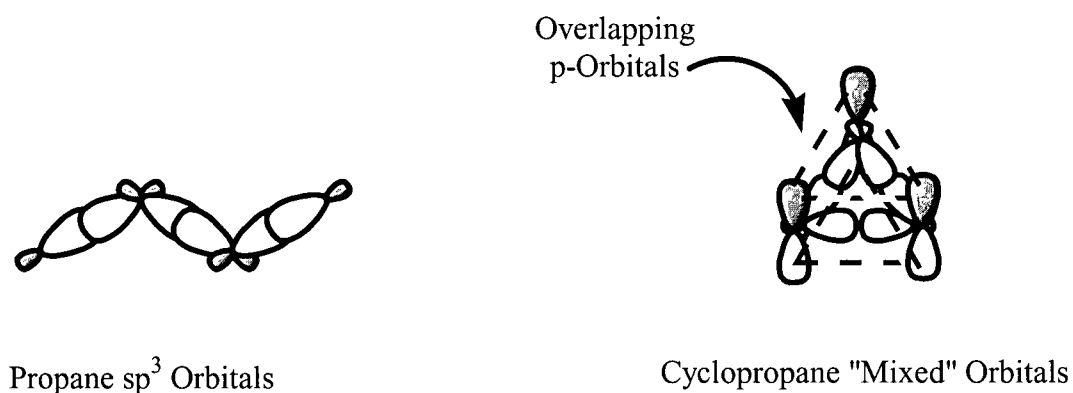


Figure 2-9. Cyclopropane "Mixed Orbitals".

trimethylsilyl group is a relatively large molecule as compared to the hydrogens on diazomethane, and would hamper the approach of the reactive center to the dipolarophile. The trimethylsilyl group is also electron donating and should have an opposite effect on reactivity to that of the steric factor. The electron donating group would destabilize the HOMO of the dipole thus decreasing its energetic distance to the LUMO of the dipolarophile. This effect should increase the rate of the 1,3-dipolar cycloaddition. In this case, it seems that the steric consideration is the more important factor in determining the rate of the reaction, as the diazomethane reaction was shown to be more efficient.

2.2.4 Nitrile Oxides

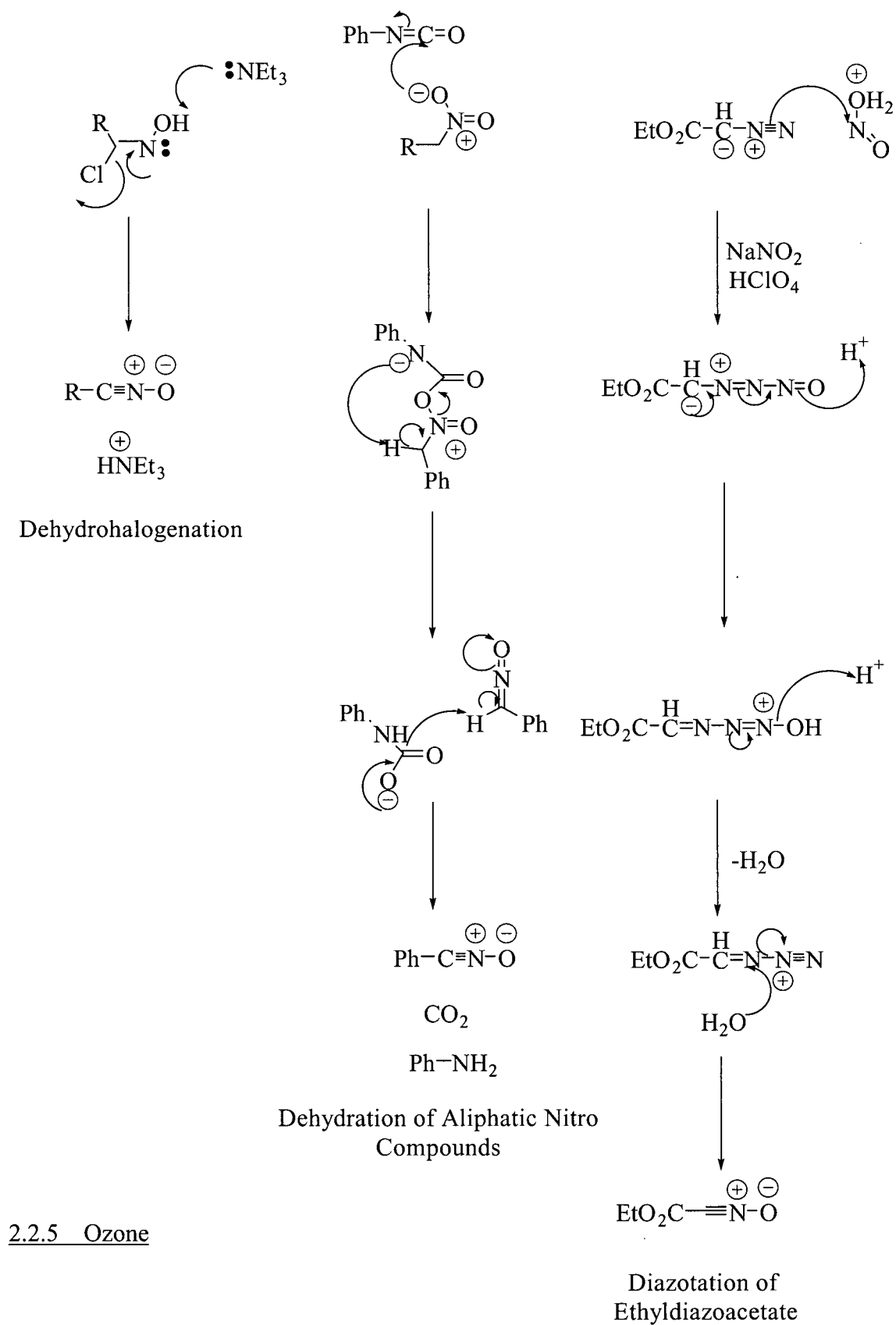
Nitrile oxides are discussed in detail in "1,3-Dipolar Cycloaddition Chemistry".¹⁶³ There are many ways to synthesize nitrile oxides.¹⁸¹ The methods described in this thesis are dehydrohalogenation of hydroximoylchlorides,²¹⁷ dehydration of aliphatic nitro groups,²¹⁷ and diazotation of ethyl diazoacetate (Scheme 2-12).²¹⁷ Nitrile oxides dimerize rapidly. The only way to combat this is to ensure that the generation of the 1,3-dipole is very slow, and that the concentration of the nitrile oxide remains low (Scheme 2-12).

Several methods of dehydrohalogenation were attempted. There were no significant results acquired from dehydrohalogenation reactions with aryl hydroximoylchlorides. The dehydration of aliphatic nitro groups was attempted in the presence of many different dipolarophiles. A reaction of 1-nitropropane was attempted with phenyl isocyanate in the presence of TPP, NiTPP, β -nitro tetraphenylporphyrin, tetrakis(p-nitrophenyl)porphyrin, ZnTPP or pFTPP. The only reaction that gave a result was the reaction with pFTPP. A spot more polar than the starting material was observed

on the tlc plate and the UV-Vis spectrum of the crude product showed the longest wavelength absorption band growing more intense as the reaction progressed, but nothing was isolated from this reaction.

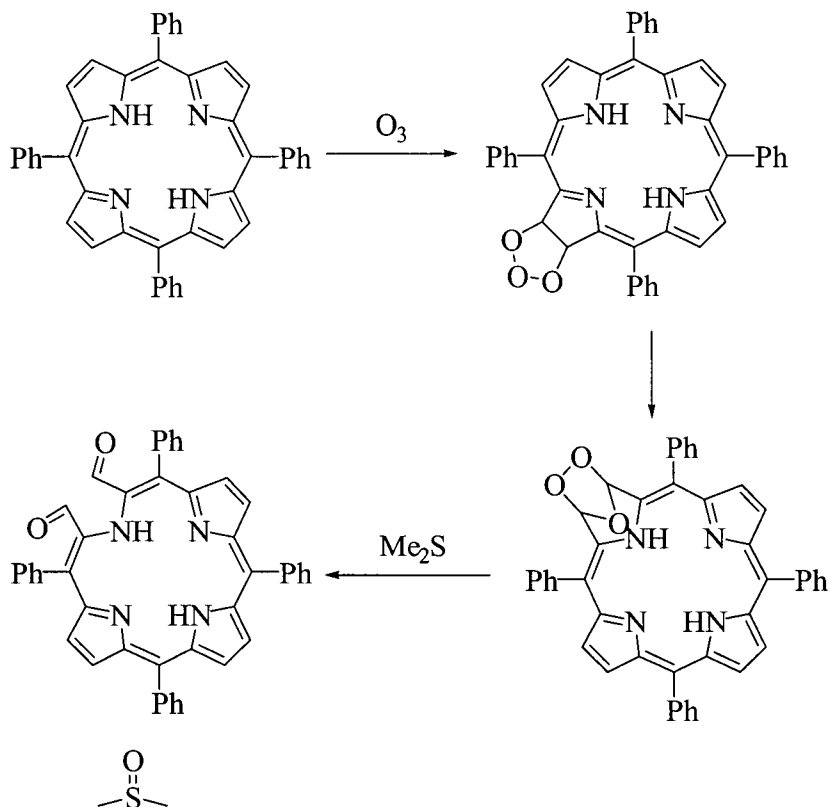
The diazotation of ethyldiazoacetate to form the nitrile oxide was done in the presence of pFTPP or TPP. The reaction with pFTPP was unsuccessful. The reaction with TPP, gave a more polar green spot on a silica tlc plate, however, a product could not be isolated.

The reactions with nitrile oxides were not fruitful. The reason for this presumably is that the reactive intermediates have exceedingly short lifespans, due to their tendency to dimerize. This makes it very difficult to promote a reaction with such an unreactive dipolarophile as a porphyrin.



Scheme 2-12. Methods of Nitrile Oxide Formation.

Being a type three dipole, it was thought that ozone might give some interesting products in reactions with porphyrins. Electrical arcing of oxygen produces



Scheme 2-13. Predicted Products of Porphyrin Ozonolysis.

ozone, and a variety of porphyrins were reacted with ozone. In these reactions, dimethyl sulfide was used to reduce the ozonide. This allows the ozonide to form two aldehydes (Scheme 2-13). If the reactions were to succeed on a porphyrin, a sechochlorin would be formed.¹⁶⁴

These reactions were performed at $0^\circ C$, samples were taken from the reaction flask at regular time intervals, quenched with dimethylsulfide, and the products were observed using silica tlc. Initially, TPP was used as the dipolarophile, and during the

reaction, the observed tlc plates showed two different spots, starting material, and a polar baseline spot. The UV-Vis spectrum showed an increasingly chlorin-like spectrum (intense high wavelength absorption). Upon work-up though, none of the chlorin spectrum, as evidenced by UV-Vis spectral analysis and the portions of the reaction that were left the longest, showed no porphyrin characteristics in the UV-Vis spectrum. It was determined that the intense high wavelength band resulted from protonation of the inner pyrrole nitrogens of the porphyrins. The only products that were obtained in the reaction with TPP, ZnTPP, DPP, NiTPP and Lu(acac)TPP were decomposition products, with no fine structure observable in the UV-Vis spectra.

2.2.6 Thiocarbonyl Ylides

Thiocarbonyl ylides are discussed in Section 1.3.4.4. Being a typical type one dipolarophile, it was thought the thiocarbonyl ylides would react best with the electron poor dipolarophile pFTPP. Two methods for the synthesis of the unstabilized thiocarbonyl ylide were used in this thesis.

The first method for synthesis of the thiocarbonyl ylide was the double desilylation of α,α' -di(trimethylsilylmethyl)sulfide with AgF. It was thought that the azomethine ylides could be synthesized via this procedure, thus possible to synthesize thiocarbonyl ylides in the same manner. The α,α' -di(trimethylsilylmethyl)sulfide was synthesized by reacting Na_2S with chloromethyltrimethylsilane.¹⁶⁵ The cycloaddition reaction was performed in a similar manner to that of the azomethine ylides (Section 2.2.1). AgF and pFTPP were stirred under N_2 in THF and the sulfide was added to this solution in THF. A silver mirror on the inside of the reaction flask appeared after stirring the reaction mixture overnight. Only one reaction product was observed on a silica tlc

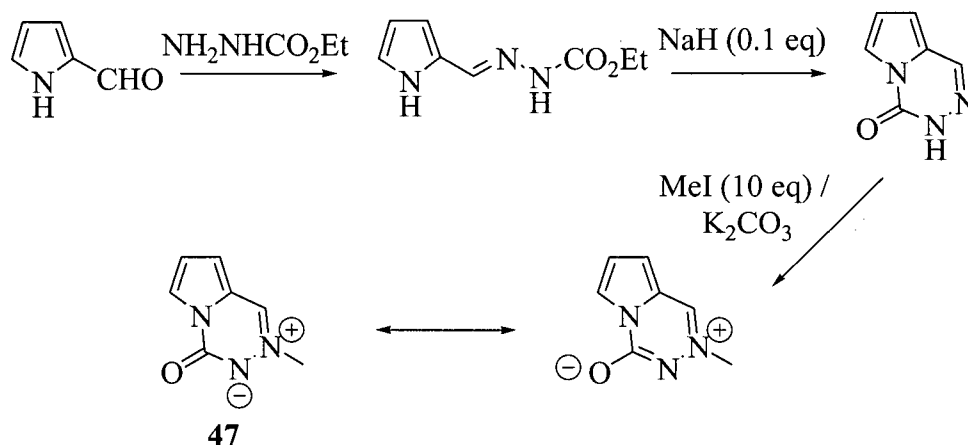
plate (R_f 0.5, 50 % $\text{CH}_2\text{Cl}_2/\text{hexane}$). This product, after purification, exhibited a characteristic metallo-porphyrin UV-Vis spectrum. The reaction was discontinued after two weeks.

The other method for the synthesis of the thiocarbonyl ylide is the elimination of disiloxane from bis(trimethylsilyl)methyl sulfoxide (Scheme 1-33).¹⁶⁶ This method has been used in cycloaddition reactions with many dipolarophiles, and works well with electron poor species, thus a reaction was attempted with pFTPP. The sulfoxide was synthesized via NaIO_4 oxidation of the sulfide.²²² The sulfoxide and the pFTPP, both dissolved in HMPA, were then added to HMPA at 100°C . Only starting material and silica tlc baseline material were recovered. This reaction was discontinued.

2.2.7 Azomethine Imines

Grashey discusses the reactions of azomethine imines in detail.¹⁶⁷ The example investigated in this thesis, mesomeric betaines,¹⁸⁵ is detailed in Section 1.3.3.1. They are functionally azomethine imines, and are intriguing because of their preference for reacting with electron rich dipolarophiles.¹²⁶ The pyrrolotriaziniumolate systems utilized in this thesis were synthesized by the method shown in Scheme 2-14. The cycloaddition reaction was attempted by heating **47** with a selected dipolarophile in toluene.¹²⁶ pFTPP, TPP and DPP were all used as dipolarophiles. The DPP reactions were attempted both with and without $\text{MgBr}_2 \cdot \text{H}_2\text{O}$ as a catalyst. The catalyst is thought to act by coordinating to the carbonyl oxygen to lower the LUMO level of the dipole,¹⁶⁸ thus making the type three cycloaddition more facile.

All of the reactions that were attempted failed to yield any products. It is possible that the steric congestion that occurs when using such a large dipole was the dominating factor.



Scheme 2-14. Synthesis of Mesomeric Betaine 47.

2.2.8 Azides (N_3^-)

Lwowski discusses azides in detail.¹⁶⁹ The cycloadditions of azides to dipolarophiles are stereospecific and reversible.¹⁸⁷ Azides are type two dipolarophiles, and can react efficiently with both electron rich and poor dipolarophiles.

Azides were reacted with both pFTPP and TPP. An excess of trimethylsilylazide was refluxed with either pFTPP or TPP in THF. The reaction with pFTPP gave a more polar red spot on a silica tlc plate. The compound that corresponds to this spot had a UV-Vis spectrum characteristic to that of a chlorin. Unfortunately, the amount of the compound isolated was small and no other structural characterizations were obtained. The possible 1,3-dipole cycloadduct structure is shown in Figure 2-10.

The second type of azide that was used in a reaction with TPP and pFTPP is NaN_3 .⁶¹ This reactant undergoes 3^-+2 cycloadditions where the products are negatively

charged. The procedure of refluxing the azide with a dipolarophile in DMF has been used to form cycloadducts with cyano dipolarophiles.²²⁸ The reacting orbital is the allyl

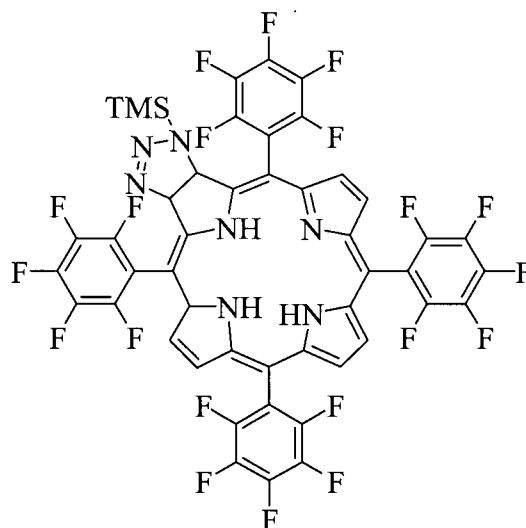


Figure 2-10. Possible Trimethylsilylazide Cycloaddition Product.

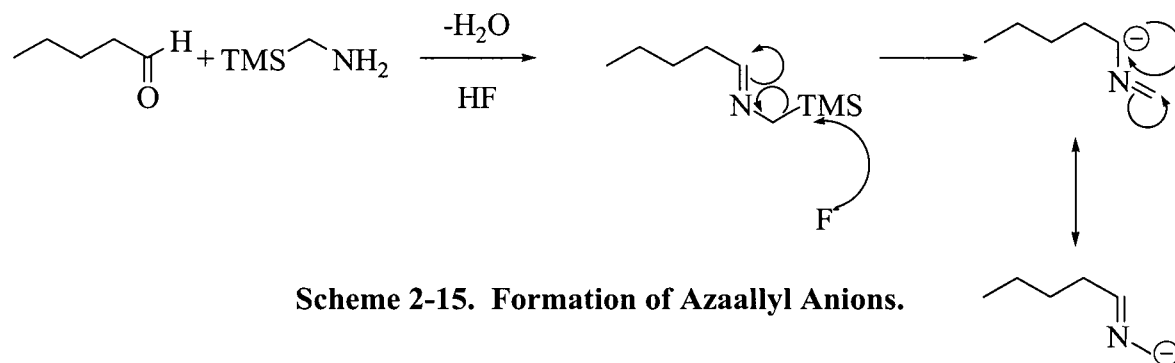
anion orbital, in the same way as the azaallyl anions react (Section 1.3.4.2). Unfortunately, none of the reactions yielded products, thus the reactions were discontinued.

2.2.9 Azaallyl Anions

Azaallyl anions are discussed in Section 1.3.4.2. These reactive intermediates have been used to react with many different dipolarophiles.¹⁷⁰ They are able to react with both electron rich and electron poor dipolarophiles.²³⁰ The reaction that was attempted in this thesis required the formation of the azaallyl anion from (2-azaallyl)silanes.¹⁷¹

The procedure consisted of first forming the (2-azaallyl)silane *in situ* at *r.t.*, and then cleaving the silyl group with HF•pyr at 50°C (Scheme 2-15). The reaction was

attempted with trimethylsilylmethylamine and *iso*-valeraldehyde to form the (2-azaallyl)silane while pFTPP and DPP were used as the dipolaophiles. The reaction did not provide any product, only starting material was recovered. The reactions were discontinued.



Chapter Three: Conclusions and Suggestions For Future Work

In this thesis, the synthesis, isolation and characterization of novel chlorins were investigated. Initially the reactions between carbonyl ylides and porphyrins were performed. The TPP reaction with TCNEO yielded compound **40** in moderate yield, which was then hydrolyzed and methylated to form compound **41**. The pFTPP reaction with non-stabilized carbonyl ylide, synthesized from α,α' -dichloromethylether, yielded compound **44** in moderate yield. These results suggest that electron rich TPP will undergo 1,3-dipolar cycloaddition with electron poor carbonyl ylides in what might be a LU controlled process, while the electron poor pFTPP will undergo 1,3-dipolar cycloaddition with non-stabilized carbonyl ylides in an HO controlled process. This concept could be investigated further with the variety of dipoles and dipolarophiles available.

Novel chlorins were then synthesized via reaction between electron deficient pFTPP and non-stabilized azomethine ylides synthesized from α,α' -di(trimethylsilylmethyl)amines to form compounds **36a-38a**. These results are evidence that electron deficient porphyrins are required to undergo 1,3-dipolar cycloaddition with type one dipoles such as azomethine ylides, as many porphyrins were investigated, with only pFTPP yielding a successful reaction. In continuation of this research, there are a variety of amines available for use in the synthesis of α,α' -di(trimethylsilylmethyl)amines which could then be used in 1,3-dipolar cycloadditions with various electron deficient porphyrins.

Diazomethane was used to synthesize novel chlorin **45** via 1,3-dipolar cycloaddition with pFTPP. **45** was then subjected to heat in refluxing mesitylene, or sunlight, both of which caused the extrusion of N₂ to form **46**. Again, the successful 1,3-dipolar cycloaddition reaction between diazomethane and pFTPP shows the requirement for electron deficient porphyrins in reaction with type one dipoles, as this reaction has never been reported to be successful with TPP or other electron rich porphyrins. In continuation of this research, other electron deficient porphyrins could be investigated in 1,3-dipolar cycloadditions with diazomethane.

The purpose of this thesis was to synthesize novel chlorins for their use as photosensitizers in PDT. Investigation of the chlorins synthesized in the course of this thesis for use in PDT would yield insight into the physical properties of photosensitizers as the fluorinated chlorins have not been investigated for this purpose.

Chapter 4: Experimental

4.1 Instrumentation and Materials

Mass Spectra

Mass spectrometric analyses were carried out by the B. C. Regional Mass Spectrometry Center at the University of British Columbia, Department of Chemistry. Low and high resolution mass spectra were obtained by liquid secondary ion mass spectrometry (LSIMS), and were determined on a KRATOS Concept IIIHQ hybrid mass spectrometer. Molecular ions are designated as MH^+ .

UV-Vis Spectra

UV-Vis spectra were taken on a Carey 50. Wavelengths for each absorption maximum (λ_{max}) are reported in nanometers (nm).

Nuclear Magnetic Resonance Spectrometry

Proton nuclear magnetic resonance spectra (1H -NMR) were recorded on the following spectrometers: Bruker WH-400 (400 MHz), Bruker AV-400 (400 MHz) and Bruker AMX-500 (500 MHz). The positions of the signals are given as chemical shifts (δ) in parts per million (ppm) with respect to tetramethylsilane; however, the internal reference standard used in each case was the residual proton signal present in the deuterated solvent. Reported chemical shifts are followed in parentheses by the multiplicity of the peak, the coupling constant in Hz, and the number of protons. In some cases, 1H COSY experiments were used in order to ascertain structures.

Chromatography

Chromatographic purification's of compounds were carried out using silica gel 60, 70-230 mesh, supplied by E. Merck Co.. Thin layer chromatography (tlc) was carried out

on pre-coated silica gel plates (Merck 60, 230-400 mesh) with aluminum backing and fluorescent indicator (F₂₅₄). Preparative thin layer chromatography was performed on pre-coated 10 cm × 10 cm, 1 or 2 mm thick Merck silica gel plates.

Reaction conditions

Due to inherent light sensitivity of these compounds, all reactions were performed in a dark fumehood or surrounded by aluminum foil.

Reagents and Solvents

Unless otherwise specified, reagents were used as supplied by the Aldrich Chemical Company. Solvents were reagent grade and purified using standard literature procedures when necessary. Deuterated solvents were supplied by Cambridge Isotope Laboratory.

4.2 General Procedures and Data

Tetraarylporphyrin Synthesis

Tetra(*para*-nitrophenyl)porphyrin (T(*p*-NO₂)PP) was synthesized by Alder's method.¹⁷² The method involves the refluxing of the appropriate benzaldehyde and pyrrole in propionic acid (500 mL). This solution was concentrated to 100 mL and filtered through silica gel. The filtrate is concentrated again and purified by chromatography on silica gel (50 % CH₂Cl₂/hexane).

T(*p*-NO₂)PP: R_f 0.77 (silica; CH₂Cl₂); UV-Vis (CH₂Cl₂) λ_{max} 422, 518, 554, 592, 648; ¹H-NMR (400 MHz, CDCl₃, ppm) δ = 8.75 (s, 8H), 8.68 (d, J = 6.86 Hz, 8H), 8.59 (d, J = 6.84 Hz, 8H).

pFTPP was synthesized by the method of Drenth.¹⁷³ This method proceeds by adding 800 mL of distilled CH₂Cl₂ to a 2 L flask. To this 100 mL of 0.10 M pyrrole and

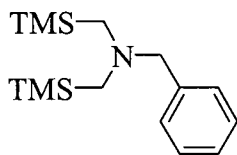
100 mL of 0.10 M benzaldehyde are added and the solution was purged with N₂ for 5 min. After 5 min. 4 mL of 0.5 M BF₃·Et₂O was then added, and the solution was stirred in the dark under N₂ for 24 h. 7.4 mol of DDQ was then added to the solution, and stirred for another 1 h, after which the solution is concentrated (200 mL) under reduced pressure and 20 g of alumina was added. The product is then purified by column chromatography on neutral alumina (30 % CHCl₃/hexane).

pFTPP: R_f 0.77 (silica; 50 % CH₂Cl₂/hexane); UV-Vis (CH₂Cl₂) λ_{max} (log ε) 411 (4.52), 507 (4.37), 584 (3.99), 658 (3.79); ¹H-NMR (200 MHz, CDCl₃, ppm) δ = 8.80 (s, 8H), -2.50 (s, 2H).

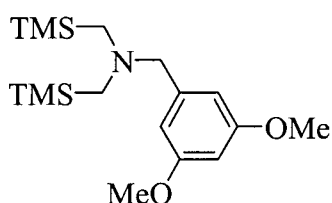
Zinc 2-nitro-5, 10, 15, 20-tetraphenylporphyrin (β -NO₂TPP) was produced by the following procedure.¹⁷⁴ ZnTPP is dissolved in 50 % CH₂Cl₂/CH₃CN and stirred under N₂ in the absence of light. AgNO₂ was dissolved in CH₃CN and was followed by I₂ dissolved in CH₂Cl₂. The reaction was left for 2 h in the dark, and then concentrated under reduced pressure. The final product was then purified by column chromatography on silica gel (75 % CHCl₃/hexane).

β -NO₂TPP: UV-Vis (CHCl₃) λ_{max} (log ε) 425 (5.28), 558 (4.20), 603 (4.14), ¹H-NMR (200 MHz, CDCl₃, ppm) δ = 9.18 (s, 1H), 8.80 (br s, 6H), 7.95-8.25 (m, 8H), 7.5-7.85 (m, 12H).

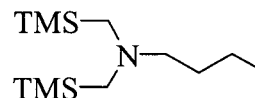
Synthesis of α, α' -(disilylmethyl)amines¹⁷⁵ (36, 37 and 38).



36



37



38

A solution of benzylamine (2 g, 18.6 mmol), chloromethyltrimethylsilane (4.56 g, 37.3 mmol) and potassium carbonate (5.14 g, 37.3 mmol) were refluxed in dry acetonitrile under N₂ for 68 h. The potassium carbonate was filtered off, and the mixture was concentrated under reduced pressure. The crude product was purified by column chromatography. The yield of the final product **36** was 76 %. Compound **37** was produced in the same manner using 3.12 g (18.6 mmol) of 3,5-dimethoxybenzylamine, 4.56 g (37.3 mmol) of chloromethyltrimethylsilylamine and 5.14 g (37.3 mmol) of potassium carbonate. The yield was 51 %. Compound **38** required 1.36 g (18.6 mmol) of *n*-butylamine, 4.5 g (37.2 mmol) of chloromethyltrimethylsilane and 5.14 g (37.2 mmol) of potassium carbonate. The yield of **38** was 59 %.

36: R_f 0.6 (silica; 20 % EtOAc/hexane); ¹H-NMR (400 MHz, CDCl₃, ppm) δ = 7.20 (m, 5H), 3.40 (s, 2H), 1.80 (s, 4H), 0.00 (2, 18H).

37: R_f 0.6 (silica; 20 % EtOAc/hexane); ¹H-NMR (400 MHz, CDCl₃, ppm) δ = 6.52 (d, J = 1 Hz, 2H), 6.32 (t, J = 1 Hz, 1H), 3.72 (s, 6H), 3.30 (s, 2H), 1.85 (3, 4H), 0.00 (s, 18H).

38: R_f 0.5 (silica; 20 % EtOAc/hexane); ¹H-NMR (400 MHz, CDCl₃, ppm) δ = 2.23 (t, J = 7.08 Hz, 2H), 1.86 (m, 4H), 1.31 (m, 4H), 0.88 (t, J = 7.08 Hz, 2H), 0.00 (s, 18H).

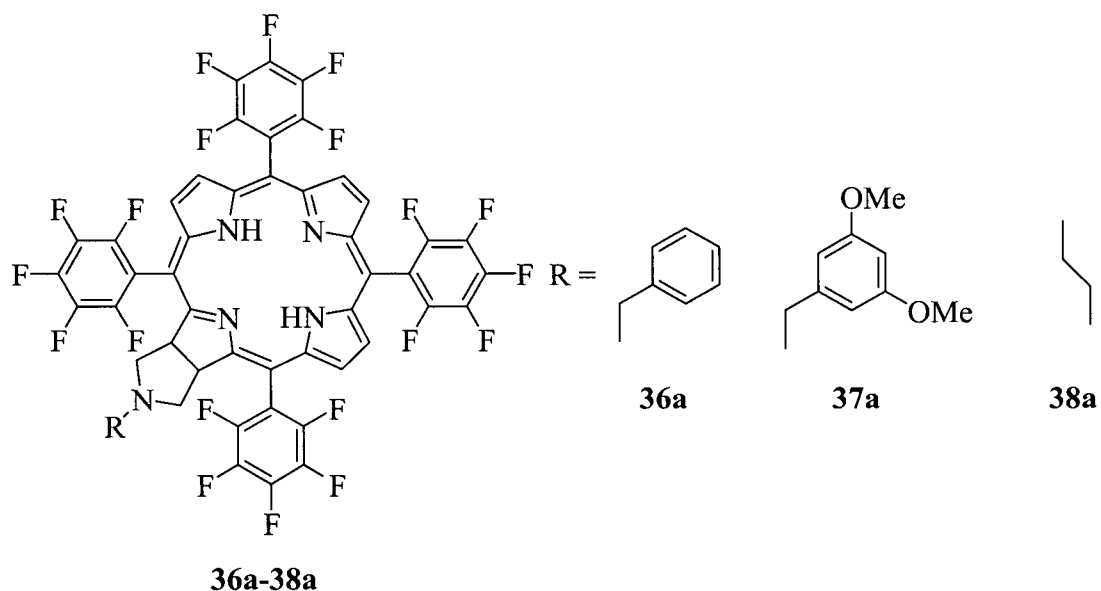
Synthesis of α,α' -(disilylmethyl)-*n*-cyanomethylamine (**39**)

A solution of **37** (500 mg, 1.79 mmol) in dry CH₂Cl₂ (5 mL) was added to a solution of cyanogen bromide (209 mg, 1.97 mmol) slowly at *r.t.*. Almost immediately, silica tlc showed complete consumption of **37**, and the reaction was halted. 2 mL of triethylamine was added to the reaction mixture, which was then washed twice with

0.5 M HCl, and then twice with H₂O. The crude product was purified using column chromatography on silica gel (5 % EtOAc/hexane) to give the pure product in 58 % yield.

39: R_f 0.7 (silica; 20 % EtOAc/hexane); ¹H-NMR (400 MHz, CDCl₃, ppm) δ = 2.5 (s, 4H), 0.20 (s, 18H). MS (EI) m/z calculated for C₉H₂₂N₂Si₂: 214.13216, found 214.13265 m/z (MH⁺ = 100 %).

Reaction of α,α'-(disilylmethyl)amines with pFTPP.¹⁹⁴



Two dry round bottom flasks are fitted with N₂ inlets. To one was added 50 mg (0.0513 mmol) of pFTPP and 129 mg (1.026 mmol) of AgF. To the other was added 177.7 mg (0.636 mmol) of dry **36**. 1 mL of THF was added to both flasks, and the solution of amine **36** was added to the other flask drop-wise via syringe. The reaction was stopped after 1 h and AgF was filtered. The products were purified by column chromatography on silica gel (20 % EtOAc/hexane). Two products were collected **36a**

(33 mg, 58 %) and **36b** (7 mg). The reaction of **37** with pFTPP proceeded in a similar manner with 50 mg (0.0513 mmol) of pFTPP, 200 mg (1.58 mmol) of AgF and 200 mg (0.589 mmol) of **37**. The reaction was left for 1 h. The products were purified in the same manner as **36a**, yielding **37a** (19 mg, 33 %) and **37b** (5 mg). The reaction between **38** and pFTPP proceeded in a similar manner to that of **36** with 50 mg (0.0513 mmol) of pFTPP, 200 mg (1.58 mmol) of AgF and 150 mg (0.607 mmol) of **38**. The products were purified in the same manner as **36a**, yielding **38a** (38 mg, 67 %).

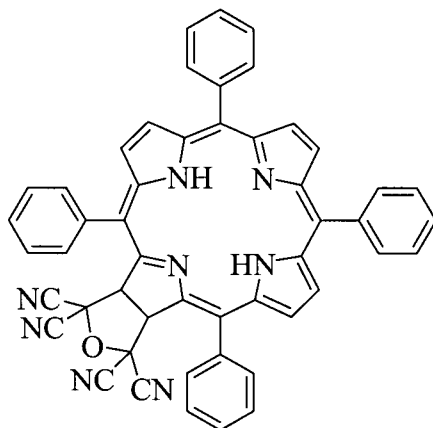
36a: R_f 0.7 (silica; 60 % CH_2Cl_2 /hexane); $^1\text{H-NMR}$ (400 MHz, CDCl_3 , ppm) δ = 8.70 (d, J = 4.78 Hz, 2H), 8.48 (s, 2H), 8.38 (d, J = 4.78 Hz, 2H), 7.25 (m, 2H), 7.08 (m, 3H), 5.17 (m, 2H), 3.41 (s, 2H), 3.09 (m, 2H), 2.56 (m, 2H), -1.80 (s, 2H). UV-Vis (CHCl_3) λ_{max} (rel. intensity) 405 (1.00), 504 (0.08), 600 (0.02), 654 (0.283). MS (LSIMS) dev. in ppm from mass calculated for $\text{C}_{53}\text{H}_{22}\text{F}_{20}\text{N}_5$: 0.15, found 1108.15575 m/z (MH^+ = 100 %).

37a: R_f 0.7 (silica; 20 % EtOAc/hexane); $^1\text{H-NMR}$ (400 MHz, CDCl_3 , ppm) δ = 8.70 (d, J = 4.78 Hz, 2H), 8.47 (s, 2H), 8.38 (d, J = 4.78 Hz, 2H), 6.3 (s, 1H), 6.16 (s, 2H), 5.15 (m, 2H), 3.57 (s, 6H), 3.34 (s, 2H), 3.10 (m, 2H), 2.56 (m, 2H), -1.80 (s, 2H). UV-Vis (CHCl_3) λ_{max} (rel. intensity) 405 (1.00), 504 (0.09), 600 (0.03), 654 (0.284). MS (LSIMS) dev. in ppm from mass calculated for $\text{C}_{55}\text{H}_{25}\text{F}_{20}\text{N}_5\text{O}_2$: -1.39, found 1168.17509 m/z (MH^+ = 100 %).

38a: R_f 0.7 (silica; 60 % CH_2Cl_2 /hexane); $^1\text{H-NMR}$ (400 MHz, CDCl_3 , ppm) δ = 8.70 (d, J = 4.78 Hz, 2H), 8.48 (s, 2H), 8.38 (d, J = 4.78 Hz, 2H), 5.20 (m, 2H), 3.15 (m, 2H), 2.51 (m, 2H), 2.24 (d, J = 7.5 Hz, 2H), 1.3 (m, 2H), 1.19 (m, 2H), 0.80 (t, J = 7.5 Hz, 3H), -1.86 (s, 2H). UV-Vis (CHCl_3) λ_{max} (rel. intensity) 405 (1.00), 504 (0.09),

600 (0.03), 654 (0.290). MS (LSIMS) dev. in ppm from mass calculated for $C_{50}H_{23}F_{20}N_5$: 1.59, found 1074.17295 ($MH^+ = 100\%$).

Reaction of tetracyanoethylene oxide with TPP to form 40

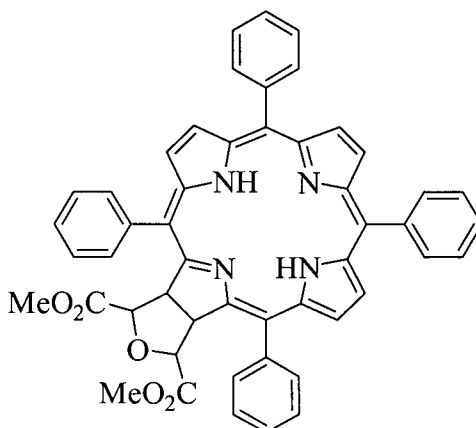


40

A solution of 200 mg (0.325 mmol) of TPP was refluxed in 50 mL of toluene. TCNEO (200 mg, 1.4 mmol) was then added to the solution. The mixture was refluxed for 1 h, concentrated under reduced pressure, and purified by preparatory tlc on 2 mm silica gel plates (50 % CH_2Cl_2 /hexane). The product **40** was obtained in 20 % yield.

40: R_f 0.7 (silica; 50 % CH_2Cl_2 /hexane); 1H -NMR (400 MHz, $CDCl_3$, ppm) δ = 8.70 (d, $J = 4.89$ Hz, 2H), 8.50 (s, 2H), 8.38 (d, $J = 4.89$ Hz, 2H), 8.13 – 7.66 (m, 20H), 6.00 (s, 2H), -2.05 (s, 2H). UV-Vis ($CHCl_3$) λ_{max} (rel. intensity) 416 (1.0), 514 (0.14), 554 (0.18), 586 (0.10), 642 (0.22). LRMS (LSIMS) 759 m/z ($MH^+ = 100\%$).

Hydrolysis and methylation of **40** to form **41**



41

A solution of **40** in concentrated HCl (5 mL), was refluxed for 8 h, and the HCl was removed under reduced pressure. The resulting polar products were then dissolved in 2 mL of DMSO, with 66 μ L of dimethylsulfate and 100 mg (0.723 mmol) of potassium carbonate. This solution was heated until no more baseline material was observed using silica tlc. Purification on preparatory tlc gave two products, one of which was **41**, 10 mg, 10 % yield.

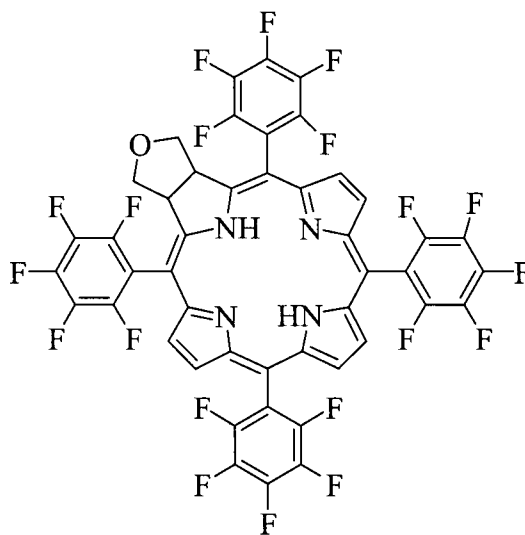
41: R_f 0.7 (silica; 60 % CH_2Cl_2 /hexane); $^1\text{H-NMR}$ (400 MHz, CDCl_3 , ppm) δ = 8.60 (d, J = 4.89 Hz, 2H), 8.45 (s, 2H), 8.28 (d, J = 4.89 Hz, 2H), 8.13 – 7.66 (m, 20H), 6.02 (s, 2H), 4.92 (s, 2H), 3.53 (s, 6H), -1.96 (s, 2H). UV-Vis (CHCl_3) λ_{max} (rel. intensities) 416 (1.00), 518 (0.10), 544 (0.09), 592 (0.07), 646 (0.14). MS (LSIMS) dev. in ppm for mass calculated for $\text{C}_{53}\text{H}_{20}\text{F}_{20}\text{N}_5$: 0.30, found 775.29228 m/z (MH^+ = 100 %).

Synthesis of α,α' -(dichloromethyl)ether¹⁷⁶

A 100 mL round bottom reaction flask was cooled in ice, 16.8 mL of conc. HCl was added to the flask, after which 24 g of paraformaldehyde was added slowly. 45.2 mL of chlorosulfonic acid was added slowly to the mixture while stirring. The mixture is stirred for 4 h at *r.t.*. The less dense organic layer was then separated from the more dense aq. layer, and was washed with H₂O twice, and with 40 % NaOH until just alkaline. The product was dried over potassium carbonate and potassium hydroxide at 0°C. The product was then used without further purification.

44a: ¹H-NMR (200 MHz, CDCl₃, ppm) δ = 5.45 (s, 4H).

Reaction of unstabilized carbonyl ylide with pFTPP to form 44



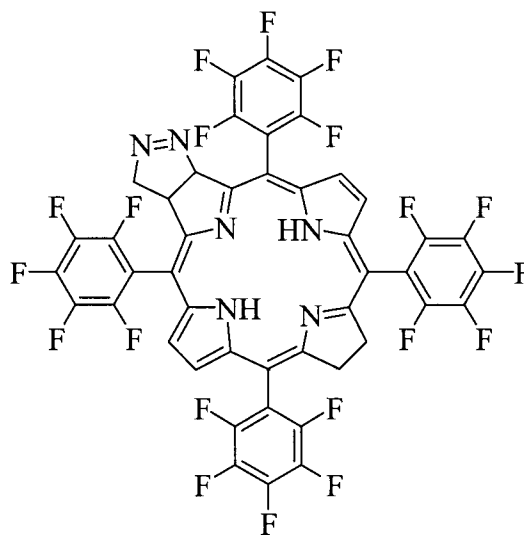
44

A suspension of lead PbCl₂ with Mn was stirred in 15 mL of dry THF for 1 h. To the mixture 50 mg (0.05 mmol) of pFTPP was added followed by 3 g (0.02 mol) NaI and 1.14 g of the α,α' -(dichloromethyl)ether. The reaction is left to stir overnight under N₂,

and stopped 12 h later. The reaction was quenched with water, and the organic products were then separated into CH_2Cl_2 . The organic layer was dried with MgSO_4 and purified by preparatory tlc on 2 mm silica gel plates (50 % CHCl_3 /hexane). The product **44** was obtained in 38 % yield.

44: R_f 0.5 (silica; 50 % CH_2Cl_2 /hexane); $^1\text{H-NMR}$ (400 MHz, CDCl_3 , ppm) δ = 8.70 (d, J = 4.90 Hz, 2H), 8.47 (s, 2H), 8.38 (d, J = 4.90 Hz, 2H), 5.33 (t, J = 4.36 Hz, 2H), 4.20 (t, J = 8.17 Hz, 2H), 4.20 (t, J = 8.17 Hz, 2H), 3.92 (dd, J = 4.36 Hz and 8.17 Hz, 2H), -1.50 (s, 2H). UV-Vis (CHCl_3) λ_{max} (rel. intensities) 414 (1.00), 506 (0.03), 603 (0.01), 656 (0.128). LRMS (LSIMS) 1019 m/z (MH^+ = 100 %).

Reaction of pFTPP with Diazomethane to give **45**



45

2 g (9.33 mmol) of Diazald[®] was dissolved in 16 mL of diethylether. This is added dropwise into the reaction chamber of a diazomethane apparatus containing 8 mL of H_2O , 8 mL EtOH and 2 g (0.0338 mmol) of KOH. The resulting gas was condensed with ether at -78°C into a flask containing 50 mg of pFTPP dissolved in 2 mL of dry

CH₂Cl₂. After all of the Diazald® is exhausted, the reaction was sealed under positive N₂ pressure and left to stir overnight. The reaction is repeated 24 h later. The solution was then concentrated under reduced pressure, and the crude product was purified by preparatory tlc on 2 mm silica gel plates (20 % CH₂Cl₂/hexane). The compound **45** was obtained in 60 % yield.

45: R_f 0.7 (silica; 50 % CH₂Cl₂/hexane); ¹H-NMR (400 MHz, CDCl₃, ppm) δ = 8.80 (d, J = 4.89 Hz, 1H), 8.77 (d, J = 4.89 Hz, 1H), 8.61 (d, J = 4.89 Hz, 1H), 8.52 (s, 2H), 8.44 (d, J = 4.89 Hz, 1H), 4.92 (s, 2H), 7.72 (d, J = 8.8 Hz, 1H), 5.11 (m, 2H), 4.92 (m, 1H), -2.09 (s, 2H). UV-Vis (CHCl₃) λ_{max} (rel. intensities) 402 (1.00), 504 (0.09), 598 (0.01), 648 (0.181). MS (LSIMS) dev in ppm from mass calculated for C₄₅H₁₂F₂₀N₆: 0.58, found 1017.08882 m/z (MH⁺ = 100 %).

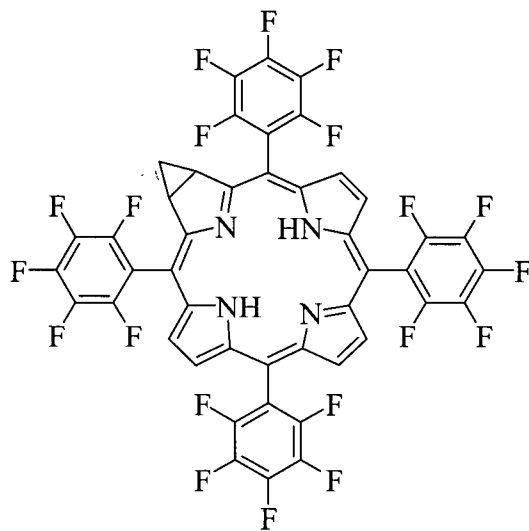
Nitrogen Elimination from Compound **45** to form **46**

Compound **45** (5 mg) was subjected to the following two experiments.

1. Compound **45** was dissolved in mesitylene and refluxed under N₂ for 1 h.
2. Compound **45** was dissolved in toluene-d₈, this was then irradiated with sunlight for 1 h.

Both reactions gave the same product **46** in nearly quantitative yield. The products were used directly for analysis without any purification.

46: R_f 0.8 (silica; 20 % CH₂Cl₂/hexane); ¹H-NMR (400 MHz, CDCl₃, ppm) δ = 8.67 (d, J = 4.78 Hz, 2H), 8.43 (s, 2H), 8.40 (d, J = 4.78 Hz, 2H), 3.90 (dd, J = 4.10 Hz, 2H), 1.90 (m, 1H), .84 (s, 1H), -1.73 (s, 2H). UV-Vis (CHCl₃) λ_{max} (rel. intensities) 410 (1.00), 508 (0.14), 606 (0.08), 662 (0.30). MS (LSIMS) dev. in ppm from mass calculated for C₄₅H₁₂F₂₀N₄: 0.73, found 988.07498 m/z (MH⁺ = 100 %).



46

Chapter 5: References

1. Dinello, R. K.; Chang, C. K. In *The Porphyrins*; Dolphin D. Ed.; Academic Press; New York, **1978**, Volume I, Chapter 7, pg. 291.
2. Hiroyuki, N.; Tsukahara, Y.; Tsuchida, F. *J. Phys. Chem. B* **1998**, *102*, 8766.
3. Groves, J.; Matsunaga, A. *Bioorganic and Medicinal Chem. Lett.* **1996**, *6*, 1595.
4. Pratviel, G.; Bernadou, J.; Meunier, B. *Angew. Chem.* **1995**, *34*, 746.
5. Tong, Y.; Hamilton, D.; Meillon, J.; Sanders, K. *Org. Lett.* **1999**, *1*, 1343.
6. Kuster, W. *Z. Physiol. Chem.* **1912**, *82*, 463.
7. Ollis, W. D. In *Aromaticity, an International Symposium*; The Chemical Society; Burlington House; **1966**, *21*, 3.
8. Janson, T.; Katz, J. In *The Porphyrins*; Dolphin, D. Ed.; Academic Press; New York, **1978**, Volume IV, Chapter 1, pg. 1-54.
9. Buchler, J. In *The Porphyrins*; Dolphin, D. Ed.; Academic Press; New York, **1978**, Volume I, Chapter 10, pg. 390-474.
10. Spyroullias, G.; Sioubara, M.; Coutsolelos, A. *Polyhedron* **1995**, *14 (23)*, 23.
11. Smith, K. M., In *Porphyrin and Metalloporphyrins*, Smith, K. M. Ed.; Elsevier Publishing Company; Amsterdam, **1975**, Chapter 1, pg. 11.
12. Kim, J.; Adler, A.; Longo, F. In *The Porphyrins*; Dolphin, D. Ed.; Academic Press; New York, **1978**, Volume I, Chapter 1 pg. 88-90.
13. Shanmugathan, S.; Edwards, C.; Boyle, R. *Tetrahedron* **2000**, *56*, 1032.
14. Czuchajowski, L.; Habdas, J.; Neidbala, H.; Wandrekar, V. *Tetrahedron Lett.* **1991**, *32*, 7511.

-
15. Milgrom, L. R. *The Colours of Life*; Oxford University Press; New York, **1997**, pg. 74.
16. Milgrom, L. R. *The Colours of Life*; Oxford University Press; New York, **1997**, pg. 75.
17. Bonnett, R. In *The Porphyrins*; Dolphin, D. Ed.; Academic Press; New York, **1978**; Structure and Synthesis Part A; Volume I, Chapter 1, pg. 4.
18. Milgrom, L. R. *The Colours of Life*; Oxford University Press; New York, **1997**, pg. 81.
19. Tome, A.; Lacerda, P.; Neves, M.; Cavaleiro, J. *J. Chem. Soc., Chem. Comm.* **1997**, 1199.
20. Tome, A.; Silva, A.; Lacerda, P.; Neves, M.; Cavaleiro, J. *J. Chem. Soc., Chem. Comm.* **1999**, 1767.
21. Gouterman, M.; Adar, F.; Weiss, C. In *The Porphyrins*; Dolphin, D. Ed; Academic Press; New York, **1978**, Volume III, Chapters 1 - 3.
22. Milgrom, L. R. *The Colours of Life*; Oxford University Press; New York, **1997**, pg. 86
23. Gouterman, M. In *The Porphyrins*; Dolphin D. Ed.; Academic Press; New York, **1978**, Volume III, Chapter 1.
24. Frydman, B.; Frydman, R.; Valasinas, A.; Bogorad, L. In *The Porphyrins*; Dolphin D. Ed.; Academic Press; New York, **1978**, Volume VI, Chapters 1 - 2.
25. Milgrom, L. R. *The Colours of Life*; Oxford University Press; New York, **1997**, pg. 36.

-
26. Milgrom, L. R. *The Colours of Life*; Oxford University Press; New York, **1997**, pg. 41.
27. Milgrom, L. R. *The Colours of Life*; Oxford University Press; New York, **1997**, pg. 45.
28. Alder, A. D.; Longo, F. R.; Finarelli, J. D.; Goldmacher, J.; Assour, J.; Korsakoff, L. *J. Org. Chem.* **1967**, *32*, 476.
29. Rothmund, P. *J. Am. Chem. Soc.* **1936**, *58*, 625.
30. Lindsey, J. S.; Scriemann, I. C.; Hsu, H. C.; Kearney, P. C. ; Marguerettaz, A. M. *J. Org. Chem.* **1987**, *52*, 827.
31. Kuroda, Y.; Murase, H.; Suzuki, Y.; Ogoshi, H. *Tetrahedron Lett.* **1989**, *30*, 2411.
32. Whitlock, H. W.; Hanauer, R. *J. Org. Chem.* **1968**, *33*, 1629.
33. Milgrom, L. R. *The Colours of Life*; Oxford University Press; New York, **1997**, pg. 56.
34. MacDonald, S.F.; Bullock, E.; Arsenault, G.P. *J. Am. Chem. Soc.* **1960**, *82*, 4384.
35. <http://www.qlt-pdt.com>.
36. Stilts, C.; Nelen, M.; Himley, D.; Davies, S.; Gollnick, S.; Oseroff, A.; Gibson, S.; Russell, H.; Detty, M. *J. Med. Chem.* **2000**, *43*, 2403.
37. Meyer-Betz, F. *Deutsches Aech. Klin. Med.* **1913**, *112*, 476.
38. Policard, A. C. R. *Hebd. Soc. Bio.* **1925**, *91*, 1422.
39. Milgrom, L. R. *The Colours of Life*; Oxford University Press; New York, **1997**, pg. 207.
40. Kato, H. *J. Photochem. Photobiol. B: Biol.* **1998**, *42*, 96.
41. Lipson, R.; Blades, E. *Arch. Dermatol.* **1960**, *82*, 508.

-
42. Milgrom, L. R. *The Colours of Life*; Oxford University Press; New York, **1997**, pg. 209.
43. Dolphin, D. *Can. J. Chem.* **1994**, *72*, 1005.
44. Lee See, K.; Forbes, I. J.; Bettes, W. H. *J. Photochem. Photobiol.* **1984**, *39*, 631.
45. Symonowicz, K. *Anticancer Res.* **1999**, *19*, 5385.
46. Gomer, C. J.; Dougherty, T. J. *Cancer Res.* **1979**, *39*, 146.
47. Foote, C. S. In *Pathology of Oxygen*; Autor, A. P. Ed.; Academic Press; **1982**, pg. 21.
48. Foote, C. S. In *Porphyrin Localization and Treatment of Tumors*; Doiron, D. R. and Gomer, C. J. Ed.; Alan R. Liss, Inc.; New York, **1984**; pg. 3.
49. Redmond, R.; Gamlin, J. J. *J. Photochem. Photobiol.* **1999**, *70*, 391.
50. Tanielian, C.; Wolff, C.; Esch, M. *J. Phys. Chem.* **1996**, *100*, 6555.
51. Fernandez, J. M. *J. Photochem. Photobiol. B: Biol.* **1997**, *37*, 131.
52. Winkelman, J. W.; Collins, G. H. *Photochem. Photobiol.* **1987**, *46*, 801.
53. Stilts, C. E.; Nelen, N. I.; Hilmey, D. G.; Davies, S. R.; Gollnick, S. O.; Oseroff, A. R.; Gibson, S. L.; Hilf, R.; Detty, M. R. *J. Med. Chem.* **2000**, *43*, 2405.
54. Ulman, A.; Manassen, J. *J. Chem. Soc., Perkin I* **1979**, *4*, 1066.
55. Symonowicz, K.; Ziolkowski, P.; Chmielewski, P. *Anticancer Res.* **1999**, *19*, 5385.
56. Richter, A. M.; Waterfield, E.M.; Jain, A. K.; Sternberg, E. D.; Dolphin, D.; Levy, J. *Br. J. Cancer* **1991**, *63*, 87.
57. Pangka, V. S.; Morgan, A. R.; Dolphin, D. *J. Org. Chem.* **1986**, *51*, 1094.
58. Aveline, B.; Hasan, T.; Redmond, R. W. *Photochem. Photobiol.* **1994**, *59*, 328.
59. Araki, K.; Silva, C.; Toma, H.; Catalani, M.; Medeiros, H.; Mascio, P. *J. Inorg. Biochem.* **2000**, *78*, 269.

-
60. Eggleton, M. K.; Crites, D. K.; McMillin, D. R. *J. Phys. Chem.* **1998**, 5506.
61. Huisgen, R. In *1,3-Dipolar Cycloaddition Chemistry*; Padwa, A. Ed.; Wiley-Interscience; New York, 1984, Volume 1, Chapter 1.
62. Curtius, T. *Ber. Dtsch. Chem. Ges.* **1883**, 16, 2230.
63. Buchner, E. *Ber. Dtsch. Chem. Ges.* **1888**, 21, 2637.
64. Buchner, E. *Ber. Dtsch. Chem. Ges.* **1889**, 22, 2165.
65. Pechmann, H. V. *Ber. Dtsch. Chem. Ges.* **1894**, 27, 1888.
66. Pechmann, H. V.; Burkard, E. *Ber. Dtsch. Chem. Ges.* **1900**, 33, 3590.
67. Schmitz, E.; Ohme, R. *Chem. Ber.* **1962**, 95, 795.
68. Mikhailova, V.; Bulat, A. *Zh. Org. Khim.* **1971**, 2223.
69. Thiele, J. *Ber. Dtsch. Chem. Ges.* **1911**, 44, 2522.
70. Clausius, K.; Weiser, H. *Helv. Chim. Acta* **1952**, 35, 1548.
71. Michael, A. *J. Prakt. Chem. (2)* **1893**, 48, 94.
72. Harries, C. *Liebigs Ann. Chem.* **1905**, 343, 311; **1910**, 374, 288; **1912**, 390, 236; **1915**, 410, 1.
73. Criegee, R. *Liebigs Ann. Chem.* **1953**, 1, 583.
74. Bailey, P.S. Thompson J. A., Shoulders, B.A. *J. Am. Chem. Soc.* **1966**, 88, 4098.
75. Criegee, R. *Angew. Chem. Int. Ed. Eng.* **1975**, 14, 745.
76. Schank, K.; Beck, H.; Buschlinger, M.; Eder, J.; Heisel, T.; Pistorius, S.; Wagner, C. *Helv. Chim. Acta* **2000**, 83, 801.
77. Werner, A.; Buss, H. *Ber. Dtsch. Chem. Ges.* **1894**, 27, 2193.
78. Grundmann, C.; Grunanger, P. In *The Nitrile Oxides* Springer-Verlag, Berlin, **1971**.
79. Grundmann, C.; Dean, J. M. *J. Org. Chem.* **1965**, 30, 2809.

-
80. Tufariello, J. *Acc. Chem. Res.* **1979**, *12*, 396.
81. Lwowski, W. In *1,3-Dipolar Cycloaddition Chemistry*; Padwa, A. Ed.; Wiley-Interscience; New York, **1984**, Volume 1, pg. 561.
82. Huisgen, R.; Szeimies, G. *Chem. Ber.* **1965**, *98*, 1153.
83. Bruice, P. Y. *Organic Chemistry*, 2nd Ed., Prentice Hall, **1998**, pg. 135.
84. Poppinger, D. *Aust. J. Chem.* **1976**, *29*, 463.
85. Poppinger, D. *J. Am. Chem. Soc.* **1975**, *97*, 7486.
86. Klopman, G. *J. Am. Chem. Soc.* **1968**, *90*, 223.
87. Sustmann, R. *Pure Appl. Chem.* **1974**, *40*, 569.
88. Houk, K. N. In *Application of Frontier Molecular Orbital Theory to Pericyclic Reactions*; Marchand, A. P., Lehr, R. E. Ed.; Academic Press; New York, *Pericyclic Reactions*, **1977**, Vol. 2, pg. 181.
89. Elender, K.; Riebel, P.; Weber, A.; Sauer, J. *Tetrahedron* **2000**, *56*, 4263.
90. Caramella, P.; Gandour, R. W.; Hall, J. A.; Deville, C. G.; Houk, K. N. *J. Am. Chem. Soc.*, **1977**, *99*, 385.
91. Geittner, J. Ph. D. Thesis, University of Munich, **1974**. Geittner, J.; Huisgen, R.; Sustmann, R. *Tetrahedron Lett.* **1977**, 881.
92. Huisgen, R.; Szeimes, G. *Chem. Ber.* **1967**, *100*, 2494.
93. Rastelli, A.; Bagatti, M.; Gandolfi, R.; Burdisso, M. *J. Chem. Soc., Faraday Trans.* **1994**, *90*, 1077. Kanemasa, S.; Nisuichi, M. *J. Am. Chem. Soc.* **1994**, *116*, 2324.
94. Bohm, T.; Weber, A.; Sauer, J. *Tetrahedron* **1999**, *55*, 9535.
95. Sakai, N.; Funabashi, M.; Hamada, T. *Tetrahedron* **1999**, *55*, 13703.
96. Gothelf, K. V.; Jorgensen, K. A. *Chem. Rev.* **1998**, *98*, 863.

-
97. Caramella, P.; Grunanger, P. In *1,3-Dipolar Cycloaddition Chemistry*; Padwa, A. Ed.; Wiley-Interscience; New York, **1984**, Volume 1, pg. 293.
98. Kanemasa, S.; Nishiuchi, M.; Kamimura, A.; Hori, K. *J. Am. Chem. Soc.* **1994**, *116*, 2330.
99. Simonsen, K. B.; Bayon, P.; Hazell, R.; Gothelf, K. V.; Jorgensen, K. A. *J. Am. Chem. Soc.* **1999**, *121*, 3845.
100. Kanemasa, S.; Nishiuchi, M.; Kamimura, A.; Hori, K. *J. Am. Chem. Soc.* **1994**, *116*, 3846.
101. Black, T. *Aldrichima Acta* **1983**, *16* (1), 3.
102. Regitz, M.; Heydt, H. In *1,3-Dipolar Cycloaddition Chemistry*; Padwa, A. Ed.; Wiley-Interscience; New York, **1984**, Vol. 1, 1393.
103. Huisgen, R. *Angew. Chem.* **1962**, *75*, 604.
104. Firestone, R. A., *Tetrahedron Lett.* **1980**, *21*, 2209.
105. Huisgen, R. *J. Org. Chem.* **1976**, *41*, 403-419.
106. Regitz, M.; Heydt, H. In *1,3-Dipolar Cycloaddition Chemistry*; Padwa, A. Ed.; Wiley - Interscience; New York, **1984**, Volume 1, pg. 405.
107. Rastelli, A.; Gandofi, R.; Amade; M. S. *J. Org. Chem.* **1998**, *63*, 7425-7436.
108. Rastelli, A.; Gandofi, R.; Amade; M. S. *J. Chem. Soc., Faraday Trans.* **1994**, *90*, 1077.
109. Fisera, L.; Geittner, J.; Huisgen, R. *Heterocycles* **1978**, *10*, 153.
110. Heine, H. W.; Peavy, R. *Tetrahedron Lett.* **1965**, 3123.
111. Maggini, M.; Scorrano, G.; Prato, M. *J. Am. Chem. Soc.* **1993**, *115*, 9798.
112. Gallagher, T. *J. Heterocyclic Chem.* **1999**, *36*, 1365.

-
113. Lown, W. J. In *1,3-Dipolar Cycloaddition Chemistry*; Padwa, A. Ed.; Wiley-Interscience; New York, **1984**, Volume 1, pg. 672.
114. Bohm, T., Weber, A., Sauer, J. *Tetrahedron* **1999**, *55*, 9535.
115. Elender, K.; Riebel, P.; Weber, A.; Sauer, J. *Tetrahedron* **2000**, *56*, 4261.
116. Pearson, W.; Stevens, E. *J. Org. Chem.* **1998**, *63*, 9812.
117. Linn, W.J. *J. Am. Chem. Soc.*, **1965**, *87*, 3657.
118. Hojo, M.; Naruyasu, I.; Hosomi, A. *Synlett* **1995**, *3*, 234.
119. Hojo, M. *J. Org. Chem.* **1997**, *62*, 8611.
120. Hojo, M. *J. Am. Chem. Soc.* **1996**, *118*, 3534.
121. Aono, M.; Hyodo, C.; Terao, Y.; Achiwa, K. *Tetrahedron. Lett.* **1986**, *27*, 4032.
122. Hosomi, A.; Matsuyama, Y.; Sakurai, H. *J. Chem. Soc., Chem. Comm.* **1986**, 1073.
123. Aono, M. *Tetrahedron Lett.* **1986**, *27*, 4040.
124. Bohm, T. *Tetrahedron* **1999**, *55*, 9535.
125. Huisgen, R. *J. Am. Chem. Soc.* **1985**, *108*, 6401.
126. Mloston, G.; Fabian, J. *Polish J. Chem.* **1999**, *73*, 689.
127. Steglich, W.; Gruber, P.; Heininger, H.; Kneidl, F. *Chem. Ber.* **1971**, *104*, 3816.
128. Riichter, A. M.; Waterfield, E. M.; Jain, A. K.; Sternberg, E. D.; Dolphin, D.; Levy, J. *Br. J. Cancer* **1991**, *63*, 87.
129. Hansen, H. J. In *1,3-Dipolar Cycloaddition Chemistry*; Padwa, A. Ed.; Wiley-Interscience; New York, **1984**, Volume 1, pg. 215.
130. Bunge, K.; Huisgen, R.; Raab, R. *Chem. Ber.* **1972**, *105*, 1296.
131. Dragisich, V., *Organometallics* **1990**, *9*, 2868.

-
132. Milgrom, L. R. *The Colours of Life*; Oxford University Press; New York, **1997**, pg. 74.
133. Spikes, J. D.; Bommer, J. C. *J. Photochem. Photobiol. B.: Biol.* **1993**, *17*, 135
134. Bonnett, R. *Chem. Soc. Rev.* **1995**, *24*, 19.
135. Whitlock Jr., H.; Hanauer, R.; Oester, M.; Bower, B. *J. Am. Chem. Soc.* **1969**, *91*, 7485.
136. Flitsch, W. *Adv. Heterocycl. Chem.* **1988**, *43*, 73.
137. Scheer, H.; Inhoffen, H. H. In *The Porphyrins*; Dolphin, D. Ed.; Academic Press: New York, **1978**, Volume II, Chapter 1 p. 45.
138. Tome, A.; Lacerda, P.; Neves, M.; Cavaleiro, J. *J. Chem. Soc., Chem. Comm.* **1997**, 1199.
139. DiNello, R. K.; Dolphin, D. *J. Org. Chem.* **1980**, *45*, 5196.
140. Pangka, V. S.; Morgan, A. R.; Dolphin, D. *J. Org. Chem.* **1986**, *51*, 1094.
141. Scott, A.; Irwin, A.; Siegel, L.; Shoolery, J. N. *J. Am. Chem. Soc.* **1978**, *100*, 7987.
142. Morgan, A.; Kohli, D. *Tetrahedron Lett.* **1995**, *36*, 7603.
143. Osuka, A.; Marumo, S.; Maruyama, K. *Bull. Chem. Soc. Jpn.* **1993**, *66*, 3873.
144. Brukner, C.; Dolphin, D. *Tetrahedron Lett.* **1995**, *36*, 3295.
145. Brukner, C.; Dolphin, D. *Tetrahedron Lett.* **1995**, *36*, 5196.
146. Silva, A.; Tome, A.; Meves, M.; Silva, A.; Cavaleiro, J. *Chem. Comm.* **1999**, 1767.
147. Li, G.; Chen, Y.; Missert, J.; Rungta, A.; Dougherty, T.; Grossman, Z.; Pandey, R. *J. Chem. Soc., Perkin Trans. 1* **1999**, 1785.
148. Pandey, G.; Lakshmaial, G.; Gadre, S. *Ind. J. Chem.* **1996**, *35B*, 91-98.
149. Hodge, J.; Hill, M.; Gray, H. *Inorg. Chem.* **1995**, *34*, 809.

-
150. Hageman, H. *Organic Reactions* **1953**, 7, 198.
151. Linn, W. J.; Benson, R. E. *J. Am. Chem. Soc.* **1965**, 87, 3657.
152. Hojo, M.; Aihara, H.; Sakata, K.; Hosomi, A. *J. Org. Chem.* **1997**, 62, 8610.
153. Linn, W. J.; Benson, R. E. *J. Am. Chem. Soc.* **1965**, 87, 3657.
154. McAlpine, J. Ph.D. Thesis **1999**, University of British Columbia.
155. Fadel, A.; *Tetrahedron* **1991**, 47, 6265.
156. Grundy, J.; James, B.; Pattenden, G.; *Tetrahedron Lett.* **1972**, 757.
157. Shea, K.; Jaquinod, L.; Smith, K. *J. Org. Chem.* **1998**, 63, 7019.
158. Hojo, M.; Aihara, H.; Sakata, K.; Hosomi, A. *J. Org. Chem.* **1997**, 62, 8610; Takai, K.; Kaihara, H.; Ikeda, N. *J. Org. Chem.* **1997**, 62, 8612.
159. Black, H. *Aldrichimica Acta* **1983**, 16, 3.
160. Regitz, M. In *1,3-Dipolar Cycloaddition Chemistry*; Padwa, A. Ed.; Wiley-Interscience; New York, **1984**, Volume 1, pg. 393.
161. Meier, H.; Zeller, K. P. *Angew. Chem.* **1977**, 89, 876.
162. Callot, H. *Tetrahedron Lett.* **1972**, 11, 1011.
163. Caramella, P.; Grunanger, P. In *1,3-Dipolar Cycloaddition Chemistry*; Padwa, A. Ed.; Wiley-Interscience; New York, **1984**, Volume 1, pg. 291.
164. Adams, K. R.; Bonnett, R.; Burke, P. J.; Salgado, A.; Valles, M. A. *J. Chem. Soc., Chem. Comm.* **1993**, 1860.
165. Russel, G., Ochrymowycz, L. A. *J. Org. Chem.* **1970**, 35, 2107.
166. Aono, M.; Hyodo, C.; Terao, Y.; Achiwa, K. *Tetrahedron Lett.* **1986**, 27, 4039.
167. Grashey, R. In *1,3-Dipolar Cycloaddition Chemistry*; Padwa, A. Ed.; Wiley-Interscience; New York, **1984**, Volume 1, pg. 733.

-
168. Sakai, N.; Funabashi, M.; Hamada, T. *Tetrahedron* **1999**, *55*, 13708
169. Lwowski, W. In *1,3-Dipolar Cycloaddition Chemistry*; Padwa, A. Ed.; Wiley-Interscience; New York, **1984**, Volume 1, pg. 559.
170. Pearson, W.; Mi, Y. *Tetrahedron Lett.* **1997**, *38*, 5441. Pearson, W.; Stevens, E. *Tetrahedron Lett.* **1994**, *35*, 2641. *J. Org. Chem.* **1998**, *63*, 9812.
171. Pearson, W.; Clark, R. *Tetrahedron Lett.* **1999**, *40*, 4467.
172. Alder, A. D.; Longo, F. R.; Finarelli, J. D.; Goldmacher, J.; Assour, J.; Korsakoff, L. *J. Org. Chem.* **1967**, *52*, 827.
173. Made, A.; Hoppenbrouwer, R. J.; Nolte, J.; Drenth, W. *Recl. Trav. Chim. Pays-Bas.* **1988**, *107*, 15.
174. Baldwin, J.; Crossley, M.; DeBernardis, J. *Tetrahedron* **1982**, *38*, 685.
175. Pandey, G.; Lakshmaiah, G.; Gadre, S. *Indian J. of Chem.* **1996**, *35B*, 95.
176. *Org. Syn. Vol.* 36, 1.